DIGITALCOMMONS
@WAYNESTATE

Wayne State University

Wayne State University Dissertations

1-1-2015

Soy Isoflavones Mediate Radioprotection Of Normal Lung Tissue By Modulating The Radiation-Induced Inflammatory Response

Lisa Marie Abernathy
Wayne State University,

Follow this and additional works at: http://digitalcommons.wayne.edu/oa_dissertations

 Part of the Cell Biology Commons, Immunology and Infectious Disease Commons, and the Molecular Biology Commons

Recommended Citation
Abernathy, Lisa Marie, "Soy Isoflavones Mediate Radioprotection Of Normal Lung Tissue By Modulating The Radiation-Induced Inflammatory Response" (2015). *Wayne State University Dissertations.* Paper 1326.

This Open Access Dissertation is brought to you for free and open access by DigitalCommons@WayneState. It has been accepted for inclusion in Wayne State University Dissertations by an authorized administrator of DigitalCommons@WayneState.

SOY ISOFLAVONES MEDIATE RADIOPROTECTION OF NORMAL LUNG TISSUE BY MODULATING THE RADIATION-INDUCED INFLAMMATORY RESPONSE

by

LISA MARIE ABERNATHY

DISSERTATION

Submitted to the Graduate School

of Wayne State University,

Detroit, Michigan

in partial fulfillment of the requirements

for the degree of

DOCTOR OF PHILOSOPHY

2015

MAJOR: IMMUNOLOGY & MICROBIOLOGY

Approved by:

_____

Advisor Date

_____

_____

_____

© COPYRIGHT

LISA M. ABERNATHY

2015

All Rights Reserved

DEDICATION

This dissertation is dedicated, in loving memory, to Ian Eric Knox Simpson.

ACKNOWLEDGEMENTS

First and foremost, I would like to express my deep gratitude to my research mentor Dr. Gilda Gali Hillman for her unconditional support that she has offered me from the moment I met her. I aspire to emulate her professional and personal strength, integrity, and passion for family and the pursuit of knowledge. Working under her guidance has been such a pleasure and what I learned from her about life, both inside and outside of the lab, is truly invaluable. She will always have a special place in my heart.

I want to thank my committee members Dr. Wei-Zen Wei, Dr. Harley Tse, and Dr. Michael Joiner for their wonderful guidance. Our meetings were crucial to the development of this dissertation project. I would like to thank Dr. Kang Chen for giving me the opportunity to teach and guiding me in my postdoctoral job search. His vast knowledge of immunology will never cease to amaze me, and I appreciate the time he took to advise me.

I am also grateful to the Immunology & Microbiology department chair Dr. Paul Montgomery and department graduate officer Dr. Thomas Holland. Dr. Holland has always gone above and beyond for me during times of medical emergencies, and I could not have continued in the program unhindered without his creative solutions. Additionally, I would like to express my appreciation to the department office staff Lynette, Nancy, and Mary for always having the answers to our many questions. I would also like to thank all of the Wayne State University School of Medicine graduate and medical students that have become friends over the years.

I have been fortunate enough to meet several talented students that I have had the honor of mentoring in The Hillman Lab. I enjoyed training these students, including Future Docs Shoshana Rothstein, David Hoogstra, as well as the freshly minted Dr. John David. I look

forward to seeing where the future takes these talented upcoming physicians. Also, I would like to thank Chris Yunker, an extremely hardworking technician, for being a helpful constant presence in the lab. Lastly, thank you to Matthew Fountain, you are my lab baby brother. Thank you for always being so quick to help and eager to learn.

I would like to thank all of my beautiful friends that have supported me through this journey with their love. Brittany Koenig Stewart has been particularly supportive during my graduate career. She has this extraordinary ability to bring our loved ones together, whether the times are good or bad. A special thanks to Lois and Tom Gueli and of course, Nona's gravy. Words cannot express my appreciation and adoration for them and their family. I am lucky to be surrounded by such amazing people, and choosing these friends that have become family is my greatest accomplishment.

Finally, I would like to thank my family. My parents Afaf and Tony have been extremely supportive of me every windy step of the way. I hope that bringing up a daughter with a severe chronic disease coupled with relentless ambition has not only been challenging but also rewarding. My mom is no doubt my biggest fan and has an instilled in me a humble self-confidence that I value more and more the older I get, and for that I am forever grateful. My dad fostered a love of science in me before I was even old enough to read, and I am thankful that we can share a special bond over our lifelong intellectual quests. I appreciate my big sister Hana for teaching me to love unconditionally and accept what I cannot control, and my little brother Mark who inspires me every day with his newfound pursuit of education and knowledge. My nephews Adam and Zach have always made me so proud, and I hope I make them proud, too. A very heartfelt thank you to William Close, you are my rock, my fellow graduate student, and so much more to me. I look forward to our future together in science and beyond.

TABLE OF CONTENTS

LIST OF TABLES

LIST OF FIGURES

CHAPTER 1

Introduction

I. Physiological and immune functions of the lung

The lung is an internal organ that is constantly exposed to the external environment. It is also frequently targeted by infectious pathogens. The physiologic function of the lungs are critical for good health and collateral tissue damage is detrimental, which presents an immunologic dilemma for the host. While one of the most crucial functions of the lung is to serve as the organ of gas exchange, it also has a major role in mediating host defense (1).

Breathing (ventilation) is the physiologic aspect of respiration, the means of gas exchange in lungs. Carbon dioxide exchange (CO_2) is produced during the oxidation of food molecules and is exchanged for oxygen (O_2) found in outside air. Fresh air is moved into and out of the airways through the trachea and into the bronchi by convection of the air. Bronchioles terminate into alveoli, where subsequent movement of gases between alveoli and blood in pulmonary capillaries are mediated by the random movement of O_2 and CO_2 molecules from regions of high to low concentrations (2). The pulmonary interstitium contains elastic and collagen fibers that confer the elasticity and structural integrity of lung tissues, and is rich in fibroblasts. The interstitium separates the endothelium and epithelium of pulmonary tissue. The pulmonary interstitium is a supportive structure composed of a thin layer of cells found between alveoli. Growth of this fibrous tissue is responsible for pulmonary fibrosis that results in patients experiencing breathing difficulty. A schematic of mammalian lung anatomy can be found in Figure 1.1.

The lung is an organ that can be divided into two major anatomical compartments: the bronchoalveolar space, clinically and experimentally accessible by lavage, and all else encompassed in the lung tissue (3). Under homeostatic conditions, alveolar macrophages account for up to 95% of all leukocytes in the lungs bronchoalveolar air spaces, vastly out numbering lymphocytes (1-4%) and neutrophils (~1%) (4).

The lung epithelium, including mucus and ciliated epithelial cells that line the bronchi and bronchioles, serves as a physical barrier to protect from environmental insults such as infectious agents and harmful particulate matter (5). Mucus traps potentially damaging particles and transports them by action of the mucociliary escalator that covers the nose, bronchi, and bronchioles. Antimicrobial surfactant proteins are able to opsonize bacteria. Respiratory epithelium is capable of directly sensing pathogens and even releasing cytokines such as interleukin-25 (IL-25), IL-33, and thymic stromal lymphopoietin (TSLP). These innate processes inherent to the lung parenchyma are generally able to maintain the semi-sterility of the lungs without the intervention of the conventional immune system.

The largest population of lung leukocytes at stead state are alveolar macrophages (6), which are the major orchestrators of pulmonary immune and inflammatory responses. These tissue-resident macrophages, also known as dust cells in reference to their function, are located in alveolar spaces and are highly active given their position at an important boundary between inside the body and the outside environment (7). Their role in the non-infected host is to repress the induction of immune responses. Resident alveolar macrophages are constantly encountering inhaled material due to their anatomical position; thus, it is critical to the health of the host that these cells are kept in a relatively quiescent state and have an anti-inflammatory phenotype to prevent collateral damage to the lung parenchyma in response to innocuous antigens and

maintain homeostasis (7). This is apparent by the downregulation of the phagocytic cell membrane receptor CD11b (8), which is a canonical surface marker on most macrophage subsets typically used to identify macrophages. Instead, alveolar macrophages are identified phenotypically by their co-expression of F4/80 and CD11c (9).

Neutrophils play an indispensable role in the innate immune response to lung infection as they are the first cells recruited in injured tissues (10). Intriguingly, the lungs appear to play an immunoprotective role by physical sequestration of activated neutrophils during inflammatory conditions by filtering primed neutrophils from circulation and being a site for de-priming (11). Whether this phenomenon is active or passive remains unknown. Regardless, it is interesting that activated inflammatory cells would enter the lung for deactivation, highlighting the potent anti-inflammatory force of the lung microenvironment.

Dysfunction of immunological processes in the lung results in injury to this organ, which can be detrimental to the host's viability and quality of life.

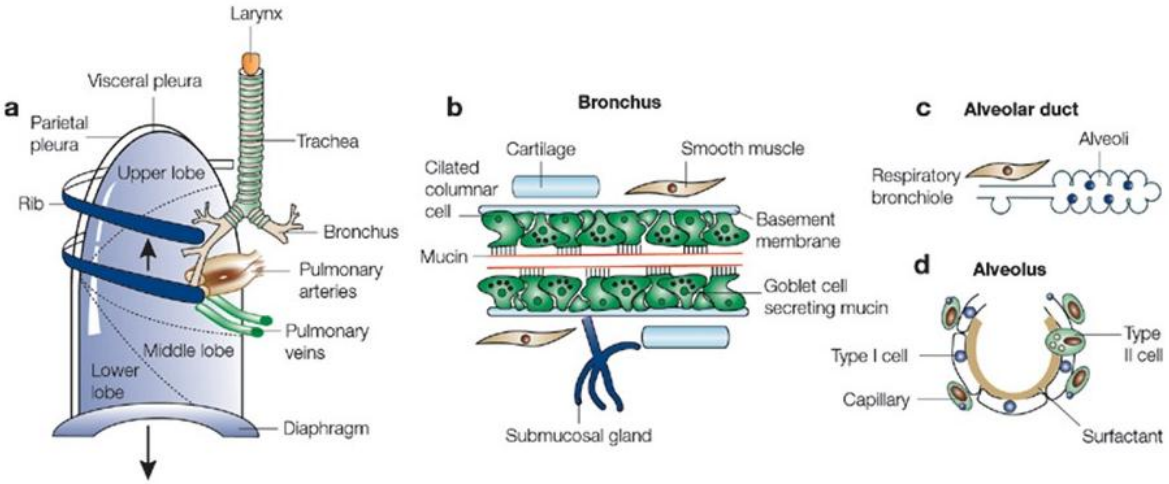

Figure 1.1. Diagram of lung anatomy and cross-sections of bronchi, bronchioles, alveolar ducts, and alveoli. A) Gross anatomy of the lung and thorax. B) Bronchial wall. C) Terminal airway and alveoli. D) Alveolar structure. *Richard M. Effros, Anatomy, development, and physiology of the lungs. GI Motility online (2006)*.

II. Radiation-induced lung injury

A. Adverse effects of radiation therapy for lung cancer. Radiation therapy is defined as the medical use of ionizing radiation to kill malignant cells and control tumor growth. It has become the most important nonsurgical modality for the treatment of cancer, with nearly 1 million people of the approximately 1.4 million who developed cancer receiving treatment with radiation in the United States *(American Society for Therapeutic Radiation Oncology)*. Radiation therapy is advantageous over surgery, being that it is non-invasive and potentially organ preserving. Additionally, radiation therapy is tremendously cost effective, as it only accounts for 5% of the total cost of cancer care (12).

Radiation therapy utilizes ionizing radiation, which causes mitotic cell death followed by tissue repair and remodeling (13). The severity of tissue damage depends on several factors, including radiation dose, quality, fractionation, tissue radiosensitivity, and the repair and repopulation capacity of the organ (14). The degree of radiosensitivity of an organ refers to its relative susceptibility to ionizing radiation (15). The radiosensitivity of a tissue is directly correlated to the proliferative potential of its constituent cells and inversely proportional to the degree of their differentiation. Due to the lack of regenerative capacity, the lung is one of the most radiosensitive normal tissues in the body (16). The high radiosensitivity of the lung parenchyma is the major dose-limiting factor in thoracic radiation therapy.

The therapeutic ratio of radiation therapy refers to the balance between the probability of tumor control or cure and the risk of normal tissue complications. The probability of curing a tumor increases with increasing radiation dose (17). However, it is an unavoidable consequence that normal tissue will be included in the radiation field. Thus, a fundamental and ongoing problem of radiation therapy is that the desired anti-tumor effect is coupled with injury to

surrounding, otherwise normal and healthy tissues (Figure 1.2). One promising strategy to improve the therapeutic ratio of radiation therapy is to administer it in combination with a radiation protector or mitigator, (see *Chapter 1, Section IIE* for current treatments of RILI).

Radiation-induced lung injury (RILI) to normal tissue is a major concern in non-small cell lung cancer (NSCLC). Radiotherapy given concurrently with chemotherapy is the conventional treatment for locally advanced NSCLC presenting as unresectable, stage III disease in approximately 50,000 Americans per year. There is an associated overall 5-year survival rate of 20%, emphasizing the need to improve the efficacy of concurrent chemo-radiotherapy (18, 19). High intensity radiotherapy could be more effective but the therapeutic ratio is limited by lung tissue toxicity.

RILI was first described in 1898, shortly after Wilhelm Röentgen discovered x-rays and Antoine Becquerel discovered radioactivity as various forms of radiation used to treat cancer (20). The distinction between two distinct types of RILI was not made until 1925. Molecular and cellular damage occur immediately after tissue exposure to ionizing radiation, yet the clinical and physiopathological features are often delayed for weeks, months, or years after treatment. RILI leads to compromised lung function, including diffusion and gas exchange, affecting the breathing capacity of patients and their overall quality of life (21-23). Clinically significant RILI occurs in about 30% of patients receiving thoracic irradiation for lung cancer (24), while concurrent chemotherapy increases this incidence (25).

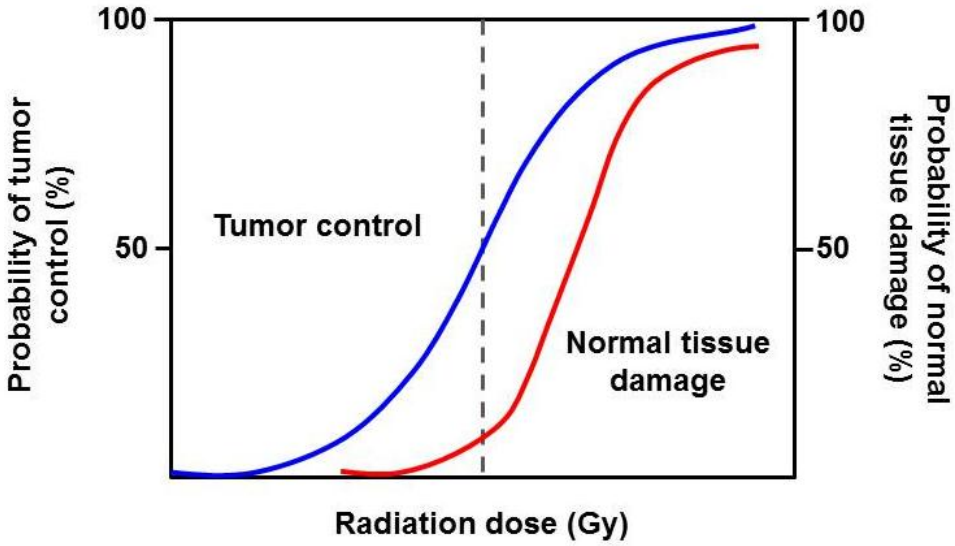

Figure 1.2. Dose-response curve for radiation therapy. Radiation therapy treatment schedules aim to maximize tumor cure while minimizing normal tissue toxicity. The dotted line represents a theoretical dose associated with an optimal therapeutic outcome. The probability of normal tissue damage increases with radiation dose. *Adapted from Barnett, GC et. al. 2009, Joiner, M.C. and Van Der Kogel, A.J. 2009.*

B. Radiation-induced lung injury: Early and late effects. It is important to make a distinction both clinically and biologically between early and late radiation side effects to provide insight towards the development of novel therapeutic interventions. Radiation pneumonitis occurs in the acute phase, within 4-12 weeks after completion of radiation therapy (26). Clinically, patients with pneumonitis present with shortness of breath, chest pain, cough, congestion and fever (27). Radiation fibrosis occurs in the late phase, develops within 6-12 months after the completion of radiation therapy, and can continue to progress for over 2 years before becoming stable (26). Patients may present in the clinic with progressive chronic dyspnea (i.e., difficulty breathing), and radiologic findings which are consistent with lung fibrosis and include lung tissue retraction, pleural thickening, volume loss, and tracheal deviation toward the irradiated region (28). Thus, RILI is classically divided temporally, according to the time of symptom appearance, as either the early, acute inflammatory phase or the late, chronic fibrotic phase. These two distinct yet closely related phases of RILI are characterized by particular histologic lesions and may occur sequentially or independently.

Radiation-induced pneumonitis and fibrosis is driven by a complex process involving an early inflammatory process triggered by damage to lung parenchyma, epithelial cells, vascular endothelial cells and stroma that involves induction of pro-inflammatory cytokines and chemokines which recruit inflammatory immune cells in the lung tissue resulting in pneumonitis and late fibrosis (23, 29, 30). Initially, oxidative injuries after radiation induce expression of pro-inflammatory cytokines. These ensuing cytokines subsequently mediate the recruitment of inflammatory cells into the injured tissue. Infiltrating inflammatory cells are stimulated and activated, producing additional mediators, resulting in a cytokine cascade (31, 32). The expansion and perpetual activation of inflammatory cells, and components of the lung

parenchyma, lead to clinical pneumonitis. Activated cells produce molecular mediators and growth factors that affect the proliferation and gene expression of lung fibroblasts (33). This process leads to increased collagen synthesis and deposition, eventually leading to the development of lung fibrosis.

C. Cellular mediators of radiation-induced lung injury. The lung is composed of approximately 50 distinct cells types (2). Rube *et. al.* first formally proposed a multicellular cross talk hypothesis involving the interaction of a multitude of cells that reside in a given tissue to explain the development and pathogenesis of radiation injury (34). According to this model, all cells in the irradiated lung such as endothelial and epithelial cells as well as inflammatory cells actively contribute to RILI. Alveolar epithelial cells consist of type I and type II pneumocytes (Figure 1.1D). Type I pneumocytes cover more than 90% of the alveolar epithelium surface. Type II pneumocytes secrete surfactant and regulate surface tension. Radiation-induced apoptosis of type I pneumocytes leads to the proliferation of type II pneumocytes, which reduces the regenerative capacity of the alveolar epithelium. In response to radiation-induced injury and inflammatory stress, lung fibroblasts differentiate into myofibroblasts and this turnover contributes to the formation of scar tissue through the generation of collagen, fibronectin, and other ECM components by myofibroblasts (35). Early radiation responses in the lung may be driven by activation or damage of lung epithelial or endothelial cells, while fibroblasts are likely contributors to late radiation fibrotic responses. The interaction of these lung cells with inflammatory cell subsets in the lung after radiation undoubtedly plays an important role in the pathology and progression of RILI.

Studies carried out in immunocompromised mice lacking functional T and B cells demonstrate that radiation pneumonitis and fibrosis occur in the absence of functional

lymphocytes (36), indicating that cells of the adaptive immune system are not required for the induction or promotion of RILI. Rather, innate immune cells appear to be the major contributors to the pathology associated with radiation toxicities in the lung, with a particular emphasis on macrophages.

Given the sheer abundance of macrophages in the lungs in the steady state, it is no surprise that these cells are central players in inflammatory, immunoregulatory, and repair processes. Alveolar macrophages exhibit a great capacity to functionally contribute to pulmonary inflammation and anti-microbial defenses (37). In contrast, interstitial macrophages have been shown to have more immunoregulatory roles in the maintenance of lung homeostasis and during pathologic conditions (38). It is interesting to note that after thoracic irradiation, macrophages are prominently found at inflammatory and fibrotic foci in the lungs (39).

Classically activated M1 macrophages are generated inflammatory cytokines (TNF-α, GM-CSF, IFN-γ) M1 macrophages and mediate acute inflammation, kill intracellular microbes, and participate in Th1 reactions. M2 macrophages can be generated through alternative activation by IL-4, IL-13, IL-10, TGF-β, or immune complexes, and have an immunosuppressive phenotype. M2 macrophages participate in Th2 and Treg reactions (40). M1 macrophages produce NOS2, which generates reactive NO species, thus promoting inflammation. M2 macrophages produce Arg-1, which generates L-orthonine, a precursor of proline, from arginine (41). Proline enhances collagen synthesis, thus promoting tissue repair and resolution of inflammation (42). The M1 phenotype predominates during the acute inflammatory phase, and then switches to M2 during wound-healing phase (43).

Neutrophils possess potent antimicrobial properties and are the first cells to be recruited to sites of inflammation. Neutrophils are known to contribute to acute lung injury (44). However,

a specific role for neutrophils in RILI has been unclear. Myeloperoxidase (MPO) is an abundant constituent of activated neutrophils and its presence in tissues is a marker of neutrophil recruitment (45). Increases in MPO expression and activity have been detected in irradiated lungs (46, 47), suggesting that activated neutrophils contribute to mediating lung damage after thoracic irradiation.

D. Molecular mediators of radiation-induced lung injury. Radiation disrupts endothelial and epithelial cell barrier integrity by interrupting adherens junctions that bind cells together within tissues. E-cadherin is an adhesion molecule expressed on epithelial cells (48). Normal expression of lung E-cadherin is critical for the maintenance of tight junctions between epithelial cells and for maintenance of normal barrier function of airway epithelium. Decreased E-cadherin expression in the lung would be indicative of a disrupted epithelial barrier, which can result in the recruitment of inflammatory cellular and molecular mediators and drive chronic inflammation.

Direct killing of cells by ionizing radiation releases damage-associated molecular patterns (DAMPs) into the extracellular milieu, stimulating an inflammatory response (49). Furthermore, irradiation induces pro-inflammatory and chemotactic cytokine gene expression programs in lung parenchymal cells, including leukocytes, fibroblasts, endothelial, and epithelial cells. These molecular mediators including, IL-1β, IL-6, and TNF-α, can subsequently recruit inflammatory cells to the injured tissue or influence the phenotype of resident leukocyte subsets already present in the lung, stimulating susceptible cells to further produce cytokines. These levels fluctuate over time during the radiation tissue damage response, producing a cyclic cytokine cascade, as observed by cycles of increased and decreased cytokine release (30).

During the process of a normal wound healing response, inflammation after tissue injury is resolved and ECM breakdown products are removed. . In contrast, lung injury induced by radiation leads to lung fibrosis, in which the inflammation is unresolved due to a process akin to an aberrant wound healing response (30, 50). Lung fibrosis that occurs after thoracic radiation is analogous to a "wound that won't heal", since regulatory feedback mechanisms are not observed, resulting in inflammatory cells and myofibroblasts that remain constitutively active. These cells in irradiated tissue therefore are perpetually receiving tissue repair signals.

Fibrogenesis and excessive ECM and collagen deposition are key contributors in the development of late radiation effects and fibrosis in the lung. Fibrosis is an endpoint in response to tissue injury that is characterized by the replacement of normal, functional tissue by collagen-rich matrix (51). Chronic inflammation in the lung can lead to pulmonary fibrosis. Transforming growth factor (TGF-β) is a pleotropic cytokine produced by numerous inflammatory, mesenchymal, and epithelial cells (52, 53). TGF-β has a multitude of functions and has been implicated in the formation of lung fibrosis (54). Several studies showed potential for TGF-β as a serum marker of RILI (55-57); however, their findings were not confirmed by a subsequent prospective study that evaluated plasma TGF-β levels (58). Strategies to target TGF-β for the mitigation of radiation-induced pulmonary toxicity need to be tested prospectively in the clinic to determine if inhibiting this pathway in humans is safe and effective.

E. Limitations of current management of radiation-induced lung injury. Management strategies for RILI can be classified under the following three categories of intervention: protection, mitigation, and treatment (59). Protectors are designed to prevent normal tissue damage and are administered prior to radiation, while mitigators and treatments are given during or after a course of radiation therapy, or after RILI symptoms emerge (60). Despite decades of

research, there is a disproportionately low number of radioprotectors presently in use and they are limited to selected cancers. Several therapies have been investigated to minimize radiotoxicity yet there is currently no known optimal radioprotective therapy for RILI, particularly for the treatment of late fibrosis (22, 61). Limitations include the safety profile of these agents along with the risk of tumor protection from a desired radiation effect.

Prospective controlled studies in humans have not been performed to determine the efficacy of potential therapies for RILI. Steroid therapy is the current treatment for symptomatic patients with subacute onset of RILI, and unfortunately its use is accompanied with extensive side effects (62, 63). Glucocorticoids, antibiotics, or heparin may be administered prophylactically despite a lack of efficacy in reducing the incidence of radiation pneumonitis (24, 25, 62), and symptoms tend to recur when therapy is discontinued. Furthermore, patients with established radiation-induced fibrosis are unlikely to benefit from glucocorticoid therapy (64).

A key feature of wound healing and fibrosis, regardless of the cause, is remodeling of the extracellular matrix (ECM) and excessive deposition of the ECM component collagen (65). Accordingly, therapies that inhibit collagen synthesis such as colchicine, penicillamine, interferon-gamma (IFN-γ), or pirfenidone, were thought to potentially alter the progression of radiation fibrosis. Currently, it is unknown whether drugs that inhibit collagen synthesis and deposition will slow further fibrosis.

Pentoxifylline has been studied as a treatment for radiation fibrosis. It is a methylxanthine derivative that improves microvascular blood flow and inhibits platelet aggregation. In an open label drug trial, the effect of oral pentoxifylline was evaluated in patients with soft tissue post-irradiation fibrosis of the neck, chest wall, pelvis, or extremities (66). Although pentoxifylline has immunomodulatory properties mediated by inhibition of pro-inflammatory cytokines (67),

particularly TNF-α and IL-1 (68, 69), it was found to be ineffective in the treatment of chronic radiation-induced fibrosis. A separate randomized double-blind study of pentoxifylline taken orally 3 times a day concomitantly with radiation therapy showed a modest benefit in the prevention of radiation-induced pulmonary toxicity, in a small sample size of 16 lung cancer patients (70).

Angiotensin converting enzyme (ACE) inhibitors are a class of drugs primarily used to treat hypertension and congestive heart failure by relaxing blood vessels, leading to reduced blood pressure and decreased oxygen demand from the heart (71). Captopril, an ACE inhibitor, reduced radiation-induced lung fibrosis in a preclinical rat model (72). In a retrospective study that included patients that received radiation therapy for lung cancer, ACE inhibitors reduced clinically significant acute radiation pneumonitis compared to matched patients not on ACE inhibitors (73). Prospective studies must follow up to confirm these findings. Whether ACE inhibitors also decrease radiation fibrosis remains to be clinically investigated.

Amifostine, known as WR-2721 or the trade name Ethyol®, is a radioprotector currently being investigated as a therapy to reduce the incidence and severity of radiation pneumonitis in normal tissues. It was first developed by the Anti-Radiation Drug Development Program of the U.S. Army in the 1960's as a potential agent to protect against ionizing radiation exposure (74). Amifostine has been shown to eliminate free radicals in tissues generated by radiation therapy, resulting in cytoprotection, and is currently the only radioprotector in clinical use (61). The results of randomized studies revealed that this drug is particularly promising for radioprotection in patients being treated for head and neck cancers. It is approved for xerostomia (i.e., dry mouth) in patients following head and neck irradiation (75).

Amifostine is an inactive prodrug that is dephosphorylated by alkaline phosphatase in normal endothelium to the active thiol metabolite, WR-1065, which can act as a free radical scavenger. The decreased vascularity of the tumor and the differential expression of alkaline phosphatase in normal versus malignant tissues contribute to the selective cytoprotective effects of amifostine. In a study evaluating a protective role of amifostine for pulmonary toxicities in patients with stage II or III NSCLC receiving concurrent chemoradiotherapy, amifostine significantly reduced acute pneumonitis in patients receiving radiation therapy (23% vs 3.7%, p=0.037) (76). Unfortunately, disadvantages of amifostine include the need for daily intravenous infusions, prohibitive price, and associated systemic effects such as severe nausea and vomiting which resulted in treatment discontinuation in over 20% of patients enrolled in a phase III randomized trial in head and neck cancer (77).

Understanding the cellular and molecular mechanisms of the inflammatory processes involved in RILI may lead to the development of more effective prophylactic and therapeutic interventions.

III. Soy isoflavones

A. Beneficial properties of soy. Plant-based foods are a multifaceted assortment of chemicals, including both nutrients and biologically active compounds that are nonnutrients (78). The latter are referred to as nutraceuticals or phytochemicals. There are records of soy use in China that date back to the eleventh century B.C., although the plant did not reach Europe and the United States until the 18th century *(National Cancer Institute)*. The soybean is a versatile plant that can be processed into a variety of products for dietary consumption including soy milk, miso, tofu, soy flour, and soy oil (79). Soy foods contain many phytochemicals that may have health benefits, including phytic acid, sterols, saponins, isoflavones, and lignans (80). Among these, soy isoflavones have been the significant focus of research due to their possession of a plethora of biological activities including anti-inflammatory, antioxidant, chemopreventative, and antitumor effects.

Isoflavones are always present in significant amounts in soybeans and serve an important physiologic function for the host. Isoflavones in soybean plants promote infection of plant roots by beneficial, mutualistic soil bacteria (81). Soy isoflavones facilitate a symbiotic relationship between soybean and *Rhizobium* bacteria by inducing the transcription of nodulation genes expressed in the *Rhizobium* bacteria. This results in the rhizobia inducing the formation of nodules on roots of soybean plants (82). Rhizobia also fix nitrogen which the plant can then use for growth.

Soy isoflavones are known as phytoestrogens due to their similarity in structure to the human female hormone 17-β-estradiol, and their ability to bind estrogen receptors *in vitro* and induced estrogen-like effects *in vivo* (83). However, phytoestrogens have relatively weak estrogen activity compared to animal estrogens (84), and isoflavones have a greater affinity for

estrogen receptor beta (ER-β) than for estrogen receptor alpha (ER-α) (85). Phytoestrogens such as soy isoflavones can also have estrogen receptor antagonist activity by interacting with and blocking binding sites from endogenous estrogen (86). Their mode of biological action involve both ER-dependent and ER-independent mechanisms. Genistein is the most abundant and bioactive soy isoflavone (87). Other isoflavones found in soybeans include daidzein and glycitein. Isofavones are also beneficial to the soybean plant as a survival mechanism during times of stress due to the antioxidant, antimicrobial, and antifungal properties of these phytoestrogens (88).

The combined effect of multiple isoflavones in preventing or treating cancer compared to that of a single isoflavones has been investigated in preclinical studies, by our group and others, indicating that administering mixtures of isoflavones increases effectiveness of the individual compounds (89, 90). Isoflavones act as chemopreventative agents as suggested by epidemiological studies (91-93), and a high-soy diet is associated with a decreased risk of prostate cancer (94-96).

B. Molecular structures and metabolism. Soy isoflavones are diphenolic compounds that share a structural similarity to estrogen, as presented in Figure 1.3 (adapted from (97) and (98)). These compounds possess a variety of biological activities including the ability to act as an antioxidant. Genistein, in particular, is a potent tyrosine-specific kinase inhibitor (99). This leads to its chemoprotectant activities against chronic inflammatory disorders, cancers, and cardiovascular disease.

Isoflavones are present in soybeans primarily as β-glucosides, their inactive form, becoming active in the plant when the sugar molecule is cleaved. Soy isoflavones are quite heat-stable, thus cooking soy foods does not change the total isoflavone content or nutraceutical value

(100). Glycosidic isoflavones are not readily bioavailable in humans due to the sugar-binding moiety that prevents their crossing through enterocytes, and hydrolysis is required for gut absorption and bioavailability. After oral uptake, isoflavones are unconjugated and absorbed by the gastrointestinal tract, and can be detected in plasma as soon as 30 minutes after the consumption of soy products (101). Intestinal β-glucosidases catalyze hydrolysis of the sugar moiety and the gut microflora metabolize the aglycones (102). Unconjugated aglycones are produced after hydrolysis, which can be further metabolized into p-ethyphenol (from genistein) and equol (from daidzein). During metabolism, formononetin and biochanin A are demethylated to daidzein and genistein, respectively (Figure 1.3). The resulting metabolite levels can differ to a great extent and depend on the individual microflora. The majority of the absorbed aglycones are immediately re-conjugated and have two possible fates: enter circulation to be available to the body or return to the intestinal lumen through the portal circulation to be absorbed in the large intestine (103). Conjugated isoflavones are no longer functional or bioactive. Only 1% of the isoflavones in human plasma are circulating in the active, aglycone form; they are predominantly inactive glucuronides (75%) and sulfates (24%), named in reference to their conjugates. Isoflavone levels in plasma reach a maximum concentration by 6 hours following soy product consumption (101). Once these compounds are in the body they are re-conjugated to glucuronides and excreted in the urine.

Levels of serum isoflavones in our murine studies following treatment with 1 mg/day of a mixture of soy isoflavones reflected typical *in vivo* metabolism with significant levels of daidzein (1.6 μM) and genistein (1.7 μM) (90). These levels are comparable to plasma concentrations of 1–4 μM soy isoflavones measured in Asian populations consuming foods rich in soy isoflavones, in contrast to levels of 10-30 nM found in Western populations (36).

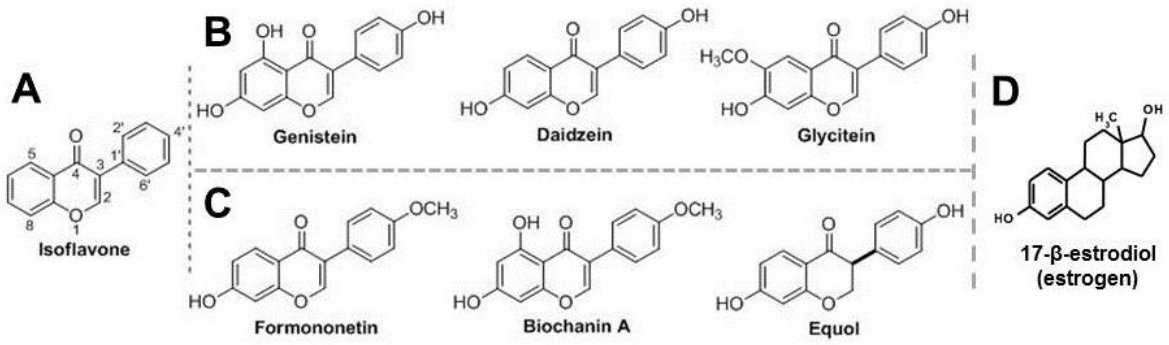

Figure 1.3. Molecular structures of soy isoflavones and endogenous 17-β-estradiol (estrogen). (A). Structure of isoflavone backbone. (B). The major isoflavones in soybean are genistein (50%), daidzein (40%), and glycitein (10%). (C). Biochanin A and formononetin are derivatives of genistein and daidzein, respectively. Equol is a breakdown product of daidzein, however only ~30-50% of people have the intestinal microbiota to produce equol. (D). Structure of the primary female sex hormone, estrogen. Adapted from Kurosu 2011 (97) and Day *et. al.* 2002 (98).

C. Soy isoflavones and the immune system. The most extensively studied isoflavone in respect to effects on the immune system is genistein, which was shown to regulate immune function (104). Genistein has been shown to have strong immune modulatory effects on macrophages, via inhibition of the production of TNF-α (105). Genistein may also downregulate cytokine-induced pro-inflammatory pathways in human brain microvascular endothelial cells (106), and soy isoflavones have been shown to have anti-inflammatory mechanism via modulation of leukocyte-endothelial cell interactions in a study of atherosclerosis (107).

Nuclear factor κB (NF-κB) activation is a molecular common denominator between inflammation and cancer (108). This transcription factor is constitutively active in a large number of cancers and is critical for tumor cell survival. Our lab has previously shown in tumor cells that soy isoflavones target critical survival pathways that are upregulated and constitutively activated in cancer cells, including NF-κB, which are responsible for the transcription (109). In contrast, normal cells do not constitutively express activated NF-κB, and activation of this transcription factor is important for the expression of pro-inflammatory gene programs. Differential expression of soy isoflavones targets in tumor cells versus normal cells is a potential mechanism of specificity for soy effects in cancer models.

D. Controversy associated with the use of phytoestrogens. Soy isoflavone intake among people in the Western world (0.15-1.7 mg per day) (110-112) is about 100-fold less than that of Asians (15-50 mg per day) (113-116). The incidence of breast and prostate cancers is lower among Asians compared to people in the Western world (117), thus soy consumption appears to be related to the decreased risk of cancer recurrence and/or mortality.

The first report linking isoflavones and cancer was almost 30 years ago when it was shown that genistein is a potent inhibitor of multiple protein tyrosine kinases relevant to cancer

cell growth and proliferation (118). The use of soy isoflavones in patients with or at risk of developing breast cancer was proposed when they were shown to inhibit the proliferation of several types of cancer cells (119).

Interest in isoflavone metabolism was piqued when it was realized that phytoestrogens are capable of disrupting normal endocrine function and their estrogenic properties were connected to infertility in animals (120, 121). A well-documented incident involves an outbreak of infertility in sheep in Australia that were grazing red clover that contained a high percentage of the isoflavone formononetin, which was being metabolized into equol by intestinal bacteria (122). When these sheep were switched to a genetically modified clover lacking isoflavones the infertility was ameliorated. Interestingly, it has been hypothesized that phytoestrogens may have evolved in plants as a protective mechanism by interfering with reproduction of grazing animals (97). Despite the detrimental effects of soy isoflavones reported in animal fertility, the effects of isoflavones on human reproductive function have not been sufficiently identified. An explanation for this discrepancy may lie in the vast difference in isoflavone exposure between animals and humans. The amount of isoflavones in the clovers consumed by the Australian sheep that caused their infertility was estimated to be about 20-100 g per day, which is up to 2000-fold higher than the amount of isoflavones achievable by humans consuming a high soy isoflavone diet (15-50 mg per day) (123, 124). Therefore, it is not likely that humans on a diet with a typical soy intake will achieve comparable levels of biologically active isoflavones to impact fertility, despite the ability of phytoestrogens to disrupt the endocrine system in animals and cause infertility.

There have been numerous prospective epidemiologic statues that have evaluated the impact of soy intake on the prognosis of breast cancer survivors after diagnosis (Table 1) (125-131). A recent meta-analysis of 35 studies in pre- and/or post-menopausal women reporting an

association between soy isoflavones intake and breast cancer risk found that there is indeed no harmful association between intake of soy isoflavones and breast cancer (132). Taken together, the overwhelming evidence to date suggests that soy foods are not harmful for breast cancer survivors to consume. There is no evidence-based basis for advising breast cancer patients against the consumption of soy foods, further supporting the safety of soy isoflavones.

Study	Location	Follow up (years)	(N)	Age (range or mean)	ER+ / ER-	Tamoxifen use (yes / no)	Median isoflavones intake (mg/d)
Boyapati *et. al*. 2005	China	5.5	1,459	25 - 64	383 / 142	Not reported	Not reported
Guha *et. al.* 2009	USA	6.3	1,954	18 - 79	1,594 / 337	1,443 / 410	Not reported
Shu *et. al.* 2009	China	3.9	5,033	20 - 75	3,181 / 1,772	2,622 / 2,408	47
Kang *et. al.* 2010	China	5.1	524	Not reported	447 / 77	438 / 0	25.6
Caan *et. al.* 2011	USA	7.3	2,763	18 - 70	Not reported	1,816 / 920	0.23
Woo *et. al.* 2012	Korea	2.7	339	25 - 77	Not reported	195 / 144	~13
Zhang *et. al.* 2012	China	4.3	616	45.7 ± 6.2	378 / 238	350 / 266	17.3

Table 1. Description of epidemiologic studies evaluating the effects of soy intake on breast cancer prognosis. Prospective studies in different countries have evaluated the impact of post-diagnosis soy intake on the prognosis of breast cancer survivors and have overwhelmingly concluded that soy isoflavones consumption in breast cancer survivors is safe, and even beneficial in some instances. Table adapted from *Messina et. al. It's Time for Clinicians to Reconsider Their Proscription Against the Use of Soyfoods by Breast Cancer Patients. Oncology (2013)* (133).

E. Soy isoflavones for the treatment of radiation injury. We have previously demonstrated in mice receiving a single high dose of thoracic irradiation (Figure 1.4) that soy isoflavones have the dual capability of protecting normal lung tissue from radiation injury while simultaneously enhancing radiation damage in the tumor (36, 134, 135). In a pre-clinical lung cancer model, supplementation with a mixture of soy isoflavones (genistein, daidzein, and glycitein) given pre- and post-thoracic irradiation mitigated the vascular damage, inflammation and fibrosis caused by high dose radiation injury to lung tissue suggesting that soy can alter the radiation-induced inflammatory response (36, 134). In naïve mice, soy protected the lungs against adverse effects of radiation including skin injury, hair loss, increased breathing rates, inflammation, pneumonitis and fibrosis (135). The soy isoflavone genistein and the superoxide dismutase mimetic EUK-207 were observed to mitigate radiation-induced lung damage in naïve rats. These compounds inhibited late occurring pulmonary fibrosis and reduced levels of activated macrophages and TGF-β1 expression (136).

These outcomes in naïve mice corroborated our findings in lung tumor models and provided further evidence for a radioprotective effect of soy isoflavones. It is important to note that soy isoflavones also sensitized cancer cells to radiation both *in vivo* and *in vitro* in pre-clinical tumor models of lung cancer, demonstrating a differential effect of radioenhancement on lung tumors with simultaneous radioprotection of normal lung tissue (36, 134, 137).

In support of a clinical application of soy isoflavones for radioprotection in lung cancer, the use of soy isoflavones as radioprotectors was found to be safe in human clinical trials (138). Prostate cancer patients receiving radiation therapy and soy tablets had reduced radiation toxicity and resulted in improved urinary, sexual and gastrointestinal functions (139). These findings suggest that soy isoflavones used as a complementary intervention to radiotherapy for lung

cancer could potentially reduce lung toxicity and provide improved therapeutic benefit to patients. While the anti-oxidant and disease preventative effects of a soy-rich diet have been investigated, an immune-mediated mechanism of radioprotection by soy isoflavones in normal tissues remains to be elucidated.

Alteration of the host immune response by radiation therapy through the triggering of a potent inflammatory response is a key contributor to the tissue-damaging pathology of RILI. Soy isoflavones may inhibit this inflammatory process or promote tissue repair. The research objective of this dissertation is to investigate radioprotection mediated by soy isoflavones in normal lung tissue by dissecting the radiation-induced inflammatory response (Figure 1.5). The clinical goal is to improve the therapeutic ratio of high-dose radiation therapy on the tumor target and reduce the radiation dose-limiting toxicity of radiation therapy to the normal lung.

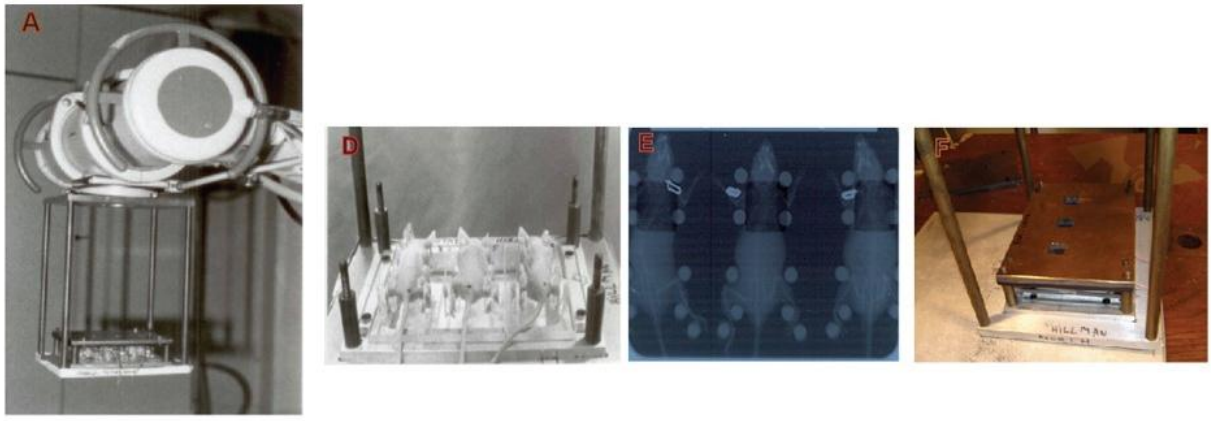

Figure 1.4. Selective delivery of high-dose radiation therapy to lungs. Radiation is delivered to the thoracic cage comprising the whole lung. Three anesthetized mice, in jigs, are positioned under a 6.4 mm lead shield with 3 cut-outs in an aluminum frame mounted on the X-ray machine to permit selective irradiation of the lung in 3 mice at a time, as previously described (134). The radiation dose to the lung and the scattered dose to areas of the mouse outside of the radiation field are carefully monitored. To minimize backscattering of radiation, the bottom of the aluminum frame that holds the jigs was hollowed out and the backplate of the jig was thinned to 1.6mm thickness. Under these conditions and the lead shielding, the X ray dose to the shielded regions was reduced to 1% of the dose to the irradiated field. The dose rate was 101 cGy/min and half value layer was 2 mm Cu. Photon irradiation was performed at a dose of 10 Gy with a Siemens Stabilipan X-ray set (Siemens Medical Systems, Inc., Erlangen, Germany) operated at 250 kV, 15 mA with 1 mm copper filtration at a distance of 47.5 cm from the target.

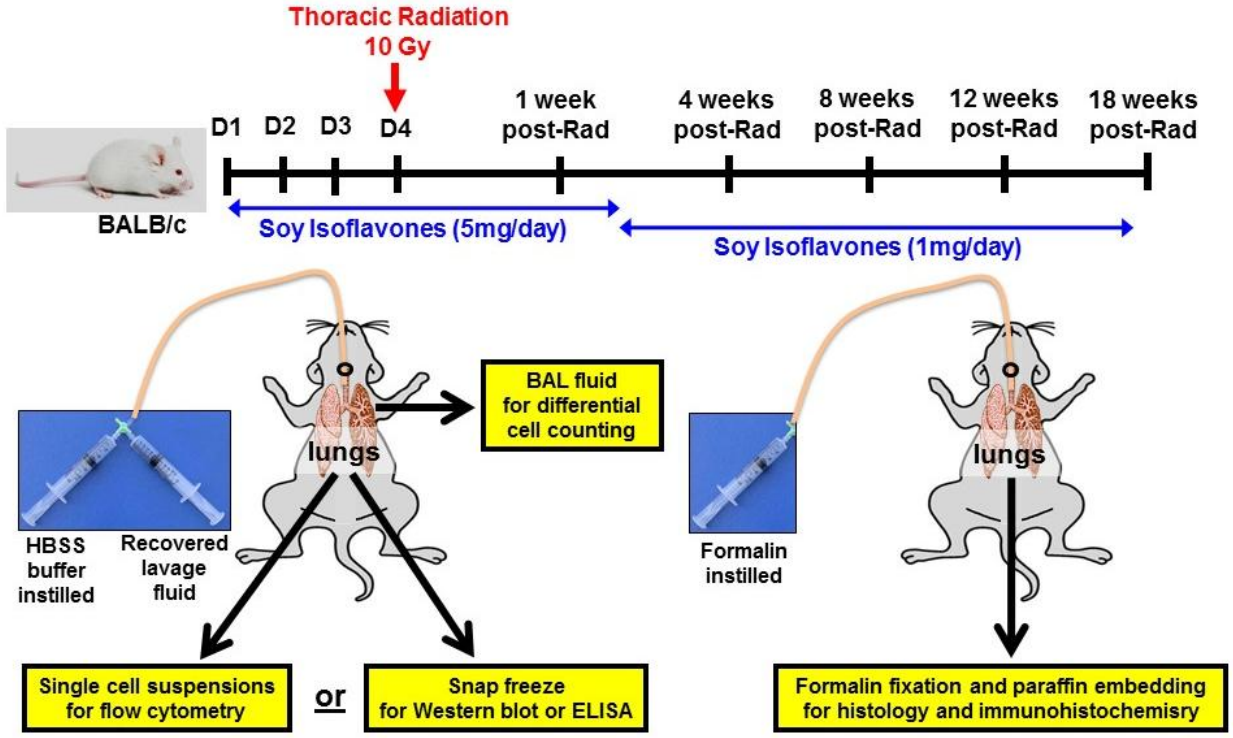

Figure 1.5. Experimental design and treatment strategy. Mice were pre-treated with oral soy isoflavones each day for 3 days at a dose of 5mg/day (equivalent to 250mg/kg). Then, the lung was selectively irradiated with 10 Gy. Soy treatment was continued on a daily basis for 5 more days at 5mg/day. Then mice were treated with a lower soy dose of 1mg/day (equivalent to 50mg/kg), given daily 5 days a week for up to 18 weeks. The rationale for giving a higher dose of soy isoflavones for pre-treatment and just after radiation is to optimize the effect of soy, based on previous studies (36, 140). At different time points after radiation, separate mice from each treatment group were either processed for flow cytometry studies or homogenized for ELISA, snap frozen for western blot, or mice were used to fix lungs *in situ* with formalin for histology studies.

CHAPTER 2

Soy Isoflavones Promote Radioprotection of Normal Lung Tissue by Inhibition of Radiation-Induced Activation of Macrophages and Neutrophils

ABSTRACT

Thoracic radiotherapy for the treatment of lung cancer is limited by morbidity-associated toxicities. Normal lung tissue damage after radiation therapy results from a chronic inflammatory response, leading to pneumonitis and fibrosis. Soy isoflavones mitigate inflammatory infiltrates and radiation-induced lung injury, but the cellular inflammatory mediators altered during radioprotection are unknown. Oral treatment with a mixture of soy isoflavones (genistein, daidzein, and glycitein) before and after administration of a high dose thoracic radiation at 10 Gy led to a reduction in infiltration and activation of alveolar macrophages and neutrophils in both the bronchoalveolar and lung parenchyma compartments. Soy treatment protected $F4/80^{+}CD11c^{-}$ interstitial macrophages which are known to play a regulatory role in inflammation and are decreased by radiation. Furthermore, soy isoflavones reduced the levels of nitric oxide synthase-2 (NOS2) expression but increased arginase-1 (Arg-1) expression in the lung parenchyma after radiation, suggesting a switch from pro-inflammatory M1 macrophage to an anti-inflammatory M2 macrophage phenotype. Soy also prevented the influx of activated neutrophils in lung caused by radiation. The modulation of macrophage and neutrophil responses to radiation by soy isoflavones could play a role in the resolution of radiation-induced chronic inflammation in the lung.

INTRODUCTION

Radiation pneumonitis is caused by an early inflammatory process triggered by damage to lung parenchyma, epithelial cells, vascular endothelial cells and stroma. This process involves induction of pro-inflammatory cytokines and chemokines which recruit inflammatory immune cells to the lung tissue resulting in pneumonitis and late fibrosis (29, 30, 141). Early acute pneumonitis occurs by 2-4 months after radiotherapy, while late chronic pneumonitis manifests clinically over 6-24 months (21, 23). At late stages, radiation-induced pulmonary fibrosis results from aberrant resolution of inflammation in contrast to classical wound healing processes (30). These adverse events after radiotherapy affect patients' breathing and their quality of life. Various strategies to decrease the extent of pneumonitis have been investigated but need further research efforts (142).

We have reported in preclinical mouse models that supplementation of soy isoflavones with thoracic irradiation mitigates radiation-induced inflammatory cytokines, infiltration of inflammatory cells and fibrosis (36, 134, 135), but the cellular mediators of radioprotection remain unclear. In Chapter 2, we investigate the role of macrophages and neutrophils in the mitigation of radiation-induced inflammatory events by soy isoflavones in lung tissue. Macrophages are recruited as a first response to radiation-induced damage in the tumor microenvironment or in normal tissues (143). Macrophages play distinct roles in the early versus late stages of inflammatory response (144-146). Monocytes can differentiate into functionally different macrophage subsets. Inflammatory cytokines (TNF-α, GM-CSF, IFN-γ) generate classically activated M1 macrophages that mediate acute inflammation and participate in Th1 reactions (40). M2 macrophages can be activated by IL-4, IL-13, IL-10, TGF-β, or immune

complexes, participate in Th2 and Treg reactions, and promote tumor growth and fibrosis (43, 147). M1 predominates during acute inflammation, and then switches to M2 during the wound-healing phase at later stages (43). We tested whether soy influences macrophage skewing to M1 or M2 subsets, and if this altering of macrophage phenotypes could dictate normal lung response to radiation-induced damage.

Activation and infiltration of neutrophils is a hallmark event in the progression of acute lung injury (44), and have been shown to be involved in radiation-induced alveolitis (46). Therefore, the effect of soy isoflavones on infiltration and activation status of neutrophils was studied after radiation to the lungs. Our findings suggest that soy can inhibit the infiltration and activation of macrophages and neutrophils induced by radiation in lung parenchyma. Radiation induced a pro-inflammatory M1 macrophage phenotype in lungs, while mice receiving soy isoflavones and radiation switched to an anti-inflammatory M2 macrophage subtype. These data indicate that soy isoflavones modulate the cellular mediators of the inflammatory response induced by radiation.

MATERIALS AND METHODS

Mice

Female BALB/c mice (Harlan, Indianapolis, IN) 5-6 weeks old, were housed and handled in animal facilities accredited by the Association for Assessment and Accreditation of Laboratory Animal Care. The animal protocol was approved by Wayne State University Institutional Animal Care and Use Committee.

Soy isoflavones

The soy isoflavone mixture G-4660 used is a pure extract of 98.16% isoflavones from soybeans consisting of 83.3% genistein, 14.6% daidzein and 0.26% glycitein (manufactured by Organic Technologies and obtained from the National Institutes of Health [NIH], Bethesda, MD). The soy isoflavone mixture was dissolved in DMSO and mixed with sesame seed oil at a 1:20 ratio just prior to treatment to facilitate gavage and avoid irritation of the esophagus by DMSO (36, 134, 135).

Lung irradiation

Radiation was delivered to the thoracic cage comprising the whole lung. Three anesthetized mice, in jigs, were positioned under a 6.4 mm lead shield with 3 cut-outs in an aluminum frame mounted on the X-ray machine to permit selective irradiation of the lung in 3 mice at a time, as previously described (134). The radiation dose to the lung and the scattered dose to areas of the mouse outside of the radiation field were carefully monitored. To minimize backscattering of radiation, the bottom of the aluminum frame that holds the jigs was hollowed

out and the backplate of the jig was thinned to 1.6mm thickness. Under these conditions and the lead shielding, the X ray dose to the shielded regions was reduced to 1% of the dose to the irradiated field. The dose rate was 101 cGy/min and half value layer was 2 mm Cu. Photon irradiation was performed at a dose of 10 Gy with a Siemens Stabilipan X-ray set (Siemens Medical Systems, Inc., Erlangen, Germany) operated at 250 kV, 15 mA with 1 mm copper filtration at a distance of 47.5 cm from the target.

Experimental design

Mice were pre-treated with oral soy isoflavones each day for 3 days at a dose of 5mg/day (equivalent to 250mg/kg). Then, the lung was selectively irradiated with 10 Gy. Soy treatment was continued on a daily basis for 5 more days at 5mg/day. Then mice were treated with a lower soy dose of 1mg/day (equivalent to 50mg/kg), given daily 5 days a week for up to 18 weeks. The rationale for giving a higher dose of soy isoflavones for pre-treatment and just after radiation is to optimize the effect of soy, based on previous studies (36, 140). At different time points, separate mice from each treatment group were either processed to harvest bronchoalveolar lavage (BAL) fluid for differential cell counting and lungs for flow cytometry studies or snap frozen for western blot, or mice were used to fix lungs *in situ* with formalin for histology studies as detailed below.

Analysis of immune cells by differential cell counting in BAL fluid and flow cytometry on single-cell suspension from lungs

BAL was performed prior to lung resection at 1, 8, 12, and 18 weeks after irradiation. To obtain BAL fluid, phosphate-buffered saline (PBS) was gently instilled into the lungs and

withdrawn through an incision of the trachea. The BAL fluid samples were centrifuged at 1500 rpm for 5 minutes at 4° C and supernatant was discarded. Cells were resuspended in media and loaded onto slides using a cytospin centrifuge (Cytospin 3 Cell Preparation System, Thermo Shandon, UK). Cell preparations were stained using a DiffQuik staining kit (IMEB Inc., San Marcos, CA,) and differential cell counts of leukocyte subsets were performed by counting at least 300 nucleated cells (148).

Following collection of BAL fluids, the same mice provided the lungs for flow cytometry studies. Lungs were excised, minced, and digested with 0.4 mg/mL collagenase IV for 45 minutes at 37° C. Digested lungs were passed through a wire mesh, then a 0.7 μm nylon mesh. Red blood cells were removed by incubating in red blood cell lysis buffer for 2 minutes at room temperature. Single-cell suspensions obtained from the lungs were incubated with Fc receptor-blocking antibody (eBioscience, San Diego, CA) prior to staining to reduce non-specific binding. For morphological characterization of lung leukocytes, cells expressing the pan-leukocyte marker CD45 were sorted by fluorescence-activated cell sorting (FACS) using a BD FACSVantage SE (BD Biosciences). $CD45^+$ cell subsets were gated according to cell size [forward scatter (FSC), x-axis] and granularity [side scatter (SSC), y-axis]. Cell subsets obtained from each gate were spun onto slides using a cytospin (Thermo Shandon, Pittsburgh, PA), and stained using a DiffQuik staining kit (IMEB Inc., San Marcos, CA). To determine the phenotype of immune cells, cells were immunostained using a 5-color fluorophore combination of fluorescent antibodies consisting of CD45-APC, CD11b-FITC, F4/80-PE, CD11c-APC-eFluor780, and Ly6G-PerCp-Cy5.5 (eBioscience). Fixable viability dye eFluor 450 (eBioscience) was used to exclude dead cells from analysis. Cells were analyzed by flow cytometry using a BD LSR II flow cytometer (BD Biosciences, San Jose, CA) in the

Microscopy, Imaging and Cytometry Resources Core at Wayne State University School of Medicine, followed by analysis on FlowJo v10 software (Tree Star Inc., Ashland, OR).

Immunohistochemistry (IHC)

Mice were sacrificed and lungs were intratracheally instilled with 10% buffered formalin and resected, embedded in paraffin, and sectioned. Sections were blocked with IHC Tek Antibody Diluent (IHC World, Woodstock, MD) then incubated with primary purified monoclonal antibodies directed against F4/80, nitric oxide synthase 2 (NOS2), arginase-1 (Arg-1), Gr-1 (Ly6C/Ly6G), and myeloperoxidase (MPO) (Abcam, Cambridge, UK) overnight at 4° C. Lung sections were then incubated with biotinylated secondary antibodies (Vector Labs, Burlingame, CA) at 1:300 for 1 hour at room temperature. Staining was amplified with the avidin-biotin system Vectastain ABC Reagent Kit (Vector Labs) and visualized with the Vector DAB Substrate Kit for peroxidase (Vector Labs). Sections were counterstained with IHC-Tek Mayer's Hematoxylin (IHC World, Woodstock, MD) and mounted with Permount mounting media (Electron Microscopy Sciences, Hatfield, PA). Macrophage and neutrophil infiltrations in the lung tissue after radiation were evaluated on a Nikon E800 microscope (Nikon Inc., Melville, NY). Quantitation of the number of $F4/80^{+}$ alveolar macrophages and measurement of the cell areas were performed using ImageJ software (NIH, Bethesda, MD) in 10 fields of 40x per slide. For quantitation of overall level of staining, whole slide imaging was performed using a slide scanner and DensitoQuant analysis (3D Histech). The percentage of positive area was calculated as the total number of positive pixels divided by total number of pixels.

Preparation of lung tissue protein lysates and western blot analysis

Mice were sacrificed at 12 weeks post-irradiation. Lungs were resected and snap frozen. To prepare lung tissue protein lysates, frozen lungs were thawed, weighed, and homogenized in 10% w/v of lysis buffer using a gentleMACS tissue dissociator (Miltenyi Biotec, Bergisch, Germany). The suspension was centrifuged at 4000 x g for 5 minutes at 4°C and the protein extracts were frozen at -80°C until analysis. For western blot analysis, total lung protein extracts (50 μg) were loaded and separated on 10% sodium dodecyl sulfate polyacrylamide gel electrophoresis (SDS-PAGE) and transferred to Whatman membranes (GE Healthcare Life Sciences, Pittsburgh, PA). Membranes were incubated with anti-myeloperoxidase (MPO) antibody (Abcam, Cambridge, MA; 1:1000) overnight at 4°C. Membranes were washed and incubated with horseradish peroxidase-conjugated secondary antibody (Vector Labs, 1:2000) at room temperature for 1 hour. Immunoreactive protein bands were visualized by SuperSignal West Pico Chemiluminescent Substrate (Thermo Scientific, Waltham, MA) and captured on a digital imaging system (Fotodyne Inc., Hartland, WI). Membranes were re-probed with anti-β-actin Ab as a loading control (137).

Statistical analysis

Data are expressed as mean ± SEM. Comparisons between means of two treatment groups were analyzed by two-tailed unpaired Student's t test using GraphPad Prism version 6.0 software (GraphPad Software Inc., San Diego, CA). A value of $p<0.05$ was considered statistically significant.

RESULTS

Effect of radiation and soy isoflavones on immune cell subsets recovered from bronchoalveolar space. We previously demonstrated that soy isoflavones decreased the extent of inflammatory infiltrates induced by radiation in lung tissues (36, 134, 135). To identify the nature of inflammatory infiltrates in lungs induced by radiation and the effect of soy isoflavones on these cells, we first analyzed immune cell subsets recovered from bronchoalveolar lavage (BAL) (148). Mice were pre-treated with soy isoflavones for 3 days, and then received 10 Gy irradiation administered to the whole lung. Soy treatment was continued for 5 days/week for up to 18 weeks and BAL fluids were harvested at early and late time points post-radiation, including 1, 8, 12 and 18 weeks after radiation. Differential cell counts to identify the morphology of immune cells were performed and the percentages of macrophages, neutrophils, and lymphocytes were calculated (Figure 2.1). Activated macrophages presented a morphology of enlarged foamy cells (Figure 2.1A, inset) that was clearly distinct from non-activated small macrophages and were counted separately. Alveolar macrophages constituted 80% to 90% of cells recovered from BAL fluids, and the majority presented as small non-activated macrophages in control BAL (Figure 2.1). Soy did not alter the morphology of these macrophages. In contrast, as early as one week after radiation, there was a significant decrease from 90.7±0.8% to 24.1±2.9% in small macrophages compared to control ($p<0.0001$) with a concomitant significant increase from 9.1±0.7% to 75.8±3.0% in enlarged foamy activated macrophages ($p<0.0001$) (Figure 2.1A). This trend was consistently observed at later time points of 8, 12 and 18 weeks after radiation (Figure 2.1B, C, D). The ratios of activated versus non-activated macrophages were reversed in BAL fluids from mice treated with radiation and soy. There was a significant

increase in non-activated macrophages associated with a concomitant decrease in activated enlarged foamy macrophages ($p<0.01$) that was consistently observed at 8, 12 and 18 weeks after radiation and these ratios were comparable to the levels of control mice or mice treated with soy alone. For example, at 18 weeks after radiation, there was a significant increase in the percentage of enlarged, foamy macrophages to 79.0±6.7% compared with 14.6±5.3% in control ($p=0.0003$) (Figure 2.1D). Soy significantly inhibited this radiation-induced increase to 33.1±8.3% compared with radiation alone ($p=0.0091$) (Figure 2.1D). These data demonstrate that radiation induced a rapid activation of macrophages that persisted for a long time as shown at 18 weeks. It should be noted that soy consistently inhibited this activation of macrophages over time and the macrophage morphology presented as small non-activated macrophages.

Whereas BAL fluids from healthy untreated mice have undetectable numbers of neutrophils and lymphocytes, neutrophil counts showed a significant increase induced by radiation at 12 weeks (19.0±2.1%, $p<0.0001$) which was decreased in radiation and soy isoflavones-treated mice (8.4±3.2%, $p<0.05$) (Figure 2.1C). A measurable increase in BAL lymphocytes was also observed after radiation; however, this increase was not seen in radiation and soy-treated mice.

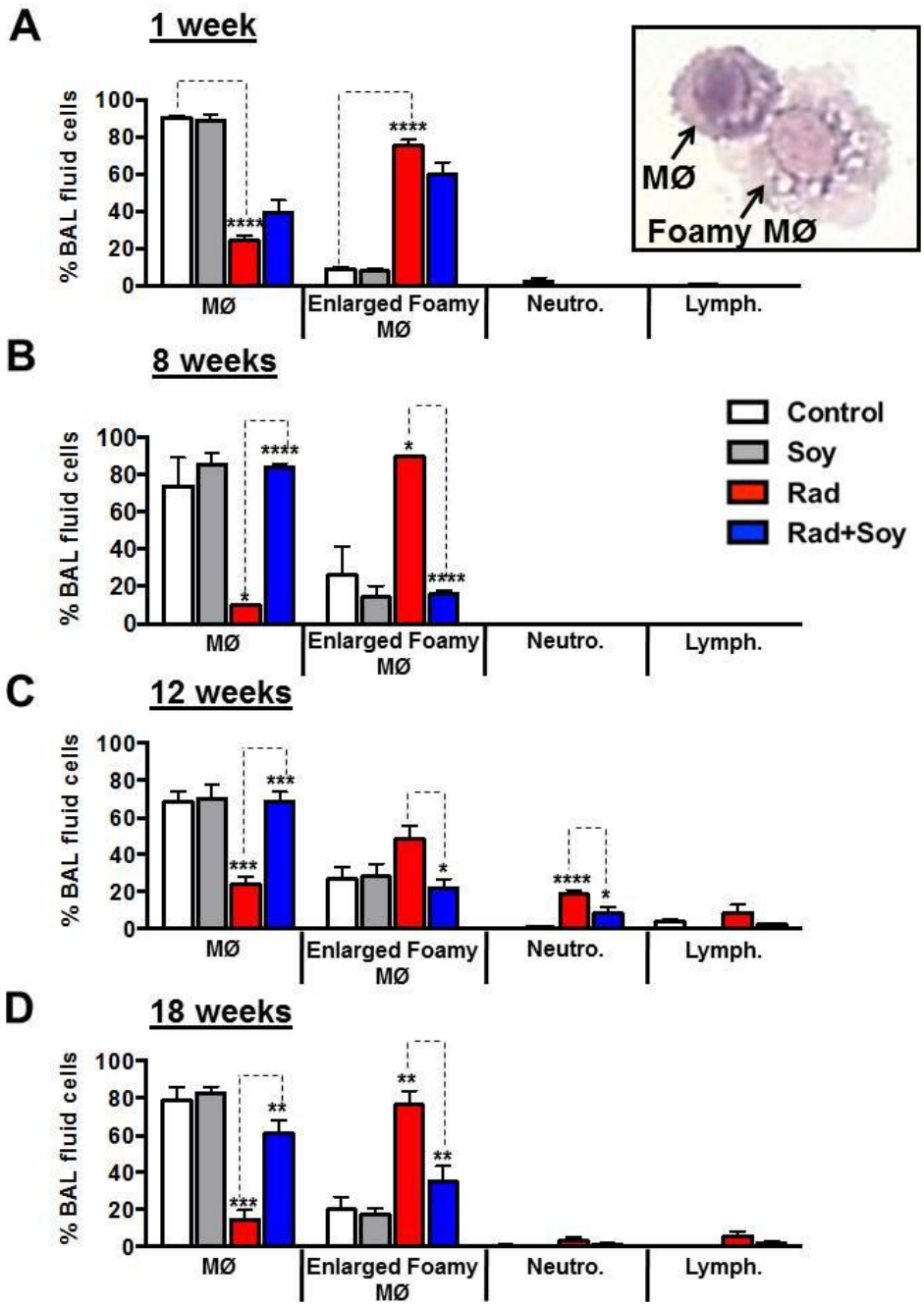

Figure 2.1. Effect of soy isoflavones on immune cells obtained from BAL fluid at different time points after radiation. BAL fluids were harvested at early and late time points post-radiation. At 1 week (A), 8 weeks (B), 12 weeks (C), and 18 weeks (D) post-radiation, differential cell counts on BAL fluid cytospins were performed and the percentages of macrophages, neutrophils, and lymphocytes were calculated. The ratios of non-activated macrophages and enlarged, foamy activated macrophages (see inset 1A), as well as those of neutrophils and lymphocytes, are shown from BAL fluid obtained from treated and control mice. The data are presented as mean ± SEM (n = 3-5 mice/group/time point) and p-values shown represent significant differences between radiation + soy compared to radiation alone. *p<0.05, **p<0.01, ***p<0.001, ****p<0.0001, radiation compared to control or radiation + soy compared to radiation alone.

Flow Cytometry phenotypic analysis of immune myeloid cells infiltrating lung parenchyma following treatment with radiation and soy isoflavones. Morphological analysis of the immune cell subsets in the bronchoalveolar compartment revealed that radiation caused a switch from non-activated to predominantly activated macrophages at 2-4 months after radiation, whereas soy isoflavones prevented radiation-induced macrophage activation. To further analyze the phenotype of myeloid cells involved in the radioprotection of lungs by soy isoflavones, we have also analyzed the lung parenchyma compartment by processing lung tissue into single cell suspensions and analysis of immune cell subsets by immunofluorescence staining and flow cytometry.

Lung cell suspensions were immunostained using a 5-color fluorophore combination of antibodies directed against CD45, CD11b, F4/80, CD11c, and Ly6G from lungs treated with soy, radiation or radiation + soy at 12 weeks after radiation, as detailed in Materials and Methods. Macrophages were gated based on differential expression of F4/80 and CD11c to analyze interstitial macrophages (IM, $F4/80^{+}CD11c^{-}$) and alveolar macrophages (AM $F4/80^{+}CD11c^{+}$) (Figure 2.2A) (149). Percentages of $F4/80^{+}CD11c^{-}$ IM subsets showed a significant decrease in interstitial macrophages induced by radiation compared to control ($p<0.05$), whereas this treatment with soy isoflavones protected this population in irradiated lung tissue ($p<0.05$) (Figure 2.2A). $F4/80^{+}CD11c^{+}$ AM subsets did not show difference between treatments (Figure 2.2A), in contrast to BAL findings that showed an increase in AM by radiation and decrease by radiation + soy. The discrepancies between the evaluations of alveolar macrophages in the BAL compartment versus the lung tissue compartment could be due to initial lavage of loose alveolar macrophages to collect BAL fluid and subsequent processing of lungs for FACS. Therefore, we assume that alveolar macrophages activated by radiation were washed out and recovered in the

BAL resulting in no AM increase observed in lung tissue. Further analysis to resolve this discrepancy is presented in IHC studies below (Figure 2.3). Neutrophils were gated by expression of CD11b, and Ly6G/Gr-1 markers within the $CD45^+$ population (Figure 2.2B) (150). $CD11b^+Ly6G^+$ neutrophils in lungs are significantly increased after radiation compared to control (p=0.01), however supplementation of soy to radiation did not significantly change the percent of neutrophils (Figure 2.2B).

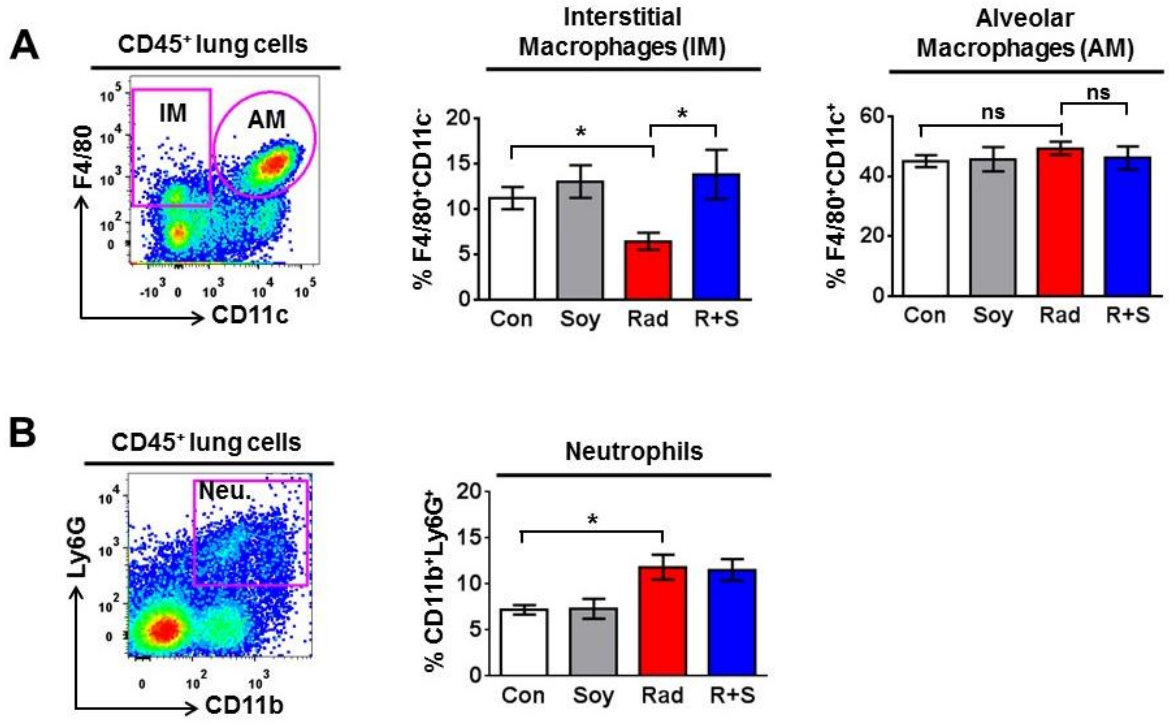

Figure 2.2. Flow cytometry analysis of macrophages and neutrophils isolated from lung tissues. (A). Interstitial and alveolar macrophages analysis. At 12 weeks after radiation, lungs from control (Con) mice, and mice treated with soy (Soy), radiation (Rad) or radiation + soy (R+S) were dissociated into single cell suspensions. Cells were stained with anti-CD45, anti-F4/80, and anti-CD11c fluorescent antibodies to analyze interstitial ($F4/80^+CD11c^-$) and alveolar ($F4/80^+CD11c^+$) tissue macrophages within $CD45^+$ leukocyte populations by flow cytometry. Representative flow cytometry plots are presented, showing the gating strategy of $CD45^+$ myeloid lung cells for analysis of $F4/80^+CD11c^-$ interstitial macrophages (IM in pink rectangle gate) and $F4/80^+CD11c^+$ alveolar macrophage (AM in pink circle gate). Percentages of $F4/80^+CD11c^-$ IM subsets and $F4/80^+CD11c^+$ AM subsets within $CD45^+$ cells are shown for lungs from control and treated mice. The data are presented as mean ± SEM (n = 4-5 mice/group) and are representative of three separate experiments. (B). Analysis of $CD45^+CD11b^+Ly6G^+$ neutrophils. Cells were stained with fluorescent anti-CD45, anti-CD11b, and anti-Ly6G to analyze neutrophil subsets by flow cytometry. Representative flow cytometry plots are presented, showing the gating strategy for analysis of $CD11b^+Ly6G^+$ neutrophils within $CD45^+$ leukocyte populations. Percentages of $CD11b^+Ly6G^+$ neutrophils within $CD45^+$ cells are shown for lungs from control and treated mice. The data are presented as mean ± SEM (n = 5 mice/group) and are representative of two separate experiments. *p<0.05, radiation compared to control or radiation + soy compared to radiation alone.

Skewing toward anti-inflammatory M2 macrophage phenotype in lung tissue treated with radiation and soy. The macrophages recovered from BAL fluids obtained from radiation + soy-treated mice showed a morphology of small non-activated cells in contrast to the enlarged foamy activated macrophages obtained from radiation-treated mice. To further study whether soy inhibits the activation of macrophages induced by radiation, we investigated, *in situ* in the lung tissues, macrophage subsets and their functional status in lungs treated with radiation only and radiation + soy. Lung tissue sections were stained by IHC with the pan-macrophage marker F4/80. We have previously documented that pneumonitis caused by radiation injury to lung tissue is associated with thickening of alveolar septa and inflammatory infiltrates (36, 134, 135). The architecture of the alveolar septa in soy + radiation-treated lungs was thinner akin to control lung tissue showing decreased pneumonitis compared to radiation–treated lungs (Figure 2.3A), as previously shown (134, 135). Radiation caused a striking infiltration of $F4/80^{+}$ macrophages in lungs that was observed in areas of thickened lung alveolar septa, and was more prominent at 18 weeks after radiation (Figure 2.3A, arrowheads) compared to earlier times points after radiation (data not shown). Numerous alveolar macrophages were particularly enlarged with abundant cytoplasm showing the morphology of activated macrophages compared to small macrophages in control lungs (Figure 2.3A, see arrows and inset). Lungs from mice treated with radiation + soy had a lower density of $F4/80^{+}$ macrophages at 18 weeks after radiation compared to radiation–treated lungs (Figure 2.3A). Moreover, the morphology of the alveolar macrophages was much smaller than those of radiation-treated lungs (see insets, Figure 2.3A). Quantitation of $F4/80^{+}$ cells showed that there was a significant increase in the number of alveolar macrophages in lungs treated with radiation compared to control lungs ($p<0.001$, Figure 2.3B). Irradiated mice supplemented with soy isoflavones showed a significantly reduced number of alveolar

macrophages compared to radiation alone ($p<0.001$, Figure 2.3B), to levels similar to those of control mice. Measurements of the average size of the alveolar macrophages showed that radiation increased the size of these cells significantly compared to either radiation + soy ($p<0.01$, Figure 2.3C) or control ($p<0.0001$, Figure 2.3C).

To further clarify the functional phenotype of infiltrating macrophages, the NOS2 activation marker for M1 macrophages and Arg-1 activation marker for M2 macrophages were used to differentiate between pro-inflammatory M1 macrophage phenotype and anti-inflammatory M2 macrophage phenotype. Radiation caused a prominent increase in NOS2 staining of lung tissue by 18 weeks after radiation (Figure 2.4A), that was apparent in enlarged alveolar macrophages (Figure 2.4A, inset). These findings were confirmed by slide scanning quantitation for the level of staining (Figure 2.4B). In contrast, a lower level of NOS2 staining was observed following radiation + soy (Figure 2.4A, B). Staining of lungs with Arg-1 showed a prominent increase in radiation + soy treated lungs compared to radiation alone (Figure 2.4C, D).

In situ staining revealed that radiation caused an increase in a pro-inflammatory M1 macrophage phenotype defined by high NOS2 and low Arg-1 levels at 18 weeks after radiation (Figure 2.4A, B). This is in contrast to relatively low NOS2 levels and high Arg-1 levels observed in lungs treated with radiation + soy or in controls (Figure 2.4B, C).

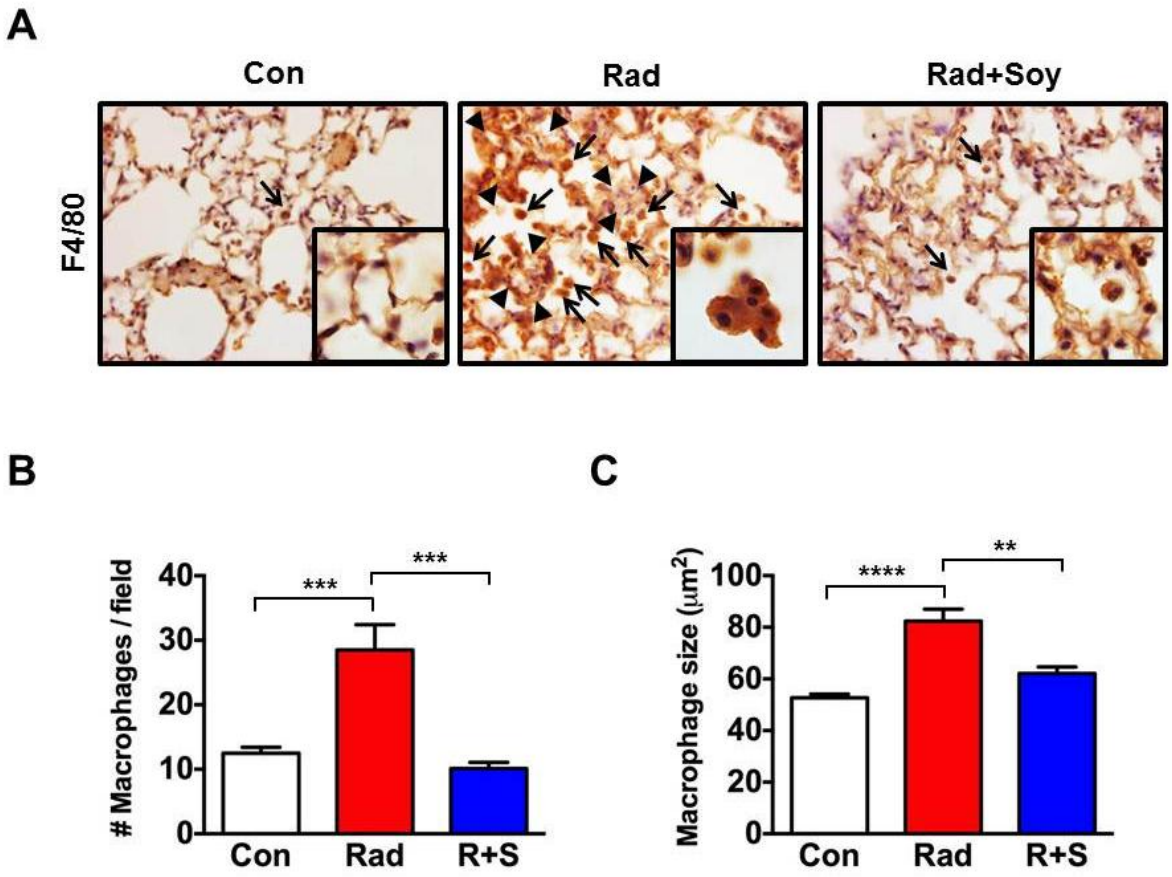

Figure 2.3. *In situ* detection of alveolar macrophages in lungs treated with radiation and soy isoflavones at 18 weeks post-radiation. Lung tissue sections were obtained from control (Con) mice and mice treated with radiation (Rad) or radiation + soy (Rad+Soy) at 18 weeks after radiation. Sections were stained by IHC for the marker F4/80 to detect alveolar macrophages in situ in the lungs. Arrows indicate positive staining of $F4/80^+$ alveolar macrophages. (A). Radiation caused a marked increase in macrophages in thickened alveolar septa areas (arrowheads). Numerous alveolar macrophages were particularly enlarged with abundant cytoplasm showing the morphology of activated macrophages compared to small macrophages in control lungs (see inset). The density of $F4/80^+$ macrophages was much lower in radiation + soy treated lungs at 18 weeks after radiation compared to radiation–treated lungs. Alveolar macrophages were smaller, resembling those of control lungs (see inset) and the architecture of the alveolar septa was thinner akin to control lung tissue showing decreased pneumonitis compared to radiation–treated lungs. (B). Using ImageJ analysis of IHC slides, the numbers of $F4/80^+$ alveolar macrophages were counted in 10 fields of 40x per slide and the average number of $F4/80^+$ cells per field ± SEM is reported for each treatment group. (C). Measurement of the $F4/80^+$ alveolar macrophage cell areas were performed using ImageJ software in 10 fields of 40x per slide and the average cell area of macrophages per field ± SEM in each treatment group is reported. The total number of macrophages counted and measured in 10 fields were 125 for control, 285 for radiation, and 101 for radiation + soy-treated mice. The means are reported in (B) and (C). All magnifications are at 40x and insets at 100x to reveal the extent of positive staining and morphology of immune cell subsets. $^{**}p<0.01$, $^{***}p<0.001$, $^{****}p<0.0001$, radiation compared to control or radiation + soy compared to radiation alone.

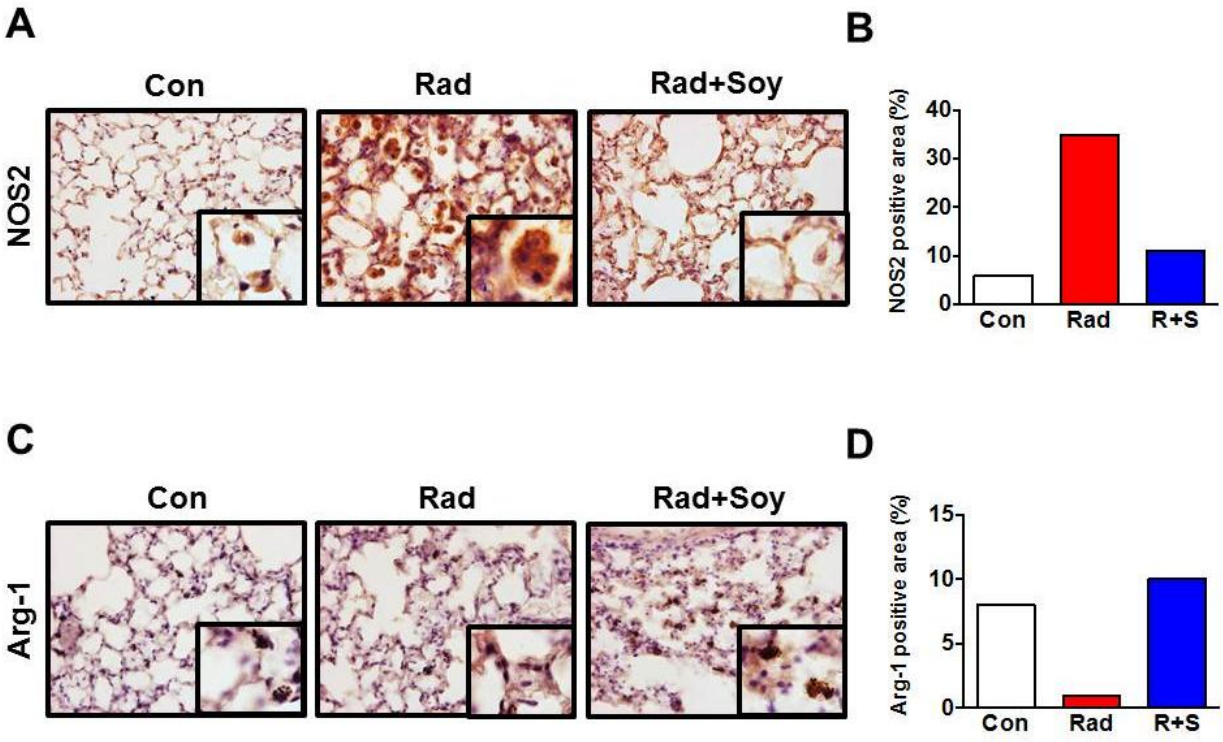

Figure 2.4. *In situ* detection of NOS2 and Arg-1 functional macrophage markers in lungs treated with radiation and soy isoflavones. Lung tissue sections were obtained from control (Con) mice and mice treated with radiation (Rad) or radiation + soy (Rad+Soy) at 18 weeks after radiation. Sections were stained by IHC for the markers NOS2 and Arg-1 to determine macrophage activation status in situ in the lungs. (A). NOS2 staining revealed an abundance of activated macrophages caused by radiation presenting as clusters of enlarged $NOS2^+$ cells in areas of pneumonitis (see insets). Lower levels of $NOS2^+$ macrophages were seen in lungs of mice treated with radiation + soy treated lungs or control which presented as smaller cells (see inset). (B). Whole slide scanning for quantitation of NOS2 positive staining confirmed these findings. (C). Compared to radiation, Arg1 expression was greater with radiation + soy. (D). Whole slide scanning for quantitation of revealed higher levels of Arg-1 in radiation + soy compared to low levels after radiation alone. For analysis of whole slide scanning, the percentage of positive area was calculated as the total number of positive pixels divided by total number of pixels. All magnifications are at 40x and insets at 100x to reveal the extent of positive staining and morphology of immune cell subsets.

Radiation-induced infiltration and activation of granulocytes/neutrophils in lung tissue is decreased by soy isoflavones. Analysis of BAL immune cells showed an increase in neutrophils by 12 weeks after radiation. *In situ* detection of granulocyte/neutrophil phenotype and function were performed by IHC staining of lung tissue sections for Gr-1 (Ly6C/Ly6G) and the neutrophil marker NIMP at 12 weeks after radiation. Radiation caused a pronounced increase in clusters of $Gr\text{-}1^+$ granulocytes in areas of thickened septa at 12 weeks after radiation (Figure 2.5, see inset). In contrast, following radiation + soy the alveolar septa were not as thickened and contained much lower levels of $Gr\text{-}1^+$ cells (Figure 2.5). NIMP staining for neutrophils followed the same patterns with increased neutrophil infiltrates induced by radiation and decreased by radiation + soy (Figure 2.5).

Concurrent with increased infiltration of $Gr\text{-}1^+$ and $NIMP^+$ cells, lungs treated with radiation also showed multiple cells with intense MPO staining (Figure 2.6). MPO^+ cells formed clusters in areas of thickened alveolar septa, which are indicative of a massive infiltration of activated neutrophils, as confirmed by quantitative analysis of the level of positive staining (Figure 2.6A, B). However, MPO^+ infiltrates were greatly reduced in lungs treated with radiation + soy (Figure 2.6A, B). These data indicate that radiation-induced neutrophil activation in lung tissue is inhibited by soy isoflavones. These findings were confirmed by western blot analysis of MPO expression in lung tissue lysates showing an increase induced by radiation, which was inhibited by the addition of soy isoflavones (Figure 2.6C).

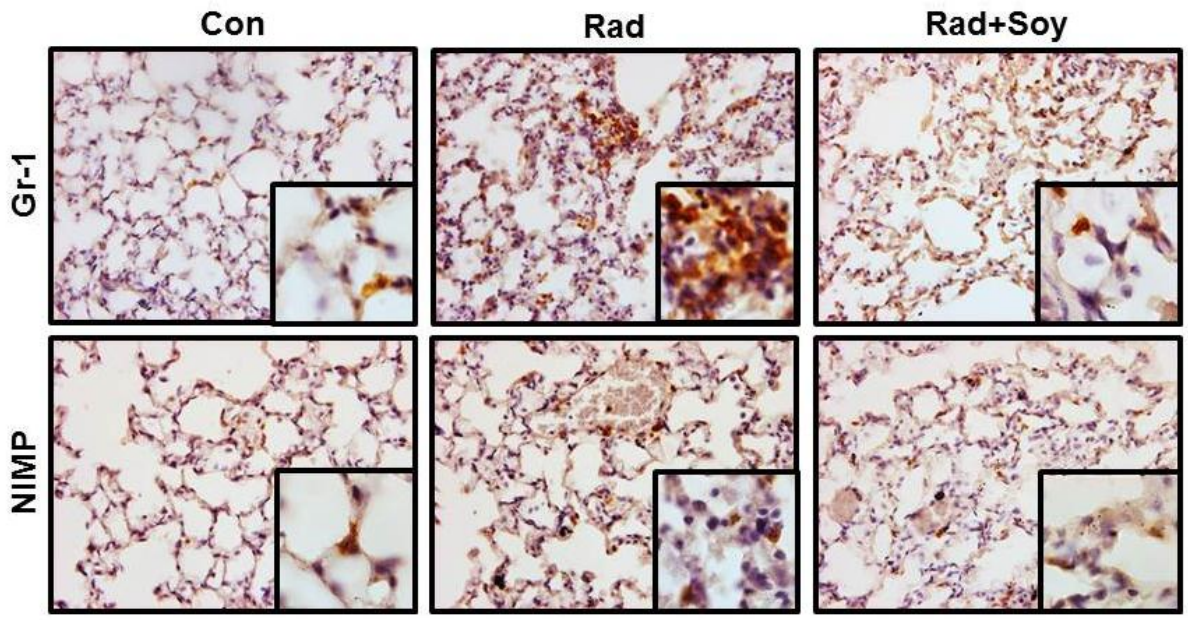

Figure 2.5. Effect of soy isoflavones on radiation-induced infiltration of granulocytes/neutrophils in lung tissue. Lungs tissue sections were obtained from control (Con) mice and mice treated with radiation (Rad) or radiation + soy (Rad+Soy) at 12 weeks after radiation. Sections were stained by IHC for Gr-1 (Ly6C/Ly6G) and NIMP to detect granulocytes/neutrophils. Staining of $Gr\text{-}1^{+}$ granulocytes showed that radiation caused a pronounced increase in clusters of granulocytes in areas of thickened septa at 12 weeks after radiation (see inset). In contrast, following radiation + soy treatment the alveolar septa were not as thickened and much lower levels of positive cells for Gr-1 were observed. All magnifications are at 40x and insets at 100x to reveal the extent of positive staining and morphology of immune cell subsets.

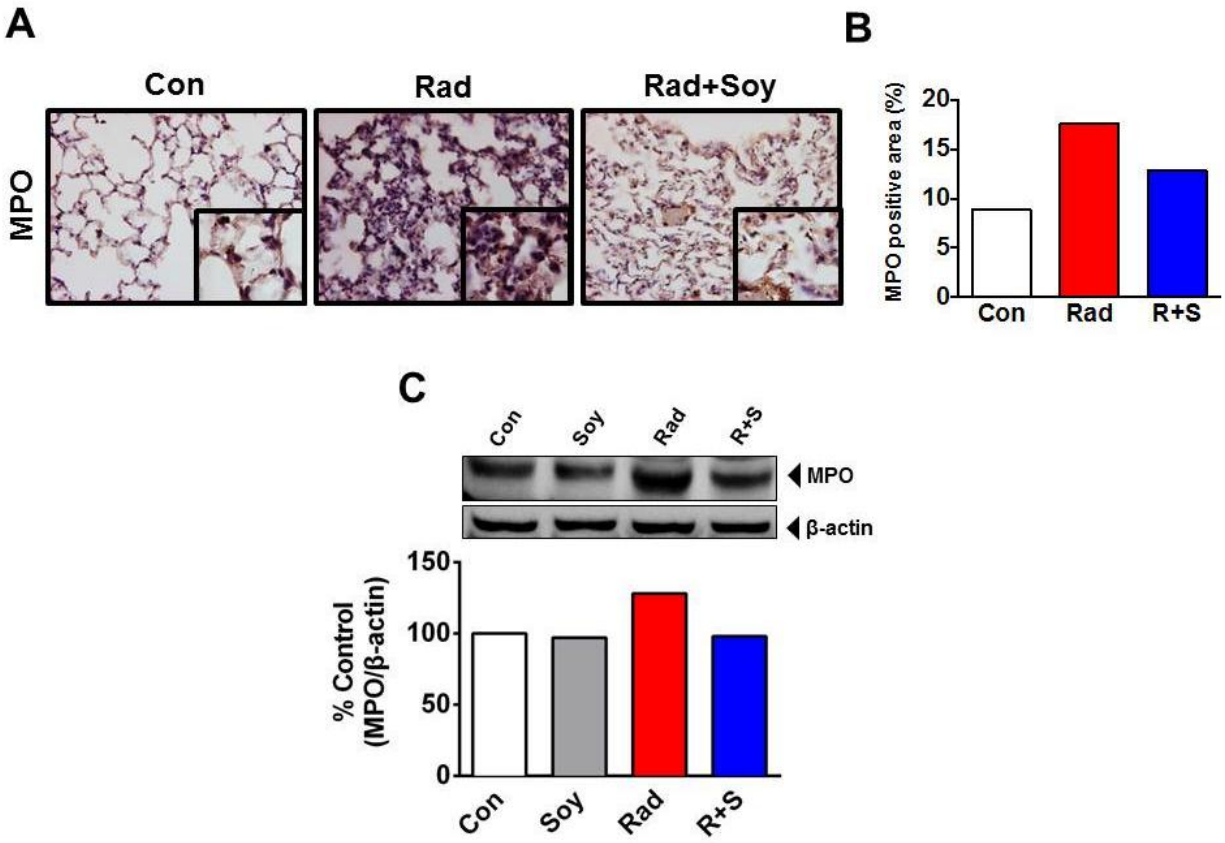

Figure 2.6. Inhibition of radiation-induced activation of neutrophils in lung tissue. Lungs tissue sections were obtained from control (Con) mice and mice treated with radiation (Rad) or radiation + soy (Rad+Soy) at 12 weeks after radiation. (A, B). Sections were stained by IHC for the neutrophil activation marker myeloperoxidase (MPO). Radiation caused extensive MPO staining in the lung tissue that is indicative of activated neutrophil infiltration. MPO^+ activated neutrophils were present in clusters in areas of thickened alveolar septa (see inset) at 12 weeks after radiation. The levels of MPO were greatly reduced in radiation + soy treated lungs. (B). Whole slide scanning for quantitation of MPO positive staining confirmed these findings. For analysis of whole slide scanning, the percentage of positive area was calculated as the total number of positive pixels divided by total number of pixels. $NIMP^+$ neutrophils were also increased in lung tissue by radiation, but not by radiation + soy. All magnifications are at 40x and insets at 100x to reveal the extent of positive staining and morphology of immune cell subsets. (C). Western blot analysis of MPO on whole tissue lysates obtained from lungs showed an increase induced by radiation, which was inhibited by the addition of soy isoflavones. Band intensities were quantified using ImageJ (NIH) densitometry analysis.

DISCUSSION

Soy isoflavones can reduce the extent of inflammatory infiltrates and vascular damage caused by radiation in the lungs (36, 134, 135), suggesting that soy modulates immune responses triggered by injury. Studies on the effect of soy and the immune system in other diseases besides cancer also support this hypothesis. A recent study suggested that genistein may down-regulate cytokine-induced pro-inflammatory pathways in human brain microvascular endothelial cells (106). Soy isoflavones have been shown *in vitro* to have anti-inflammatory mechanisms via modulation of leukocyte-endothelial cell interactions (107). The goals of our current study were to determine whether soy isoflavones modulate innate immune cells putatively involved in radiation-induced inflammation in normal lungs by examining the bronchoalveolar space and lung parenchyma compartments.

Macrophages are recruited as a first response to radiation-induced damage in the tumor microenvironment in irradiated tissues (143, 151). Alterations in lung macrophages after radiation have been observed during early and late phases of tissue injury (152, 153) supporting the idea that macrophage activation contributes, at least partially, to the pathogenesis of radiation-induced lung injury. Therefore, modulation of the response of macrophages to radiation could be a mechanism of radioprotection by soy isoflavones. By 2-4 months after radiation, an increase in the number and size of macrophages was observed both in the bronchoalveolar space and lung parenchyma compartments, indicative of macrophage activation, confirming previous reports (152, 153). Soy isoflavones durably decreased the frequency and size of macrophages found in the lung after radiation.

Our flow cytometry analysis of lung parenchyma after lavage identified subsets of residual $F4/80^{+}CD11c^{+}$ alveolar macrophages and $F4/80^{+}CD11c^{-}$ interstitial macrophages, as previously described by others (154). A decrease in interstitial macrophages was induced by radiation, whereas this cell subset was protected by the addition of soy isoflavones to radiation treatment. Interstitial macrophages have been shown to have more immunoregulatory roles in the maintenance of lung homeostasis and in pathologic conditions (38). Soy could potentially inhibit inflammatory responses by protecting interstitial macrophages. In contrast, alveolar macrophages exhibit a greater capacity to functionally contribute to pulmonary inflammation and anti-microbial defense (37). In our present study, soy isoflavones inhibited alveolar macrophage infiltration and activation induced by radiation, a mechanism that could play a role in controlling inflammatory processes. These findings suggest that soy modulation of macrophage subset functions in response to radiation may play a critical role in soy-mediated radioprotective effects in lungs. We have further studies ongoing to clarify the role of interstitial and alveolar macrophages in radiation-induced lung inflammation and their regulation by soy isoflavones.

In radiation-treated lungs, our analysis of myeloid cells *in situ* by IHC showed extensive infiltration of inflammatory cells at sites of pneumonitis, consisting of macrophages and neutrophils in the lungs. Both types of immune cells were morphologically and molecularly in a status of activation. In contrast, soy supplementation to radiation decreased both the infiltration and activation of myeloid cells. The influence of soy isoflavones on M1 and M2 macrophage polarization in irradiated lungs could be a mechanism of radioprotection. Macrophages possess the plasticity to respond to environmental stressors in tissues that functionally range from M1 pro-inflammatory to M2 immunosuppressive, anti-inflammatory phenotypes (41, 155). These two phenotypes can be distinguished by expression of NOS2 and Arg-1 (156). Normal tissue

exposed to ionizing radiation generates "damage" signals and type 1 cytokines, such as IL-1β, IL-6, and TNF-α, that classically activate macrophages (M1) and drive the acute/chronic pulmonary inflammation induced by radiation (157, 158). M1 macrophages produce NOS2, which generates reactive NO species, thus promoting inflammation. Alternatively activated macrophages (M2) can be generated by type 2 cytokines, such as IL-4, IL-10, and TGF-β, and are important for the resolution of inflammation (155, 159, 160). M2 macrophages produce Arg-1, which generates L-orthonine, a precursor of proline, from arginine (41). Proline enhances collagen synthesis, thus promoting tissue repair and resolution of inflammation (42). Our studies now demonstrate that radiation induced a pro-inflammatory M1 phenotype in lungs at late time points, while mice receiving soy isoflavones and radiation switched to an anti-inflammatory M2 subtype with increased levels of Arg-1 and decreased NOS2. These data indicate that soy isoflavones supplementation to radiation could result in skewing of alveolar macrophages from a pro-inflammatory M1 phenotype toward an anti-inflammatory M2 phenotype, which has been found to mediate the resolution of inflammation, including healing and decreased fibrosis. These data are in agreement with our previous findings demonstrating that soy isoflavones inhibited the release of pro-inflammatory cytokines including TNF-α, IL-1β, IL-6, and IFN-γ which are induced by radiation in lung tissues and promote an M1 macrophage phenotype (134).

Infiltration and activation of neutrophils into the lung are key factors that occur after damage to lung tissue (44, 152). Therefore, inhibition of the inflammatory neutrophil response induced by radiation in the pulmonary environment may result in reduced host tissue damage. Our flow cytometry studies of lung single cell suspensions showed that $CD11b^{+}Ly6G^{+}$ neutrophils were increased after radiation. Immunostaining of lung tissue sections confirmed clusters of neutrophils in sites of pneumonitis caused by radiation. These neutrophils were

activated, as confirmed by MPO staining. Treatment with soy isoflavones inhibited radiation-induced neutrophil infiltration and activation, suggesting a mechanism of protection from tissue damage by soy.

In summary, our pre-clinical study in lung suggests that a radioprotective mechanism of soy isoflavones could involve inhibition of infiltration and activation of macrophages and neutrophils in irradiated lungs. Furthermore, soy caused a polarization from M1 to M2 macrophage that could play a role in the resolution of radiation-induced acute/chronic inflammation in the lungs. It was interesting to note that soy had a protective effect on regulatory interstitial macrophages that could participate in maintaining lung homeostasis and control inflammation and tissue damage.

CHAPTER 3

Soy Isoflavones Mediate Radioprotection of Normal Lung Tissue by Promoting $CD11b^+$ Granulocyte-Associated Arginase-1

ABSTRACT

Radiation therapy for lung cancer causes normal tissue injury, including pneumonitis and fibrosis. We have shown that treatment with soy isoflavones mitigates radiation-induced lung injury, but the cellular and molecular mediators of radioprotection remain unclear. We hypothesize that soy isoflavones reduce radiation injury by promoting an anti-inflammatory phenotype in myeloid cells early in irradiated lung tissue. This chapter investigates the role of arginase-1 (Arg-1) associated with $CD11b^+$ granulocytes that could act as an immunosuppressive molecule involved in soy-mediated radioprotection of lung tissue. BALB/c mice received a single 10 Gy dose of thoracic irradiation with a mixture of soy isoflavones (83% genistein, 15% daidzein, 0.3% glycitein) given orally at 1 mg/day continuously. Lungs were harvested at 1 week post-radiation and Arg-1 was detected by Western blot and immunohistochemistry. The phenotype of lung myeloid cells associated with intracellular Arg-1 expression was analyzed by flow cytometry. Subsequent IL-1β, IL-6, and TNF-α production in lungs was measured at 4 weeks post-radiation by ELISA as readout for immunosuppression. At 1 week after radiation, both Western blot and immunohistochemistry showed that while Arg-1 levels in lung tissue are decreased by radiation, the level is maintained in radiation + soy treated lungs. Radiation and/or soy do not affect the percentage of lung $CD11b^+$ myeloid cells. However, radiation decreases the percentage of $CD11b^+Arg\text{-}1^+$ cells in lungs (p=0.0028), whereas soy isoflavones combined with

radiation caused an increase in $CD11b^{+}Arg\text{-}1^{+}$ cell subset (p=0.0096). Radiation decreases the percentage of granulocytes expressing $CD11b^{+}Ly6C^{-}Ly6G^{+}Arg\text{-}1^{+}$ (p=0.0050), while these $Arg\text{-}1^{+}$ granulocytes were not reduced in radiation + soy treated lungs (p=0.0032). At 4 weeks, soy inhibited increases in IL-1β, IL-6, and TNF-α pro-inflammatory cytokines induced by radiation in the lung. Radioprotection by soy isoflavones involves an early process of immunosuppressive events that subsequently causes a decrease downstream inflammatory cytokine expression and tissue damage by promoting $Arg\text{-}1^{+}$ granulocytes in lungs.

INTRODUCTION

Radiation pneumonitis is caused by an early inflammatory process triggered by lung tissue damage. This process occurs immediately after radiation and induces the expression and release of pro-inflammatory cytokines and chemokines which drive the recruitment of inflammatory cells into the injured tissue (29, 30, 141). Infiltrating inflammatory cells are stimulated and activated, producing additional mediators, resulting in a cytokine cascade (31, 32). The expansion and perpetual activation of inflammatory cells, as well as lung parenchyma, leads to clinical pneumonitis.

Inflammation is causally linked to radiation pneumonitis severity and outcome. In Chapter 2, our findings suggest that one radioprotective mechanism of soy isoflavones involves the inhibition of infiltration and activation of macrophages and neutrophils in irradiated lungs. On the other side of the pro/anti-inflammatory radioprotection axis, soy isoflavones may promote immunosuppressive phenotypes and anti-inflammatory molecular mediators after injury. Thus one possible mechanism of radioprotection in lung tissue could be achieved by the indirect suppression of radiation-induced pro-inflammatory cells and pathways. In Chapter 3, we investigate the role of myeloid-derived suppressor cells (MDSCs) and their expression of arginase-1 in the mitigation of radiation-pro-inflammatory cytokines by soy isoflavones in lung tissue to understand the role of immunosuppressive subsets and mediators in radioprotection of lung tissue by soy isoflavones.

MATERIALS AND METHODS

Mice

Female BALB/c mice (Harlan, Indianapolis, IN) 5-6 weeks old, were housed and handled in animal facilities accredited by the Association for Assessment and Accreditation of Laboratory Animal Care. The animal protocol was approved by Wayne State University Institutional Animal Care and Use Committee.

Soy isoflavones

The soy isoflavone mixture G-4660 used is a pure extract of 98.16% isoflavones from soybeans consisting of 83.3% genistein, 14.6% daidzein and 0.26% glycitein (manufactured by Organic Technologies and obtained from the National Institutes of Health [NIH], Bethesda, MD). The soy isoflavone mixture was dissolved in DMSO and mixed with sesame seed oil at a 1:20 ratio just prior to treatment to facilitate gavage and avoid irritation of the esophagus by DMSO (36, 134, 135).

Lung irradiation

Radiation was delivered to the thoracic cage comprising the whole lung. Three anesthetized mice, in jigs, were positioned under a 6.4 mm lead shield with 3 cut-outs in an aluminum frame mounted on the X-ray machine to permit selective irradiation of the lung in 3 mice at a time, as previously described (134). The radiation dose to the lung and the scattered dose to areas of the mouse outside of the radiation field were carefully monitored. To minimize backscattering of radiation, the bottom of the aluminum frame that holds the jigs was hollowed

out and the backplate of the jig was thinned to 1.6mm thickness. Under these conditions and the lead shielding, the X ray dose to the shielded regions was reduced to 1% of the dose to the irradiated field. The dose rate was 101 cGy/min and half value layer was 2 mm Cu. Photon irradiation was performed at a dose of 10 Gy with a Siemens Stabilipan X-ray set (Siemens Medical Systems, Inc., Erlangen, Germany) operated at 250 kV, 15 mA with 1 mm copper filtration at a distance of 47.5 cm from the target.

Experimental design

Mice were pre-treated with oral soy isoflavones each day for 3 days at a dose of 5mg/day (equivalent to 250mg/kg). Then, the lung was selectively irradiated with 10 Gy. Soy treatment was continued on a daily basis for 5 more days at 5mg/day. Then mice were treated with a lower soy dose of 1mg/day (equivalent to 50mg/kg), given daily 5 days a week for up to 4 weeks. The rationale for giving a higher dose of soy isoflavones for pre-treatment and just after radiation is to optimize the effect of soy, based on previous studies (36, 140). At different time points, separate mice from each treatment group were either processed for flow cytometry studies or homogenized for ELISA, snap frozen for western blot, or mice were used to fix lungs *in situ* with formalin for histology studies as detailed below.

Analysis of MDSC subsets and intracellular Arg-1 by flow cytometry on single-cell suspensions of lungs

Following a BAL wash, lungs were excised, minced, and digested with 0.4 mg/mL collagenase IV for 45 minutes at 37° C. Digested lungs were passed through a wire mesh, then a 0.7 μm nylon mesh. Red blood cells were removed by incubating in red blood cell lysis buffer

for 2 minutes at room temperature. Single-cell suspensions obtained from the lungs were incubated with Fc receptor-blocking antibody (eBioscience, San Diego, CA) prior to staining to reduce non-specific binding. To determine the phenotype of immune cells, cells were immunostained using a 4-color fluorophore combination of antibodies consisting of CD45-APC, CD11b-PE, Ly6C-PE-Cy7, Ly6G-PE-Cy5.5 (eBioscience). Cells were fixed with 4% paraformaldehyde in PBS and incubated with intracellular Arg-1 purified antibody (1:50, BD Biosceinces, San Jose, CA). Cells were washed in 1X Permeabilization Buffer (eBioscience) and incubated with and additional fluorescent rat anti-mouse IgG1-FITC secondary antibody (BD Pharmingen). Fixable viability dye eFluor 450 (eBioscience) was used to exclude dead cells from analysis. Cells were analyzed by flow cytometry using a BD LSR II flow cytometer (BD Biosciences, San Jose, CA) in the Microscopy, Imaging and Cytometry Resources Core at Wayne State University School of Medicine, followed by analysis on FlowJo v10 software (Tree Star Inc., Ashland, OR).

Preparation of lung tissue protein lysates and western blot analysis

Mice were sacrificed at 1 week post-irradiation. Lungs were resected and snap frozen. To prepare lung tissue protein lysates, frozen lungs were thawed, weighed, and homogenized in 10% w/v of lysis buffer using a gentleMACS tissue dissociator (Miltenyi Biotec, Bergisch, Germany). The suspension was centrifuged at 4000 x g for 5 minutes at 4°C and the protein extracts were frozen at -80°C until analysis. For western blot analysis, total lung protein extracts (90 µg) were loaded and separated on 10% sodium dodecyl sulfate polyacrylamide gel electrophoresis (SDS-PAGE) and transferred to Whatman membranes (GE Healthcare Life Sciences, Pittsburgh, PA). Membranes were incubated with anti-arginase-1 (Arg-1) antibody (eBioscience, San Diego, CA;

1:200) overnight at 4°C. Membranes were washed and incubated with horseradish peroxidase-conjugated secondary antibody (Vector Labs, 1:2000) at room temperature for 1 hour. Immunoreactive protein bands were visualized by SuperSignal West Pico Chemiluminescent Substrate (Thermo Scientific, Waltham, MA) and captured on a digital imaging system (Fotodyne Inc., Hartland, WI). Membranes were re-probed with anti-β-actin Ab as a loading control (137).

Immunohistochemistry (IHC)

Mice were sacrificed at 1 week post-irradiation and lungs were intratracheally instilled with 10% buffered formalin and resected, embedded in paraffin, and sectioned. Sections were blocked with IHC Tek Antibody Diluent (IHC World, Woodstock, MD) then incubated with primary purified monoclonal antibodies directed against arginase-1 (Arg-1) (eBioscience, San Diego, CA) overnight at 4° C. Lung sections were then incubated with biotinylated secondary antibodies (Vector Labs, Burlingame, CA) at 1:300 for 1 hour at room temperature. Staining was amplified with the avidin-biotin system Vectastain ABC Reagent Kit (Vector Labs) and visualized with the Vector DAB Substrate Kit for peroxidase (Vector Labs). Sections were counterstained with IHC-Tek Mayer's Hematoxylin (IHC World, Woodstock, MD) and mounted with Permount mounting media (Electron Microscopy Sciences, Hatfield, PA). Arg-1 expression in lung tissue after radiation was evaluated on a Nikon E800 microscope (Nikon Inc., Melville, NY).

Enzyme-linked immunosorbant assay (ELISA)

Mice were sacrificed at 4 weeks post-irradiation. Lungs were resected and snap frozen. To prepare lung homogenates, frozen lungs were thawed, weighed, and homogenized in 10% w/v of phosphate buffered saline (PBS) with Complete Protease Inhibitor Cocktail Tablets (Roche Diagnostics, Indianapolis, IN) using a gentleMACS tissue dissociator (Miltenyi Biotec, San Diego, CA). The suspension was centrifuged at 4000 x g for 5 minutes at 4°C and the supernatant was frozen at -80°C. Lung homogenates were assayed for IL-1β, IL-6, and TNF-α, using the respective Ready-SET-GO ELISA kits (eBioscience, San Diego, CA) according to manufacturer's instructions.

Statistical analysis

Data are expressed as mean ± SEM. Comparisons between means of two treatment groups were analyzed by two-tailed unpaired Student's t test using GraphPad Prism version 6.0 software (GraphPad Software Inc., San Diego, CA). A value of $p<0.05$ was considered statistically significant.

RESULTS

Effect of radiation and soy isoflavones on Arg-1 levels in lung tissue. Lungs tissue sections were obtained from control mice and mice treated with radiation or radiation + soy at 1 week post-irradiation and stained by IHC for Arg-1 to detect expression *in situ*. In control lungs, Arg-1^+ cells are evenly distributed across alveolar septa (Figure 3.1A). However, Arg-1^+ cells were sparsely found in areas of thickened septa and staining was overall greatly reduced in lungs treated with radiation (Figure 3.1A). Staining of lungs from mice receiving soy isoflavones in conjunction with radiation revealed a degree of Arg-1 positivity that was similar to control lungs (Figure 3.1A). These data indicate that radiation caused the depletion of Arg-1^+ cells normally occurring the lung, or reduced the expression of Arg-1 in cells in the lung tissue, while soy isoflavones protected from this radiation effect. These findings were confirmed by western blot analysis of Arg-1 expression in lung tissue lysates showing a decrease induced by radiation, which was inhibited by the addition of soy isoflavones (Figure 3.1B, C).

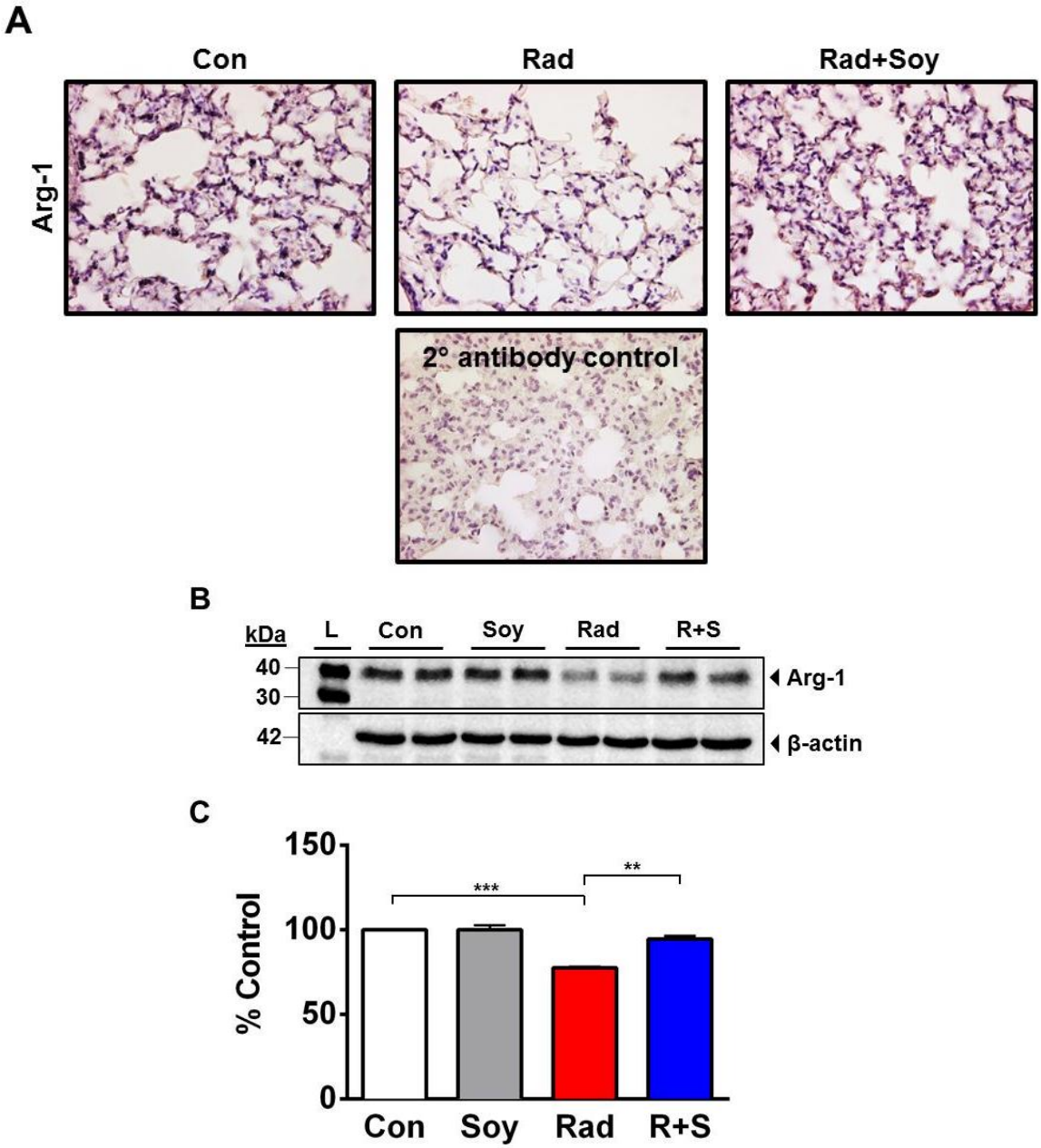

Figure 3.1. *In situ* detection of Arg-1 in lung tissue treated with radiation and soy isoflavones at 1 week post-irradiation. Lungs tissue sections were obtained from control (Con) mice and mice treated with radiation (Rad) or radiation + soy (Rad+Soy) at 1 week after radiation. (A). Sections were stained by IHC for Arg-1 to detect expression *in situ*. Staining of Arg-1^{+} cells showed that radiation caused a pronounced decrease in these cells in areas of thickened septa at 1 week after radiation. In contrast, following radiation + soy treatment, higher levels of positive cells for Arg-1 were observed and were comparable to levels in control mice. Secondary antibody alone is shown as a staining control. All magnifications are at 40x. (B). Western blot analysis of Arg-1 on whole tissue lysates obtained from lungs showed an increase induced by radiation, which was inhibited by the addition of soy isoflavones. (C). Band intensities were quantified using ImageJ (NIH) densitometry analysis. Radiation + Soy (R+S).

Effect of radiation and soy isoflavones on Arg-1 expression in CD11b$^+$ myeloid cell compartment in lung tissue. We examined myeloid cells in the lung to determine if this arginase-expressing population was being altered by radiation or soy isoflavones treatment. Lung cell suspensions were immunostained using antibodies directed against CD45 and CD11b, as well as intracellular Arg-1 from lungs treated with soy, radiation or radiation + soy at 1 week after radiation, as detailed in Materials and Methods. Intracellular Arg-1 expression in CD11b$^+$ myeloid cells in the lung was evaluated (Figure 3.2).

Radiation and/or soy isoflavones treatment did not affect the percentage of CD11b$^+$ cells in the lung at 1 week post-radiation (Figure 3.3A). However, radiation significantly decreased the percentage of Arg-1$^+$ cells within the CD11b$^+$ cellular compartment in lungs (p=0.0228) compared to control (Figure 3.3B), while lungs from Rad+Soy mice show significantly increased percentages of CD11b$^+$Arg-1$^+$ cells (p=0.0096) compared to radiation alone (Figure 3.3B).

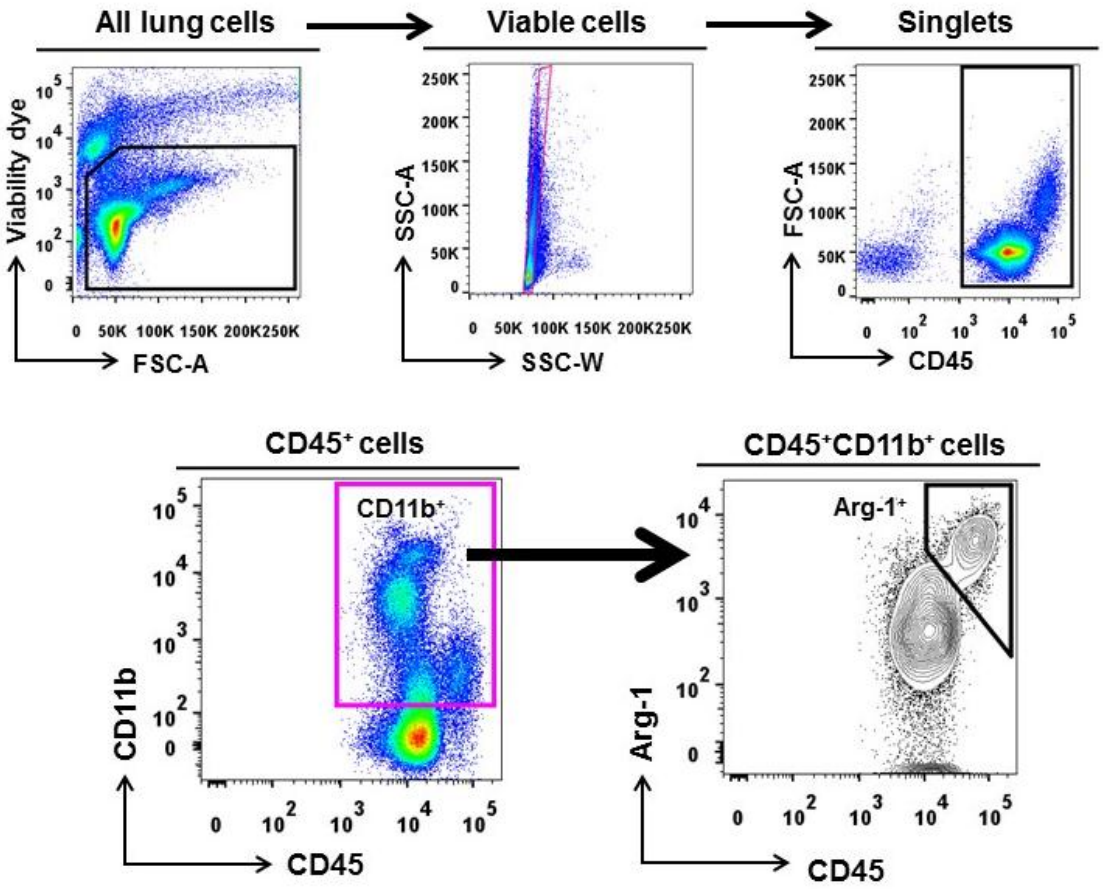

Figure 3.2. Gating strategy for the detection of intracellular Arg-1 in CD11b$^+$lung leukocytes. Single-cell suspensions obtained from the lungs were analyzed. Fixable viability dye eFluor 450 was used to exclude dead cells from analysis and gate on live cells. Side scatter are (SSC-A) and side scatter width (SSC-W) were used to identify single cell events (singlets). CD45$^+$ lung leukocytes were gated on, followed by gating on CD11b$^+$ cells within this leukocyte gate. Intracellular Arg-1 cells were gated on within the CD11b$^+$ lung leukocytes.

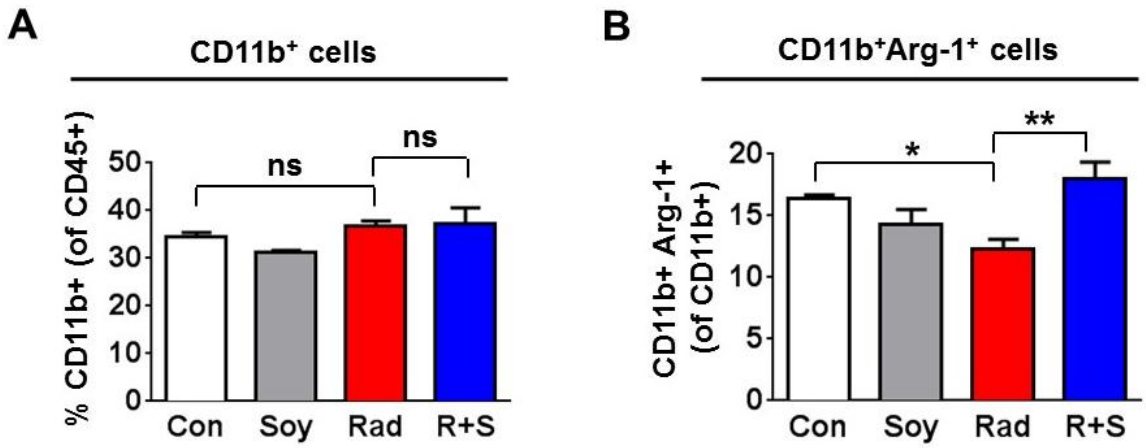

Figure 3.3. Effect of soy isoflavones on intracellular Arg-1 levels in CD11b$^+$ leukocytes in lung at 1 week post-radiation. (A). Analysis of CD45$^+$CD11b$^+$ leukocytes in lung. At 1 week after radiation, lungs from control (Con) mice, and mice treated with soy (Soy), radiation (Rad) or radiation + soy (R+S) were dissociated into single cell suspensions. Cells were stained with anti-CD45, anti-CD11b, anti-Ly6C, and anti-Ly6G fluorescent antibodies to analyze CD11b$^+$ myeloid cells within CD45$^+$ leukocyte populations by flow cytometry. Percentages of CD11b$^+$ cells within CD45$^+$ cells are shown for lungs from control and treated mice. The data are presented as mean ± SEM (n = 3 mice/group). (B). Intracellular Arg-1 expression in CD11b$^+$ lung leukocytes. After cell surface staining, cells were stained with anti-Arg-1 purified antibody followed by fluorescent anti-IgG-FITC to analyze intracellular Arg-1 in CD11b$^+$ cells by flow cytometry. Percentages of CD11b$^+$Arg-1$^+$ cells within CD45$^+$ leukocytes are shown for lungs from control and treated mice. The data are presented as mean ± SEM (n = 3 mice/group). *p<0.05, **p<0.01 radiation compared to control or radiation + soy compared to radiation alone.

Flow cytometry analysis of intracellular Arg-1 in CD11b$^+$ myeloid-derived supporessor cell subsets in lung tissue treated with radiation and soy isoflavones. To further interrogate the specific CD11b$^+$ cell populations that are augmented by radiation and soy isoflavones treatment, we examined intracellular expression of Arg-1 in monocytic- and granulocytic-MDSC subsets by flow cytometry (Figure 3.4). Lung cell suspensions were immunostained using a 5-color fluorophore combination of antibodies directed against CD45, CD11b, Ly6C, Ly6G and intracellular Arg-1 from lungs treated with soy isoflavones, radiation or radiation + soy at 1 week after radiation, as detailed in Materials and Methods. CD11b$^+$ myeloid subsets were gated based on their differential expression of Ly6C and Ly6G to analyze monocytic-MDSCs (CD11b$^+$Ly6C$^+$Ly6G$^-$) and granulocytic-MDSCs (CD11b$^+$Ly6C$^-$Ly6G$^+$) (Figure 3.4).

In order to dissect the specific CD11b$^+$ cells population responsible for Arg-1 expression in the lung, we analyzed Ly6C and Ly6G subsets (Figure 3.5A). CD11b$^+$Ly6C$^-$Ly6G$^+$ granulocytic-MDSCs highly express Arg-1 (~70% in control mice), while other CD11b$^+$ Ly6C and Ly6G subpopulations minimally expressed Arg-1. Only about 1% of monocytic-MDSCs expressed Arg-1 across all treatment groups (data not shown). Radiation and/or soy isoflavones treatment did not affect the percentage of CD11b$^+$Ly6C$^-$Ly6G$^+$ granulocytic-MDSC in the lung at 1 week post-radiation (Figure 3.5B). However, radiation significantly decreased the percentage of CD11b$^+$Ly6C$^-$Ly6G$^+$Arg-1$^+$ granulocytes in lungs (p=0.0050) compared to control (Figure 3.5C), while CD11b$^+$Ly6C$^-$Ly6G$^+$ granulocytes from Rad+Soy mice had significantly more Arg-1$^+$ cells (p=0.0032), compared to radiation alone, and these percentages were comparable to those of control lungs (Figure 3.5C).

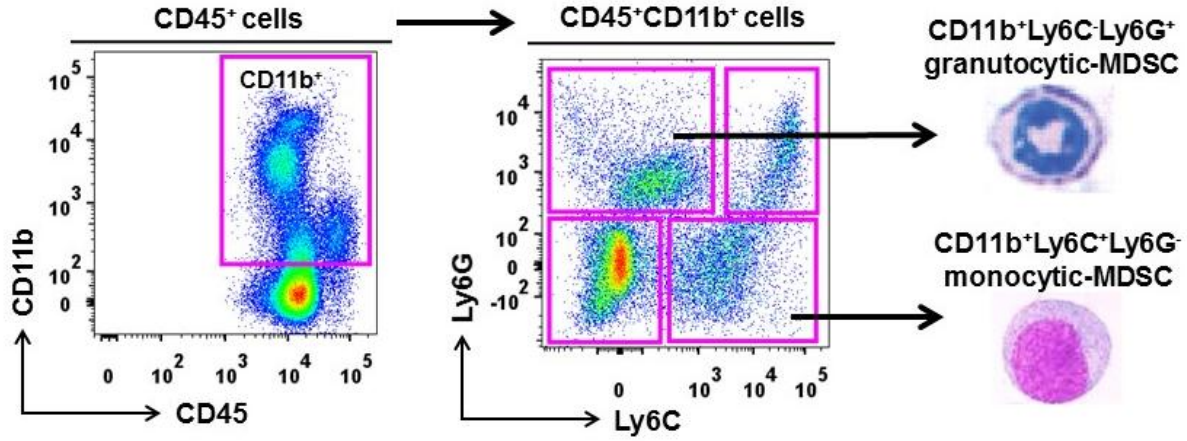

Figure 3.4. Gating strategy for granulocytic and monocytic MDSC subsets in the lungs. Single-cell suspensions obtained from the lungs were analyzed. $CD11b^+$ cells within $CD45^+$ leukocytes were gated (see Figure 3.2 for gating method). To further interrogate the specific $CD11b^+$ cell populations that are being augmented by radiation and soy isoflavones treatment, we examined in monocytic- and granulocytic-MDSC subsets by flow cytometry. $CD11b^+$ myeloid subsets were gated based on differential expression of Ly6C and Ly6G to analyze monocytic-MDSCs ($CD11b^+Ly6C^+Ly6G^-$) and granulocytic-MDSCs ($CD11b^+Ly6C^-Ly6G^+$).

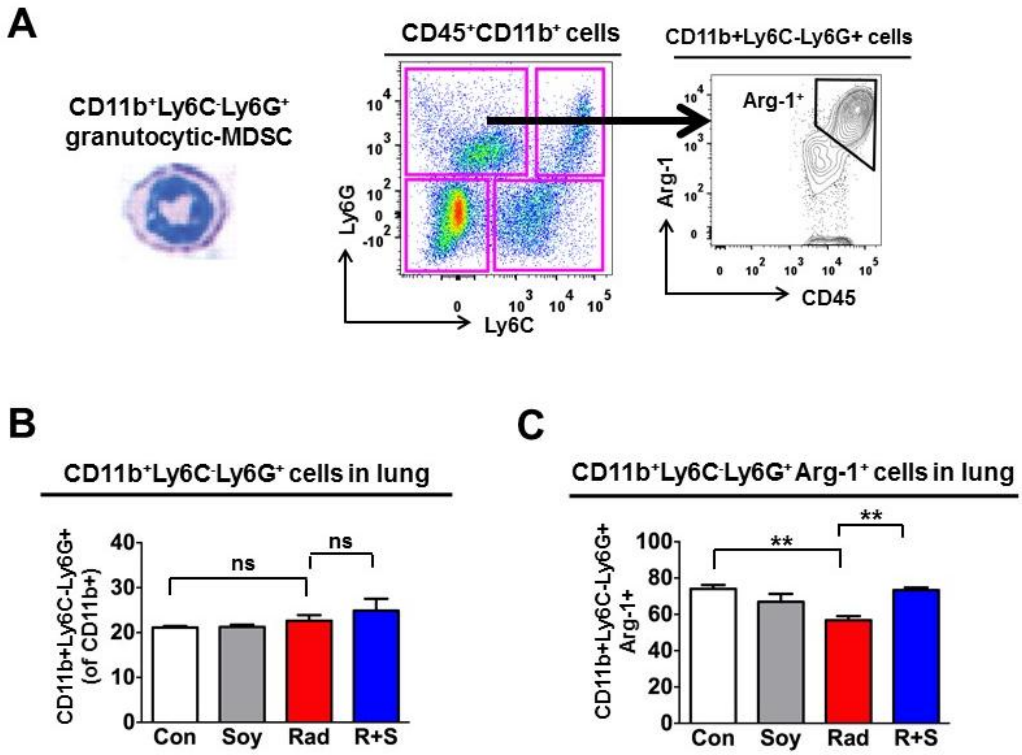

Figure 3.5. Intracellular flow cytometry analysis of Arg-1 expression in CD11b$^+$Ly6C$^-$ Ly6G$^+$ granulocytic-MDSCs at 1 week after radiation. (A). Analysis of CD11b$^+$Ly6C$^-$Ly6G$^+$ granulocytic MDSCs in lung. At 1 week after radiation, lungs from control (Con) mice, and mice treated with soy (Soy), radiation (Rad) or radiation + soy (R+S) were dissociated into single cell suspensions. Cells were stained with anti-CD45, anti-CD11b, anti-Ly6C, and anti-Ly6G fluorescent antibodies to analyze CD11b$^+$ myeloid cells within CD45$^+$ leukocyte populations by flow cytometry. (B) Percentages of CD11b$^+$Ly6C$^-$Ly6G$^+$ granulocytic MDSCs within the CD11b$^+$ gated cells are shown for lungs from control and treated mice. The data are presented as mean ± SEM (n = 3 mice/group). (C). Intracellular Arg-1 expression in CD11b$^+$ lung leukocytes. After cell surface staining, cells were stained with anti-Arg-1 purified antibody followed by fluorescent anti-IgG-FITC to analyze intracellular Arg-1 in CD11b$^+$ cells by flow cytometry. Percentages of CD11b$^+$Arg-1$^+$ cells within CD45$^+$ leukocytes are shown for lungs from control and treated mice. The data are presented as mean ± SEM (n = 3 mice/group). ***p*<0.01 radiation compared to control or radiation + soy compared to radiation alone.

Effect of soy-mediated early immunosuppressive phenotype in irradiated tissue on subsequent radiation-induced pro-inflammatory cytokine levels in lung homogenates. We showed that soy isoflavones promote an immunosuppressive granulocytic-MDSC phenotype at an early time point after radiation, with increased $CD11b^{+}Ly6C^{-}Ly6G^{+}Arg\text{-}1^{+}$ cells in irradiated lungs with in mice receiving soy isoflavones treatment. To determine if early Arg-1 expression in granulocytic-MDSCs results in a later functional anti-inflammatory effect, we measured radiation-induced pro-inflammatory cytokine expression subsequent to the soy-mediated promotion of immunosuppressive MDSC phenotype observed at 1 week. Indeed, soy isoflavones treatment inhibited radiation-induced cytokine production in lung tissue at 4 weeks post-irradiation (Figure 3.6). Inflammatory cytokines associated with radiation injury were significantly reduced by soy isoflavones supplementation, including IL-1β (p=0.0030), IL-6 (p=0.0061), and TNF-α (p=.0057). Increased Arg-1 expression at an earlier time point (1wk post-radiation) may contribute to the attenuation of pro-inflammatory cytokine expression observed in lungs at a later time point (4wks post-radiation).

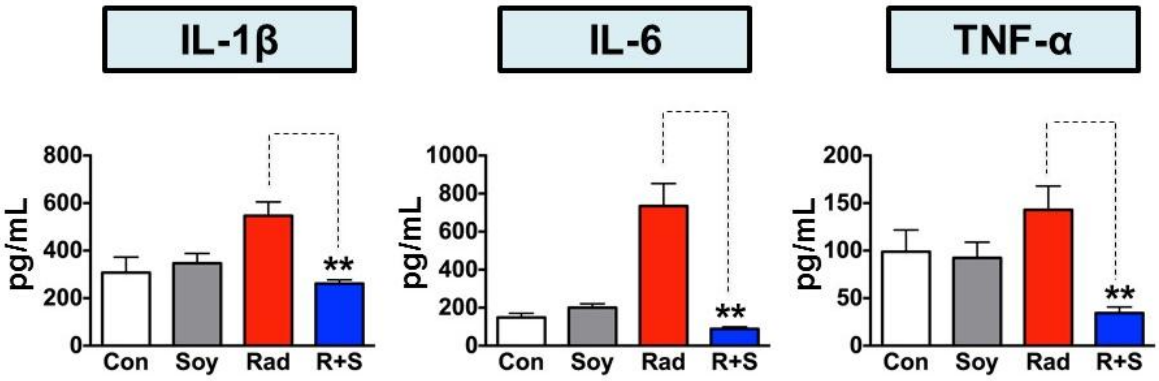

Figure 3.6. Supplementation with soy isoflavones inhibits radiation-induced cytokine production in lung tissue at 4 weeks post-radiation. Cytokine levels were measured by ELISA in lung homogenates obtained from mice at a time point of 4 weeks following irradiation. The data are presented as mean ± SEM (n = 4-9 mice/group). ***p*<0.01 radiation compared to control or radiation + soy compared to radiation alone.

DISCUSSION

Radiation-induced pro-inflammatory cytokine expression in the lung plays an important role in promoting and perpetuating inflammation that contributes to the pathology of lung injury after thoracic radiation. Acute inflammation triggered after a single dose of radiation sets off a cascade of events that is akin to an aberrant wound healing response. We have reported in preclinical mouse models that supplementation with soy isoflavones to thoracic irradiation mitigates radiation-induced inflammatory cytokines, infiltration of inflammatory cells and fibrosis (36, 134, 135), but the immunosuppressive mediators of radioprotection remain unclear. In Chapter 2, we investigated the role of macrophages and neutrophils in the mitigation of radiation-induced inflammatory events by soy isoflavones in lung tissue. Our findings suggested that a radioprotective mechanism of soy isoflavones in lung involves the inhibition of infiltration and activation of macrophages and neutrophils in irradiated lungs.

Additionally, soy isoflavones may also radioprotect

by promoting immunosuppressive phenotypes and anti-inflammatory molecular mediators after injury. Thus, radioprotection in lung tissue could also be achieved by the indirect suppression of radiation-induced pro-inflammatory cells and pathways. In this chapter, we demonstrated that soy isoflavones play a role in the promotion of an immunosuppressive phenotype in the lung at an early time point after a single dose of irradiation, and may downregulate damaging radiation-induced inflammation.

We found that arginase-1, an enzyme with an important immunosuppressive and regulatory role (42), was decreased in lungs at 1 week post-irradiation, as confirmed by IHC and western blot. Soy isoflavones supplementation protected Arg-1 levels in irradiated lungs, similar

to that of control lungs. In control lungs, Arg-1^+ cells are evenly distributed across alveolar septa while Arg-1^+ cells were sparsely found in areas of thickened septa and staining was overall greatly reduced in lungs treated with radiation. Staining of lungs from mice receiving soy isoflavones in conjunction with radiation revealed a degree of Arg-1 positivity that was similar to control lungs. These data indicate that radiation caused the depletion of Arg-1^+ cells that normally occur the lung, or reduced the expression of Arg-1 in cells lung tissue, while soy isoflavones protected from this radiation effect. These findings were confirmed by western blot analysis of Arg-1 expression in lung tissue lysates showing a decrease induced by radiation, which was inhibited by the addition of soy isoflavones. Decreased Arg-1 levels in the lung after radiation may allow for tissue damaging pro-inflammatory processes to proceed unhindered, and our data indicate that soy isoflavones may mediate radioprotection by promoting immunosuppression via Arg-1.

To identify the specific Arg-1^+ cell population affected by radiation and soy isoflavones, we performed flow cytometry studies to probe the myeloid compartment of the lungs, as these cells are known to produce arginase (161). Radiation and/or soy isoflavones treatment did not affect the percentage of $CD11b^+$ cells in the lung at 1 week post-radiation, however radiation significantly decreased the percentage of Arg-1^+ cells within the $CD11b^+$ cellular compartment in lungs compared to control. A subset of $CD11b^+$ cells showed typical characteristics of myeloid-derived suppressor cells, with a $CD11b^+Ly6C^-Ly6G^+$ immunophenotype and high arginase-1 expression (155). This population of $CD11b^+Ly6C^-Ly6G^+$ MDSCs are granulocytic in nature, given their high expression of Ly6G and lack of Ly6C. At 1 week post-radiation, we found that these granulocytic-MDSCs in irradiated lungs showed significantly less intracellular Arg-1 compared to control, while lungs from Rad+Soy mice revealed significantly increased

percentages of $CD11b^{+}Ly6C^{-}Ly6G^{+}Arg\text{-}1^{+}$ cells compared to radiation alone. These finding suggest that soy isoflavones supplementation in mice receiving a single dose of thoracic radiation promotes Arg-1 expression in a granulocytic subset of MDSCs in the lung at an early point after irradiation.

In order to determine if this early promotion of Arg-1 in granulocytic MDSCs mediated by soy isoflavones results in downstream immunosuppression at a later time point, we measured the effect of soy isoflavones treatment on pro-inflammatory cytokines levels in lung homogenates at 4 weeks post-radiation. Inflammatory cytokines are implicated in radiation-induced pneumonitis and fibrosis (30, 162). We found that soy isoflavones significantly reduced the levels of the radiation-induced pro-inflammatory cytokines IL-1β, IL-6, and TNF-α at 4 week post-radiation. These studies indicate that the early promotion of $Arg\text{-}1^{+}$ granulocytic-MDSCs by soy isoflavones in irradiated lung may result in the later inhibition of radiation-induced inflammatory cytokine release.

Arg-1 was shown to attenuate inflammatory cytokine expression in a rabbit model of atherosclerosis (163). Wang *et. al.* reported that upregulation of Arg-1 resulted in significantly decreased macrophage infiltration and inflammation in atherosclerotic plaques, corroborating our findings of soy radioprotection in lungs. In summary, our pre-clinical study in lung suggests that a radioprotective mechanism of soy isoflavones could involve the promotion of granulocytic myeloid-derived suppressor cells that express Arg-1 after radiation, resulting in subsequent downregulation of tissue damaging inflammation.

CHAPTER 4

Molecular Mediators of Radioprotection of Lung Tissue by Soy Isoflavones

ABSTRACT

Radiation-induced lung injury results from a cascade of inflammatory processes leading to clinical pneumonitis and fibrosis. Our lab has previously reported that treatment with soy isoflavones mitigates inflammation and fibrosis but the mechanism of radioprotection was unclear. In this final chapter, we investigate molecular mediators of radiation-induced inflammation modulated by soy isoflavones that protect lung tissue from injury in naïve mice. BALB/c mice received a single 10 Gy thoracic irradiation with soy isoflavones given orally at 1 mg/day, prior-to and continuously after radiation. Lungs were resected at different time points up to 18 weeks after radiation and processed for histology, western blot, and ELISA. E-cadherin, a cell adhesion molecule important airway epithelium barrier function, was assessed by IHC. Lung homogenates were processed to determine cytokine expression by ELISA and expression of NF-κB p65 by western blot. At 4 weeks post-irradiation, E-cadherin positive staining was decreased in areas of thickened septa while considerably higher levels of E-cadherin were observed following radiation + soy treatment, compared to radiation-treated lungs. Soy isoflavones modulated radiation-induced Th1/M1 pro-inflammatory cytokines more so than Th2/M2 cytokines. NF-κB p65 transcription factor subunit that plays a role in promoting inflammation was upregulated by radiation and decreased in lungs from mice treated with radiation and soy. These findings suggest that a mechanism of radioprotection by soy isoflavones involves the

regulation of radiation-induced molecular inflammatory events caused by the destruction of normal lung tissue.

INTRODUCTION

Radiation-induced pneumonitis and fibrosis is initiated by an inflammatory response triggered by tissue and cell damage that results in the cyclical induction of pro-inflammatory cytokines and chemokines which recruit inflammatory immune cells in the lung tissue and drive RILI pathogenesis (23, 29, 30). In a pre-clinical lung cancer model, we showed that supplementation with a mixture of soy isoflavones given pre- and post-thoracic irradiation mitigated the vascular damage, inflammation and fibrosis caused by high dose radiation injury to lung tissue, suggesting that soy can alter the radiation-induced inflammatory response (36, 134). In chapters 2 and 3 of this dissertation, we demonstrate that soy isoflavones inhibit radiation-induced macrophage and neutrophil infiltration and activation, while promoting immunosuppressive function of granulocytic MDSCs that are depleted in irradiated lungs. This chapter investigates the molecular mediators of inflammation modulated by soy isoflavones that protect lung tissue from radiation-induced injury in naïve mice.

Thoracic radiation therapy can damage the lung epithelial barrier integrity by interrupting adherens junctions that bind cells together within this organ. E-cadherin is a cell-cell adhesion molecule critical for the maintenance of tight junctions between cells of the airway epithelium (48). Decreased E-cadherin expression in the lung would be indicative of a disrupted epithelial barrier, which can result in the recruitment of inflammatory cellular and molecular mediators and drive chronic inflammation. Thus, the effect of soy isoflavones on the expression of E-cadherin in irradiated lung tissue was investigated.

Soy isoflavones have been shown to have anti-inflammatory properties in chronic inflammation and cardiovascular disease (164). Chacko *et. al.* demonstrated that anti-

inflammatory mechanisms of soy isoflavones include modulation of leukocyte-endothelial cell interactions in an *in vitro* blood flow assay as well as pro-inflammatory cytokine inhibition that was dependent on activation of peroxisome proliferator-activated receptor (PPAR-γ) (107). Genistein has been shown to down-regulate cytokine-induced pro-inflammatory pathways in human brain microvascular endothelial cells (106). The microenvironment in which a cytokine is released contributes to the function of that particular cytokine. Therefore, the timing and context of the milieu into which a particular cytokine is released determines functional outcome.

In chapters 2 and 3, we focused on cellular mediators of radioprotection by soy isoflavones in normal lung. In this final chapter, we further study the modulation of inflammatory response by soy isoflavones in irradiated lungs by investigating potential molecular mechanisms involved in soy radioprotection.

MATERIALS AND METHODS

Mice

Female BALB/c mice (Harlan, Indianapolis, IN) 5-6 weeks old, were housed and handled in animal facilities accredited by the Association for Assessment and Accreditation of Laboratory Animal Care. The animal protocol was approved by Wayne State University Institutional Animal Care and Use Committee.

Soy isoflavones

The soy isoflavone mixture G-4660 used is a pure extract of 98.16% isoflavones from soybeans consisting of 83.3% genistein, 14.6% daidzein and 0.26% glycitein (manufactured by Organic Technologies and obtained from the National Institutes of Health [NIH], Bethesda, MD). The soy isoflavone mixture was dissolved in DMSO and mixed with sesame seed oil at a 1:20 ratio just prior to treatment to facilitate gavage and avoid irritation of the esophagus by DMSO (36, 134, 135).

Lung irradiation

Radiation was delivered to the thoracic cage comprising the whole lung. Three anesthetized mice, in jigs, were positioned under a 6.4 mm lead shield with 3 cut-outs in an aluminum frame mounted on the X-ray machine to permit selective irradiation of the lung in 3 mice at a time, as previously described (134). The radiation dose to the lung and the scattered dose to areas of the mouse outside of the radiation field were carefully monitored. To minimize backscattering of radiation, the bottom of the aluminum frame that holds the jigs was hollowed

out and the backplate of the jig was thinned to 1.6mm thickness. Under these conditions and the lead shielding, the X ray dose to the shielded regions was reduced to 1% of the dose to the irradiated field. The dose rate was 101 cGy/min and half value layer was 2 mm Cu. Photon irradiation was performed at a dose of 10 Gy with a Siemens Stabilipan X-ray set (Siemens Medical Systems, Inc., Erlangen, Germany) operated at 250 kV, 15 mA with 1 mm copper filtration at a distance of 47.5 cm from the target.

Experimental Design

Mice were pre-treated with oral soy isoflavones each day for 3 days at a dose of 5mg/day (equivalent to 250mg/kg). Then, the lung was selectively irradiated with 10 Gy. Soy treatment was continued on a daily basis for 5 more days at 5mg/day. Then mice were treated with a lower soy dose of 1mg/day (equivalent to 50mg/kg), given daily 5 days a week for up to 18 weeks. The rationale for giving a higher dose of soy isoflavones for pre-treatment and just after radiation is to optimize the effect of soy, based on previous studies (36, 140). At different time points, separate mice from each treatment group were either homogenized for ELISA, snap frozen for western blot, or mice were used to fix lungs *in situ* with formalin for histology studies as detailed below.

Preparation of Lung Tissue Protein Lysates and Western Blot Analysis

Mice were sacrificed at 12 and 18 weeks post-irradiation. Lungs were resected and snap frozen. To prepare lung tissue protein lysates, frozen lungs were thawed, weighed, and homogenized in 10% w/v of lysis buffer using a gentleMACS tissue dissociator (Miltenyi Biotec, Bergisch, Germany). The suspension was centrifuged at 4000 x g for 5 minutes at 4°C and the

protein extracts were frozen at -80°C until analysis. For western blot analysis, total lung protein extracts (50 µg) were loaded and separated on 10% sodium dodecyl sulfate polyacrylamide gel electrophoresis (SDS-PAGE) and transferred to Whatman membranes (GE Healthcare Life Sciences, Pittsburgh, PA). Membranes were incubated with anti-NF-κB p65 antibody (eBioscience, Sn Diego, CA; 1:200) overnight at 4°C. Membranes were washed and incubated with horseradish peroxidase-conjugated secondary antibody (Vector Labs, 1:2000) at room temperature for 1 hour. Immunoreactive protein bands were visualized by SuperSignal West Pico Chemiluminescent Substrate (Thermo Scientific, Waltham, MA) and captured on a digital imaging system (Fotodyne Inc., Hartland, WI). Membranes were re-probed with anti-β-actin Ab as a loading control.15

Immunohistochemistry (IHC)

Mice were sacrificed and lungs were intratracheally instilled with 10% buffered formalin and resected, embedded in paraffin, and sectioned. Sections were blocked with IHC Tek Antibody Diluent (IHC World, Woodstock, MD) then incubated with primary purified monoclonal antibodies directed against epithelial cadherin (E-cadherin) or peroxisome proliferator-activated receptor (PPAR-γ) (eBioscience, San Diego, CA) overnight at 4° C. Lung sections were then incubated with biotinylated secondary antibodies (Vector Labs, Burlingame, CA) at 1:300 for 1 hour at room temperature. Staining was amplified with the avidin-biotin system Vectastain ABC Reagent Kit (Vector Labs) and visualized with the Vector DAB Substrate Kit for peroxidase (Vector Labs). Sections were counterstained with IHC-Tek Mayer's Hematoxylin (IHC World, Woodstock, MD) and mounted with Permount mounting media

(Electron Microscopy Sciences, Hatfield, PA). Arg-1 expression in lung tissue after radiation was evaluated on a Nikon E800 microscope (Nikon Inc., Melville, NY).

Enzyme-linked immunosorbant assay (ELISA)

Mice were sacrificed at various time points between 0-18 weeks post-irradiation. Lungs were resected and snap frozen. To prepare lung homogenates, frozen lungs were thawed, weighed, and homogenized in 10% w/v of phosphate buffered saline (PBS) with Complete Protease Inhibitor Cocktail Tablets (Roche Diagnostics, Indianapolis, IN) using a gentleMACS tissue dissociator (Miltenyi Biotec, San Diego, CA). The suspension was centrifuged at 4000 x g for 5 minutes at 4°C and the supernatant was frozen at -80°C. Lung homogenates were assayed IL-1α, IL-1β, IL-4, IL-6, IL-10, IL-13, IL-15, IL-17A, TNF-α, TGF-β, IFN-γ, and CCL2 using the respective Ready-SET-GO ELISA kits (eBioscience, San Diego, CA) according to manufacturer's instructions.

RESULTS

Effect of radiation and soy isoflavones on E-cadherin levels in lung tissue. Radiation can compromise endothelial and epithelial cell barrier integrity by interrupting adherens junctions that bind cells together within tissues. E-cadherin is an adhesion molecule expressed on epithelial cells (48). We previously showed that radiation-induced cytokines were decreased by soy isoflavones at 4 weeks post-irradiation, and thus we aimed to determine whether radiation affected cell barrier integrity at this same time point. Lung tissue sections were obtained from control mice and mice treated with radiation or radiation + soy isoflavones at 4 weeks after radiation and stained by IHC with E-cadherin. Staining of E-cadherin showed that radiation caused a pronounced loss in positive staining in areas of thickened septa (Figure 4.1). In contrast, following radiation + soy isoflavones treatment, considerably higher levels of positive staining for E-cadherin were observed, compared to radiation-treated lungs (Figure 4.1).

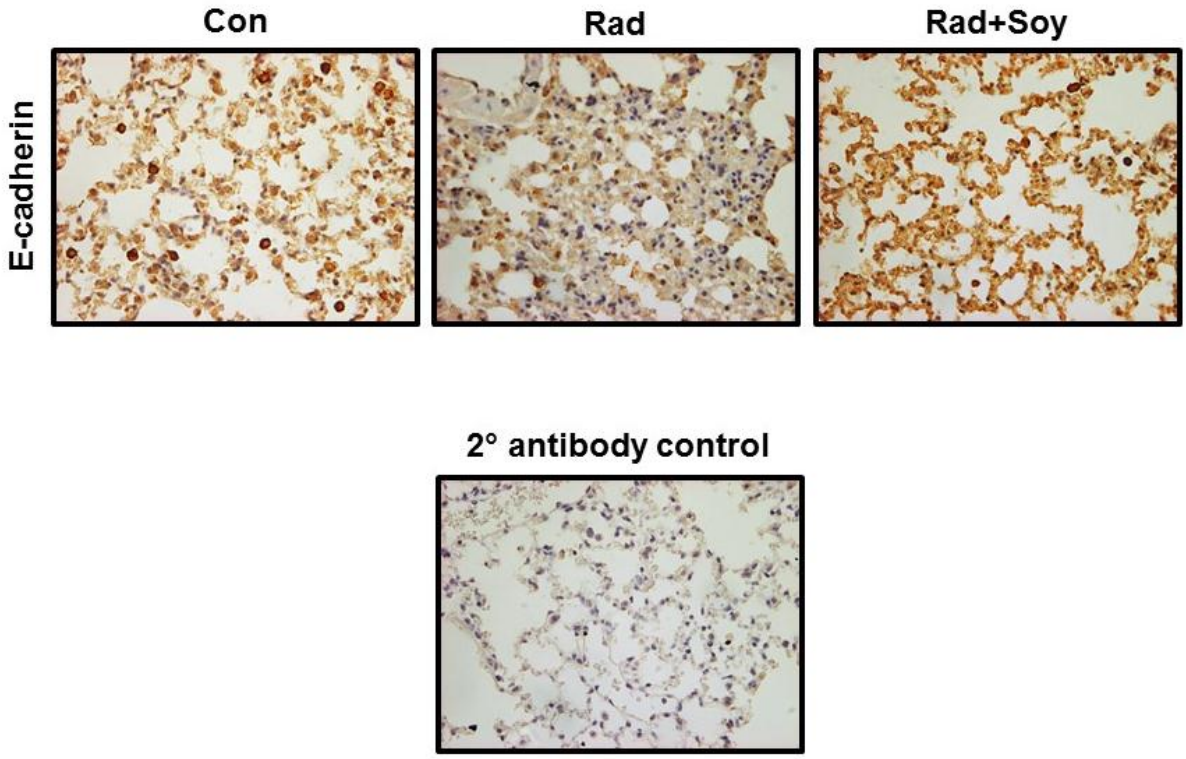

Figure 4.1. *In situ* detection of E-cadherin in lung tissue at 4 weeks after radiation ± soy isoflavones. Lungs tissue sections were obtained from control (Con) mice and mice treated with radiation (Rad) or radiation + soy (Rad+Soy) at 4 weeks after radiation. Sections were stained by IHC for E-cadherin to detect expression *in situ*. Staining of E-cadherin showed that radiation caused a pronounced decrease in positive staining in areas of thickened septa at 4 weeks after radiation. In contrast, following radiation + soy treatment, considerably higher levels of positive staining for E-cadherin were observed, compared to radiation-treated lungs. Secondary antibody alone is shown as a staining control. All magnifications are at 40x.

Effect of radiation and soy isoflavones on cytokine levels in lung tissue. The effect of soy isoflavones on the kinetics of molecular meditors of the immune system triggered by radiaiton were evaluated in lungs. Cytokine and chemokine levels following radiation were measured over time by ELISA in lung homogenates obtained mice. Pro-inflammatory cytokine levels associated with Th1/M1 immune responses were evaluated over time after a single dose of thoracic radiation (Figure 4.2). Soy isoflavones inhibited pro-inflammatory cytokines induced by radiation, including IL-1β, IL-6, TNF-α, and IFN-γ (Figure 4.2). Additionally, treatment with soy isoflavones increased IL-1β and IFN-γ at early time points of 4-24 hours post-radiation, which could play an anti-fibrotic role in the irradiated lung (Figure 4.2). There are minimal differences in the kinetics of cytokines and chemokine levels associated with Th2/M2 immune responses in lungs harvested from mice treated with radiation compared to radiation + soy (Figure 4.3).

Cytokine and chemokine levels in lungs from mice receiving daily soy isoflavones treatment or age matched controls revealed that, in general, soy isoflavones alone did not alter the cytokine or chemokine profile (Figure 4.4). This finding implies that soy isoflavones tend to modulate the immune system once an inflammatory insult has triggered the activation of pathways assoaciated with inflammation in cells and tissues.

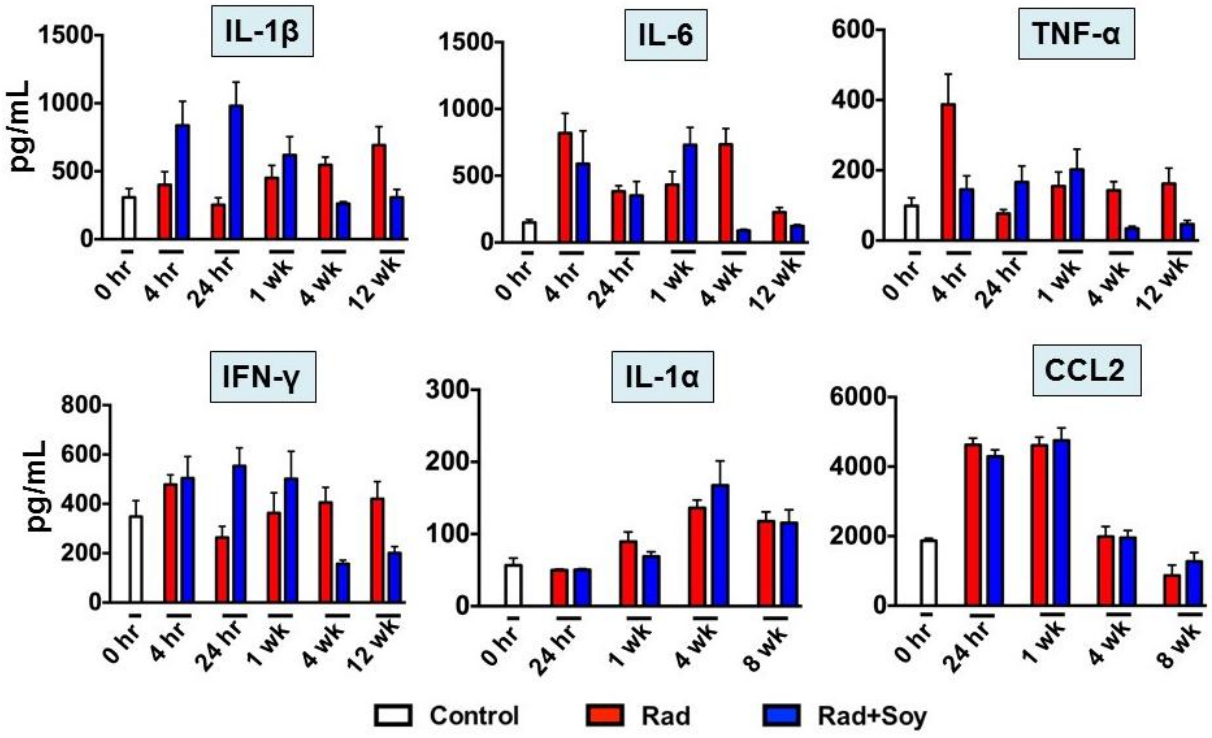

Figure 4.2. Effect of soy isoflavones on the kinetics of Th1/M1 anti-inflammatory cytokine profile in irradiated lung tissue. Cytokine and chemokine levels associated with Th1/M1 immune responses following radiation were measured over time by ELISA in lung homogenates obtained from mice.

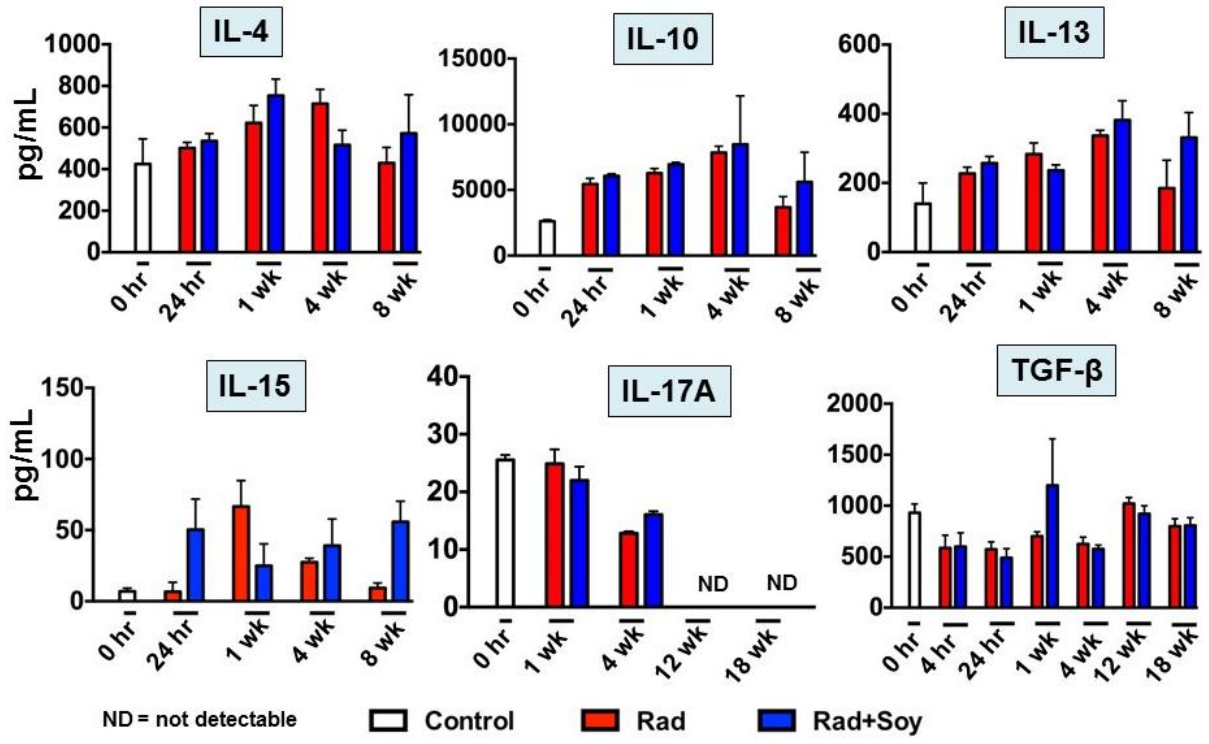

Figure 4.3. Effect of soy isoflavones on the kinetics of Th2/M2 anti-inflammatory cytokine profile in irradiated lung tissue. Cytokine levels associated with Th2/M2 immune responses following radiation were measured over time by ELISA in lung homogenates obtained from mice. ND = not detectable.

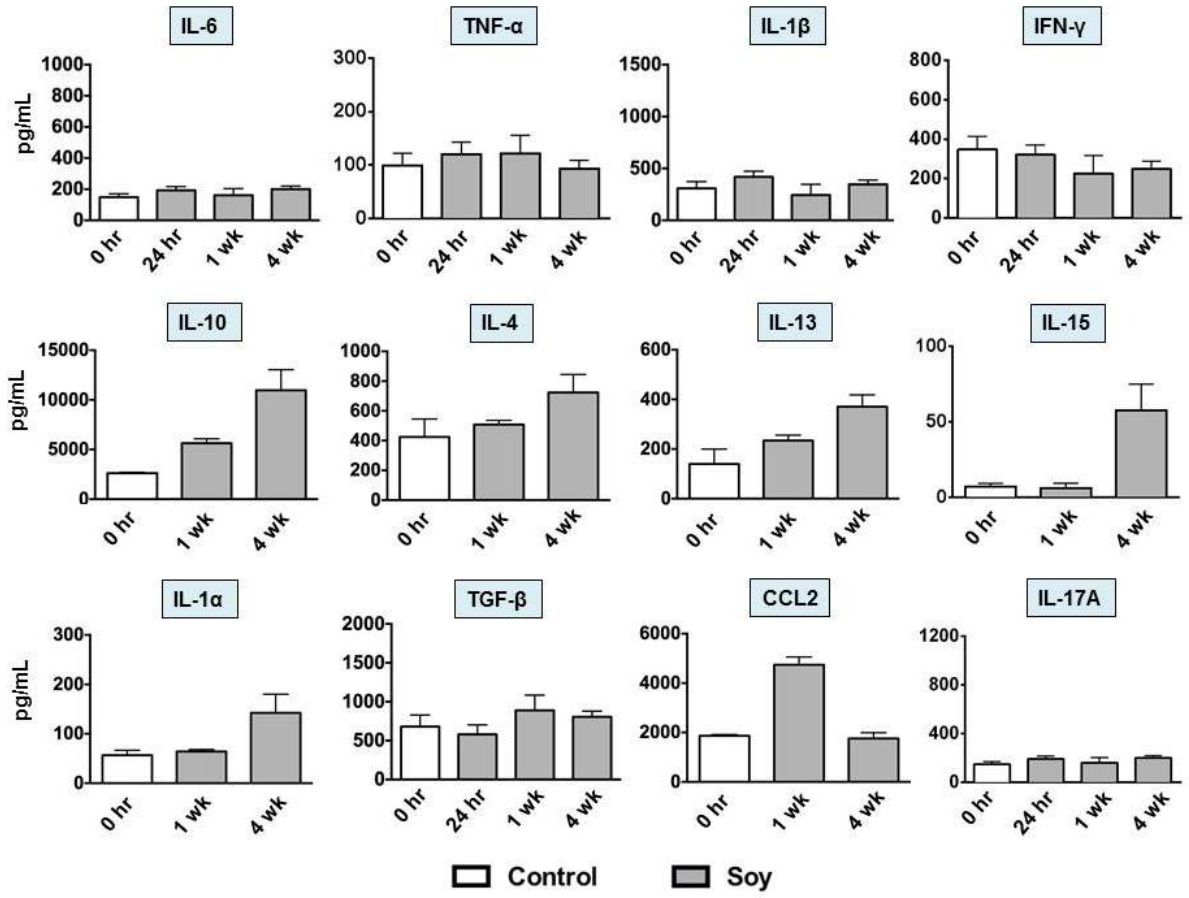

Figure 4.4. Effect of soy isoflavones treatment on homeostatic cytokine profile in lung tissue. Cytokine and chemokine levels associated with Th1/M1 or Th2/M2 immune responses were measured over time by ELISA in lung homogenates obtained mice receiving daily soy isoflavones treatment or age matched controls. In general, soy isoflavones alone did not alter the cytokine or chemokine profile.

Effect of radiation and soy isoflavones on PPAR-γ in lung tissue. PPAR-γ plays a role in M2 macrophage differentiation and activation (165). Expression of PPAR-γ in whole lung tissue as determined by western blot was increased after in both radiation-treated and radiation + soy-treated lungs (Figure 4.5A). To further evaluate the effect of soy isoflavones on the radiation-induced increase of PPAR- γ in lungs, tissue sections were obtained from control mice and mice treated with radiation or radiation + soy isoflavones at 18 weeks after radiation and stained with PPAR- γ. Interestingly, soy isoflavones altered cellular localization of PPAR-γ in alveolar macrophages at 18 weeks post-radiation. Alveolar macrophages showed cytoplasmic localization of PPAR-γ following radiation, in contrast to nuclear localization following supplementation with soy isoflavones (Figure 4.5B). Radiation caused a marked increase in PPAR-γ^{+} macrophages in thickened alveolar septa areas and spaces. Numerous alveolar macrophages showing the morphology of activated macrophages were particularly enlarged with abundant positive cytoplasmic staining compared to small macrophages in control lungs (arrows). The density of PPAR-γ^{+} macrophages was much lower in radiation + soy treated lungs at 18 weeks after radiation compared to radiation–treated lungs. Alveolar macrophages were also smaller, resembling those of control lungs and PPAR-γ positivity was more prominent in the nucleus rather than the cytoplasm, as compared to radiation–treated lungs.

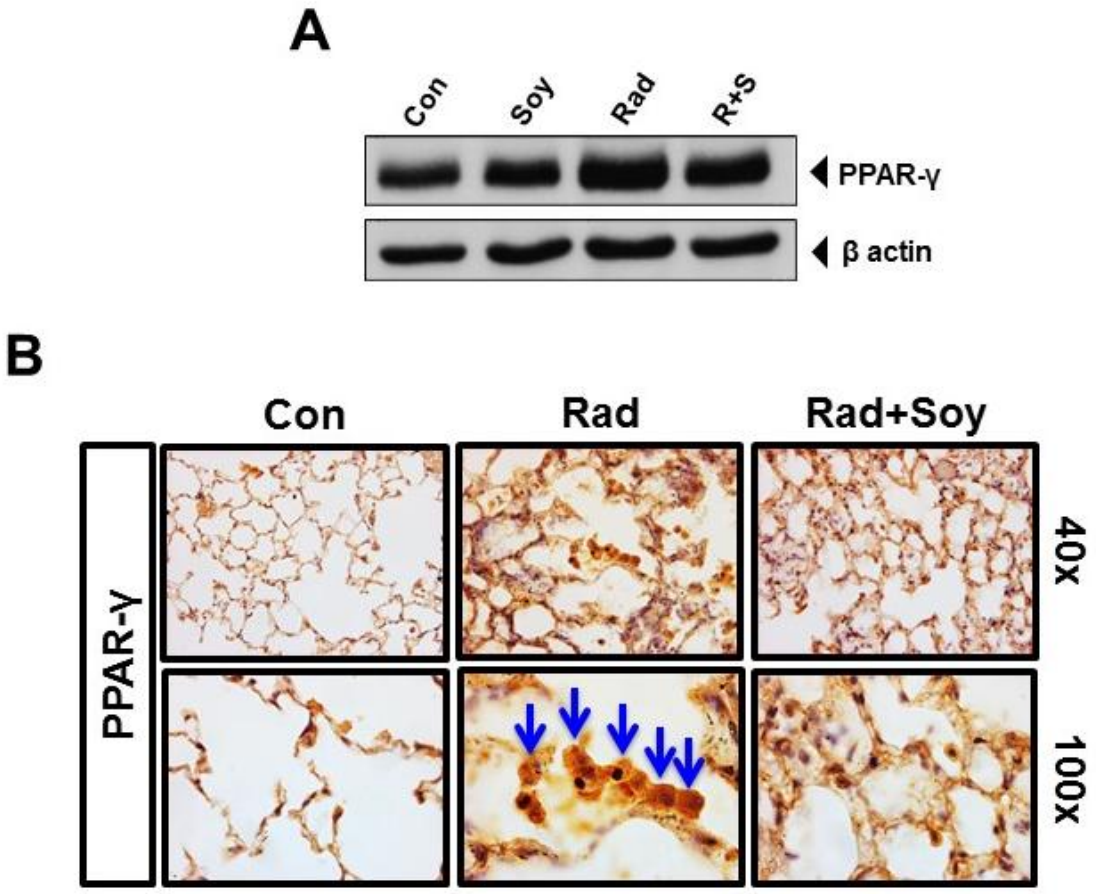

Figure 4.5. Soy isoflavones alter cellular localization of PPAR-γ in alveolar macrophages at 18 weeks post-radiation. (A). Western blot analysis of PPAR-γ on whole tissue lysates obtained from lungs showed an increase induced by radiation, including in irradiate lungs treated with soy isoflavones. Band intensities were quantified using ImageJ (NIH) densitometry analysis. (B). Lung tissue sections were obtained from control (Con) mice and mice treated with radiation (Rad) or radiation + soy (Rad+Soy) at 18 weeks after radiation. Lung sections were stained by IHC for PPAR-γ. Arrows indicate intense cytoplasmic PPAR-γ staining of alveolar macrophages. Radiation caused a marked increase in PPAR-γ^+ macrophages in thickened areas of septa and in alveolar spaces. Numerous alveolar macrophages showing the morphology of activated macrophages were particularly enlarged with abundant positive cytoplasmic staining compared to small macrophages in control lungs (arrows). The density of PPAR-γ^+ macrophages was much lower in radiation + soy treated lungs at 18 weeks after radiation compared to radiation–treated lungs. Alveolar macrophages were also smaller, resembling those of control lungs and PPAR-γ positivity was more prominent in the nucleus compared to radiation–treated lungs.

Effect of radiation and soy isoflavones on NF-κB in lung tissue. NF-κB promotes M1 macrophage pro-inflammatory gene expression (166), and we have reported that radiation upregulates that constitutively active NF-κB is in prostate cancer cells (167). Western blot analysis of normal lung tissue obtained from mice treated with radiation and/or soy isoflavones revealed that NF-κB levels were increased by radiation and was inhibited by the addition of soy isoflavones at 12 weeks (Figure 4.6A) and 18 weeks (Figure 4.6B) post-radiation.

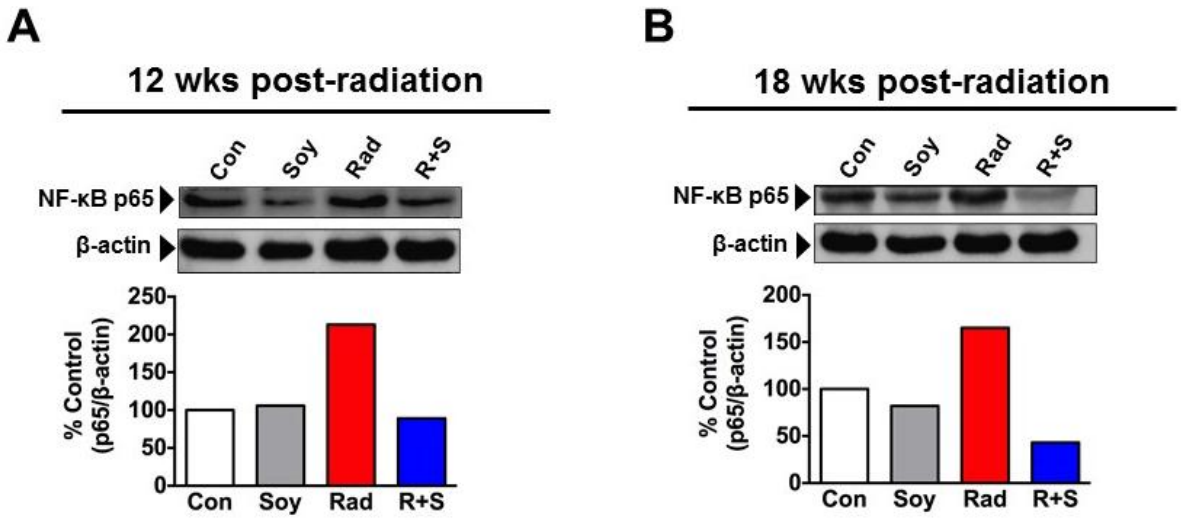

Figure 4.6. Soy isoflavones inhibit radiation-induced increase of NF-κB p65 subunit levels in lung tissue. Lungs tissue sections were obtained from control (Con) mice and mice treated with radiation (Rad) or radiation + soy (Rad+Soy) at 12 and 18 weeks after radiation. (A). Western blot analysis of NF-κB p65 on whole tissue lysates obtained from lungs at 12 weeks post-radiation showed an increase induced by radiation, which was inhibited by the addition of soy isoflavones. (B). An increase in NF-κB p65 was also observed at 18 weeks post-radiation, and an even more dramatic decrease in NF-κB p65 levels was detected in the lung at this later time point with the addition of soy isoflavones. Band intensities were quantified using ImageJ (NIH) densitometry analysis.

DISCUSSION

Radiation can compromise endothelial and epithelial cell barrier integrity by interrupting adherens junctions that bind cells together within tissues. E-cadherin is a cell-cell adhesion molecule expressed on epithelial cells (48). Normal expression of E-cadherin is critical for the maintenance of tight junctions between epithelial cells and for maintenance of normal barrier function of airway epithelium. A reduction in the lung expression of E-cadherin is indicative of a damaged, disrupted epithelial barrier that can drive recruitment of inflammatory cells and promote a cascade of damage-associated molecular events and chronic inflammation. At 4 weeks post-irradiation, we found a pronounced loss in E-cadherin in areas of thickened septa by IHC. In contrast, following radiation + soy treatment, considerably higher levels of positive staining for E-cadherin were observed, compared to radiation-treated lungs. These data suggest that soy isoflavones maintain the cell-cell junctions important for proper tissue integrity in normal lung that are damaged by thoracic irradiation.

Cytokine levels in lung homogenates of irradiated mice increase by 3-6 hours after radiation in correlation with levels measured in serum (162). The microenvironment in which a cytokine is released contributes to the function of that particular cytokine. Therefore, the timing and context of the milieu that a particular cytokine is released in determines functional outcome. The cytokine TGF-β is a canonical cytokine involved in driving fibrosis (168), whereas the cytokines IL-1β, IFN-γ, and TNF-α can play an anti-fibrotic role (169, 170). Interestingly, our model did not reveal a radiation-induced increase in TGF-β after radiation, even at a late time point of 18 week post-radiation, indicating that TGF-β may not play a pivotal role in RILI and fibrosis in our model.

Nuclear factor κB (NF-κB) activation is a molecular common denominator between inflammation and cancer (108). This transcription factor is constitutively active in a large number of cancers and is critical for tumor cell survival. Our lab has previously shown that soy isoflavones target critical survival pathways that are upregulated or constitutively activated in cancer cells, including NF-κB, which are responsible for the transcription (109). In contrast, normal cells do not constitutively express NF-κB, and activation of this transcription factor is important for the expression of pro-inflammatory gene programs. We confirmed *in vivo* in naïve mice that soy isoflavones inhibited radiation-induced NF-κB increase in the lung at 12 and 18 weeks post-irradiation. NF-κB promotes M1 macrophage pro-inflammatory gene expression (166). Peroxisomal proliferator-activated receptors (PPAR-α, β, δ, and γ) are ligand-activated transcription factors that heterodimerize with retinoid X receptor (RXR) to results gene expression (171). Promoting PPAR-γ activation by its cognate ligands have been shown to mitigate lung injury and fibrosis (172, 173). Soy isoflavones, in particular genistein, are known PPAR-γ ligands (174). PPAR-γ can influence the downregulation of pro-inflammatory mediators via trans-repression of NF-κB (175). Soy isoflavones may promote anti-inflammatory gene expression programs in the lung after thoracic radiation by interacting with PPAR-γ and downregulation of NF-κB.

In summary, our pre-clinical study in lung suggests that a radioprotective mechanism of soy isoflavones could involve the promotion of intact epithelial and endothelial tight junctions that are damaged after radiation via E-cadherin, resulting in subsequent downregulation of tissue damaging inflammation. Additionally, soy isoflavones may downregulate pro-inflammatory gene programs and cytokine expression upregulated by radiation-induced increases of NF-κB in

normal tissue, while promoting anti-inflammatory or repair pathways via the interaction of soy isoflavones with PPAR-γ.

GENERAL CONCLUSIONS

Chemoradiotherapy is currently the standard of care for unresectable locally advanced non-small cell lung carcinoma (NSCLC). However, the treatment success for this patient population has been severely constrained by post-therapy toxicity, presenting as pneumonitis and later fibrosis (176, 177). Conventional fractionated radiotherapy is associated with normal tissue side effects and poor quality of life (22). Hypofractionated radiotherapy is an emerging modality for early-stage lung cancer, which can utilize a high radiation dose per fraction over a relatively short time period to improve effectiveness of tumor destruction and increase convenience by reducing the number of visits for therapy (178-180). However, high intensity radiotherapy can also be associated with greater damage to lung tissue, emphasizing the need to develop complementary approaches to alleviate radiation-induced injury to normal lung structures and function (60).

Our pre-clinical murine studies (36, 134, 135) have already revealed that oral administration of a mixture of the soy isoflavones genistein, daidzein, and glycitein can enhance lung tumor eradication and simultaneously protect normal lung from radiation injury. While the anti-oxidant and disease preventative effects of a soy-rich diet have been investigated, prior to this dissertation project an immune-mediated mechanism of radioprotection by soy isoflavones in normal tissues remained to be elucidated.

This dissertation has focused on investigating mechanisms of radioprotection mediated by soy isoflavones in normal lung tissue by dissecting the effect of soy supplementation on the radiation-induced inflammatory responses and immunosuppressive and repair pathways in irradiated lungs. Radiation therapy triggers a potent inflammatory response is a key contributor

to the tissue-damaging pathology of RILI. Our preclinical studies in lung cancer models and naïve mice indicate that soy isoflavones inhibit this inflammatory process or even promote tissue repair.

In summary, our pre-clinical studies in lung suggest that a radioprotective mechanism of soy isoflavones likely involves both the inhibition of infiltration and activation of macrophages and neutrophils in irradiated lungs as well as the promotion of immunosuppressive myeloid-derived suppressor cells (Figure 5). Soy isoflavones inhibited the radiation-induced infiltration and activation of macrophages and neutrophils in the lung, and polarized lung macrophages from M1 to M2 macrophage phenotype. Soy inhibited alveolar macrophage activation in bronchoalveolar spaces induced by radiation and had a protective effect on regulatory interstitial macrophages that could participate in maintaining lung homeostasis and control inflammation and tissue damage. We also show that treatment with soy isoflavones downregulates pro-inflammatory gene programs and cytokine expression that are upregulated by radiation-induced increases of NF-κB in normal tissue, and may upregulating anti-inflammatory pathways via the interaction of isoflavones with PPAR-γ. Furthermore, soy isoflavones also promoted intact epithelial and endothelial tight junctions via E-cadherin that are damaged after radiation and granulocytic myeloid-derived suppressor cells that express Arg-1 after radiation, resulting in subsequent dampening of tissue damaging inflammation. These findings serve as potential mechanisms of soy-mediated radioprotection in normal lung, contributing to the resolution of radiation-induced acute and chronic inflammation that lead to pneumonitis and fibrosis.

The clinical goal is to improve the therapeutic ratio of high-dose radiation therapy on the tumor target and reduce the radiation dose-limiting toxicity of radiation therapy to the normal lung. These findings suggest that soy isoflavones used as a complementary intervention to

radiotherapy for lung cancer could potentially reduce lung toxicity and provide improved therapeutic benefit to patients.

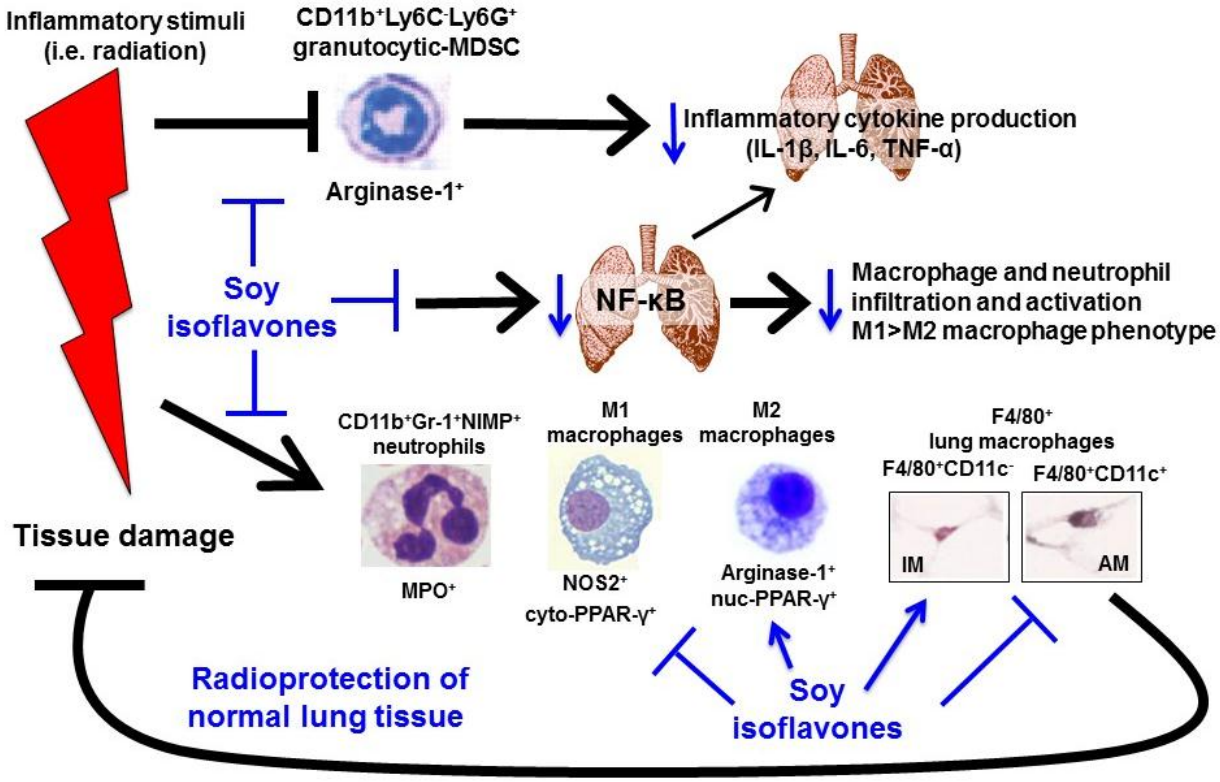

Figure 5. General conclusions and overall hypothesis. A single dose of thoracic irradiation triggers inflammatory responses in the lung that include increased NF-κB and pro-inflammatory cytokine production, as well as increases in the infiltration and activation of macrophages and neutrophils. Our findings suggest that soy can inhibit the infiltration and activation of macrophages and neutrophils induced by radiation in bronchoalveolar spaces and the lung parenchyma. Radiation induced a pro-inflammatory M1 macrophage phenotype in lungs, while mice receiving soy isoflavones and radiation switched to an anti-inflammatory M2 macrophage subtype. Soy isoflavones inhibited the radiation-induced upregulation of NF-κB and pro-inflammatory cytokine release in the lung. Soy isoflavones also had a protective effect on regulatory interstitial macrophages (IM) after irradiation and Arg-1^+ granulocytic MDSCs, while inhibiting alveolar macrophage (AM) activation induced by radiation. These data indicate that a mechanism of radioprotection by soy isoflavones in normal lung includes the modulation of innate immune cellular and molecular mediators of the inflammatory response induced by radiation.

REFERENCES

1. **Keane MP, Belperio JA, Henson PM, Strieter RM.** 2005. Inflammation, injury, and repair, p. 449-490. *In* Murray JF, Nadel JA, Mason RJ, Broaddus VC (ed.), Textbook of respiratory medicine, 4th ed. Elsevier Saunders, Philadelphia, PA.
2. **Effros RM.** 2006. Anatomy, development, and physiology of the lungs. GI Motility online.
3. **Tschernig T, Pabst R.** 2009. What is the clinical relevance of different lung compartments? BMC Pulm Med **9:**39.
4. **Martin TR, Frevert CW.** 2005. Innate immunity in the lungs. Proc Am Thorac Soc **2:**403-411.
5. **Hussain AN.** 2006. Immune system of the lungs, p. 366-368, Pathologic Basis of Disease.
6. **Guilliams M, De Kleer I, Henri S, Post S, Vanhoutte L, De Prijck S, Deswarte K, Malissen B, Hammad H, Lambrecht BN.** 2013. Alveolar macrophages develop from fetal monocytes that differentiate into long-lived cells in the first week of life via GM-CSF. J Exp Med **210:**1977-1992.
7. **Lambrecht BN.** 2006. Alveolar macrophage in the driver's seat. Immunity **24:**366-368.
8. **Holt PG.** 1978. Inhibitory activity of unstimulated alveolar macrophages on T-lymphocyte blastogenic response. Am Rev Respir Dis **118:**791-793.
9. **Roberts LM, Ledvina HE, Tuladhar S, Rana D, Steele SP, Sempowski GD, Frelinger JA.** 2015. Depletion of alveolar macrophages in CD11c diphtheria toxin receptor mice produces an inflammatory response. Immun Inflamm Dis **3:**71-81.

10. **Kruger P, Saffarzadeh M, Weber AN, Rieber N, Radsak M, von Bernuth H, Benarafa C, Roos D, Skokowa J, Hartl D.** 2015. Neutrophils: Between host defence, immune modulation, and tissue injury. PLoS Pathog **11:**e1004651.

11. **Summers C, Rankin SM, Condliffe AM, Singh N, Peters AM, Chilvers ER.** 2010. Neutrophil kinetics in health and disease. Trends Immunol **31:**318-324.

12. **Ringborg U, Bergqvist D, Brorsson B, Cavallin-Stahl E, Ceberg J, Einhorn N, Frodin JE, Jarhult J, Lamnevik G, Lindholm C, Littbrand B, Norlund A, Nylen U, Rosen M, Svensson H, Moller TR.** 2003. The Swedish Council on Technology Assessment in Health Care (SBU) systematic overview of radiotherapy for cancer including a prospective survey of radiotherapy practice in Sweden 2001--summary and conclusions. Acta Oncol **42:**357-365.

13. **Coggle JE, Lambert BE, Moores SR.** 1986. Radiation effects in the lung. Environ Health Perspect **70:**261-291.

14. **Stone HB, Coleman CN, Anscher MS, McBride WH.** 2003. Effects of radiation on normal tissue: consequences and mechanisms. Lancet Oncol **4:**529-536.

15. **Rubin P, Casarett GW.** 1968. Clinical radiation pathology as applied to curative radiotherapy. Cancer **22:**767-778.

16. **Dörr W.** 2009. Pathogenesis of normal-tissue side-effects, p. 169-190. *In* Joiner M, van der Kogel A (ed.), Basic Clinical Radiobiology Fourth Edition. CRC Press.

17. **Barnett GC, West CM, Dunning AM, Elliott RM, Coles CE, Pharoah PD, Burnet NG.** 2009. Normal tissue reactions to radiotherapy: towards tailoring treatment dose by genotype. Nat Rev Cancer **9:**134-142.

18. **van Meerbeeck JP, Meersschout S, De Pauw R, Madani I, De Neve W.** 2008. Modern radiotherapy as part of combined modality treatment in locally advanced non-small cell lung cancer: present status and future prospects. Oncologist **13:**700-708.

19. **Bradley JD, Bae K, Graham MV, Byhardt R, Govindan R, Fowler J, Purdy JA, Michalski JM, Gore E, Choy H.** 2010. Primary analysis of the phase II component of a phase I/II dose intensification study using three-dimensional conformal radiation therapy and concurrent chemotherapy for patients with inoperable non-small-cell lung cancer: RTOG 0117. J Clin Oncol **28:**2475-2480.

20. **Kelsey CR, Rosenstein BS, Marks LB.** 2012. Predicting toxicity from radiation therapy--it's genetic, right? Cancer **118:**3450-3454.

21. **Schallenkamp JM, Miller RC, Brinkmann DH, Foote T, Garces YI.** 2007. Incidence of radiation pneumonitis after thoracic irradiation: Dose-volume correlates. Int J Radiat Oncol Biol Phys **67:**410-416.

22. **Williams JP, Johnston CJ, Finkelstein JN.** 2010. Treatment for radiation-induced pulmonary late effects: spoiled for choice or looking in the wrong direction? Curr Drug Targets **11:**1386-1394.

23. **Kong FM, Hayman JA, Griffith KA, Kalemkerian GP, Arenberg D, Lyons S, Turrisi A, Lichter A, Fraass B, Eisbruch A, Lawrence TS, Ten Haken RK.** 2006. Final toxicity results of a radiation-dose escalation study in patients with non-small-cell lung cancer (NSCLC): predictors for radiation pneumonitis and fibrosis. Int J Radiat Oncol Biol Phys **65:**1075-1086.

24. **Robnett TJ, Machtay M, Vines EF, McKenna MG, Algazy KM, McKenna WG.** 2000. Factors predicting severe radiation pneumonitis in patients receiving definitive chemoradiation for lung cancer. Int J Radiat Oncol Biol Phys **48:**89-94.

25. **McDonald S, Rubin P, Phillips TL, Marks LB.** 1995. Injury to the lung from cancer therapy: clinical syndromes, measurable endpoints, and potential scoring systems. Int J Radiat Oncol Biol Phys **31:**1187-1203.

26. **Choi YW, Munden RF, Erasmus JJ, Park KJ, Chung WK, Jeon SC, Park CK.** 2004. Effects of radiation therapy on the lung: radiologic appearances and differential diagnosis. Radiographics **24:**985-997; discussion 998.

27. **Morgan GW, Breit SN.** 1995. Radiation and the lung: a reevaluation of the mechanisms mediating pulmonary injury. Int J Radiat Oncol Biol Phys **31:**361-369.

28. **Ghafoori P, Marks LB, Vujaskovic Z, Kelsey CR.** 2008. Radiation-induced lung injury. Assessment, management, and prevention. Oncology **22:**37-47; discussion 52-33.

29. **Hill RP.** 2005. Radiation effects on the respiratory system. The British Journal of Radiology **Supplement_27:**75-81.

30. **Bentzen SM.** 2006. Preventing or reducing late side effects of radiation therapy: radiobiology meets molecular pathology. Nat Rev Cancer **6:**702-713.

31. **Strieter RM.** 2008. What differentiates normal lung repair and fibrosis? Inflammation, resolution of repair, and fibrosis. Proc Am Thorac Soc **5:**305-310.

32. **Rubin P, Johnston CJ, Williams JP, McDonald S, Finkelstein JN.** 1995. A perpetual cascade of cytokines postirradiation leads to pulmonary fibrosis. Int J Radiat Oncol Biol Phys **33:**99-109.

33. **Burger A, Loffler H, Bamberg M, Rodemann HP.** 1998. Molecular and cellular basis of radiation fibrosis. Int J Radiat Biol **73:**401-408.

34. **Rubin P, Finkelstein J, Shapiro D.** 1992. Molecular biology mechanisms in the radiation induction of pulmonary injury syndromes: interrelationship between the alveolar macrophage and the septal fibroblast. Int J Radiat Oncol Biol Phys **24:**93-101.

35. **Tsoutsou PG, Koukourakis MI.** 2006. Radiation pneumonitis and fibrosis: mechanisms underlying its pathogenesis and implications for future research. Int J Radiat Oncol Biol Phys **66:**1281-1293.

36. **Hillman GG, Singh-Gupta V, Runyan L, Yunker CK, Rakowski JT, Sarkar FH, Miller S, Gadgeel SM, Sethi S, Joiner MC, Konski AA.** 2011. Soy isoflavones radiosensitize lung cancer while mitigating normal tissue injury. Radiother Oncol **101:**329-336.

37. **Franke-Ullmann G, Pfortner C, Walter P, Steinmuller C, Lohmann-Matthes ML, Kobzik L.** 1996. Characterization of murine lung interstitial macrophages in comparison with alveolar macrophages in vitro. J Immunol **157:**3097-3104.

38. **Laskin DL, Weinberger B, Laskin JD.** 2001. Functional heterogeneity in liver and lung macrophages. J Leukoc Biol **70:**163-170.

39. **Franko AJ, Sharplin J.** 1994. Development of fibrosis after lung irradiation in relation to inflammation and lung function in a mouse strain prone to fibrosis. Radiat Res **140:**347-355.

40. **Ricardo SD, van Goor H, Eddy AA.** 2008. Macrophage diversity in renal injury and repair. J Clin Invest **118:**3522-3530.

41. **Mosser DM, Edwards JP.** 2008. Exploring the full spectrum of macrophage activation. Nat Rev Immunol **8:**958-969.

42. **Barbul A.** 2008. Proline precursors to sustain Mammalian collagen synthesis. J Nutr **138:**2021S-2024S.

43. **Deonarine K, Panelli MC, Stashower ME, Jin P, Smith K, Slade HB, Norwood C, Wang E, Marincola FM, Stroncek DF.** 2007. Gene expression profiling of cutaneous wound healing. J Transl Med **5:**11.

44. **Grommes J, Soehnlein O.** 2011. Contribution of neutrophils to acute lung injury. Mol Med **17:**293-307.

45. **Bradley PP, Priebat DA, Christensen RD, Rothstein G.** 1982. Measurement of cutaneous inflammation: estimation of neutrophil content with an enzyme marker. J Invest Dermatol **78:**206-209.

46. **Haston CK, Begin M, Dorion G, Cory SM.** 2007. Distinct loci influence radiation-induced alveolitis from fibrosing alveolitis in the mouse. Cancer research **67:**10796-10803.

47. **Sener G, Jahovic N, Tosun O, Atasoy BM, Yegen BC.** 2003. Melatonin ameliorates ionizing radiation-induced oxidative organ damage in rats. Life Sci **74:**563-572.

48. **Takeichi M.** 1991. Cadherin cell adhesion receptors as a morphogenetic regulator. Science **251:**1451-1455.

49. **Kaur P, Asea A.** 2012. Radiation-induced effects and the immune system in cancer. Front Oncol **2:**191.

50. **Eckes B, Zigrino P, Kessler D, Holtkotter O, Shephard P, Mauch C, Krieg T.** 2000. Fibroblast-matrix interactions in wound healing and fibrosis. Matrix Biol **19:**325-332.

51. **Thannickal VJ, Toews GB, White ES, Lynch JP, 3rd, Martinez FJ.** 2004. Mechanisms of pulmonary fibrosis. Annu Rev Med **55:**395-417.

52. **Thompson HG, Mih JD, Krasieva TB, Tromberg BJ, George SC.** 2006. Epithelial-derived TGF-beta2 modulates basal and wound-healing subepithelial matrix homeostasis. Am J Physiol Lung Cell Mol Physiol **291:**L1277-1285.

53. **Khalil N, Bereznay O, Sporn M, Greenberg AH.** 1989. Macrophage production of transforming growth factor beta and fibroblast collagen synthesis in chronic pulmonary inflammation. J Exp Med **170:**727-737.

54. **Penn JW, Grobbelaar AO, Rolfe KJ.** 2012. The role of the TGF-beta family in wound healing, burns and scarring: a review. Int J Burns Trauma **2:**18-28.

55. **Vujaskovic Z, Groen HJ.** 2000. TGF-beta, radiation-induced pulmonary injury and lung cancer. Int J Radiat Biol **76:**511-516.

56. **Anscher MS, Kong FM, Andrews K, Clough R, Marks LB, Bentel G, Jirtle RL.** 1998. Plasma transforming growth factor beta1 as a predictor of radiation pneumonitis. Int J Radiat Oncol Biol Phys **41:**1029-1035.

57. **Fu XL, Huang H, Bentel G, Clough R, Jirtle RL, Kong FM, Marks LB, Anscher MS.** 2001. Predicting the risk of symptomatic radiation-induced lung injury using both the physical and biologic parameters V(30) and transforming growth factor beta. Int J Radiat Oncol Biol Phys **50:**899-908.

58. **De Jaeger K, Seppenwoolde Y, Kampinga HH, Boersma LJ, Belderbos JS, Lebesque JV.** 2004. Significance of plasma transforming growth factor-beta levels in radiotherapy for non-small-cell lung cancer. Int J Radiat Oncol Biol Phys **58:**1378-1387.

59. **Brizel DM.** 2007. Pharmacologic approaches to radiation protection. J Clin Oncol **25:**4084-4089.

60. **Prasanna PG, Stone HB, Wong RS, Capala J, Bernhard EJ, Vikram B, Coleman CN.** 2012. Normal tissue protection for improving radiotherapy: Where are the Gaps? Transl Cancer Res **1:**35-48.

61. **Citrin D, Cotrim AP, Hyodo F, Baum BJ, Krishna MC, Mitchell JB.** 2010. Radioprotectors and mitigators of radiation-induced normal tissue injury. Oncologist **15:**360-371.

62. **Kwok E, Chan CK.** 1998. Corticosteroids and azathioprine do not prevent radiation-induced lung injury. Can Respir J **5:**211-214.

63. **Ward HE, Kemsley L, Davies L, Holecek M, Berend N.** 1993. The effect of steroids on radiation-induced lung disease in the rat. Radiat Res **136:**22-28.

64. **Abratt RP, Morgan GW, Silvestri G, Willcox P.** 2004. Pulmonary complications of radiation therapy. Clin Chest Med **25:**167-177.

65. **Bonnans C, Chou J, Werb Z.** 2014. Remodelling the extracellular matrix in development and disease. Nat Rev Mol Cell Biol **15:**786-801.

66. **Okunieff P, Augustine E, Hicks JE, Cornelison TL, Altemus RM, Naydich BG, Ding I, Huser AK, Abraham EH, Smith JJ, Coleman N, Gerber LH.** 2004. Pentoxifylline in the treatment of radiation-induced fibrosis. J Clin Oncol **22:**2207-2213.

67. **Neuner P, Klosner G, Schauer E, Pourmojib M, Macheiner W, Grunwald C, Knobler R, Schwarz A, Luger TA, Schwarz T.** 1994. Pentoxifylline in vivo down-regulates the release of IL-1 beta, IL-6, IL-8 and tumour necrosis factor-alpha by human peripheral blood mononuclear cells. Immunology **83:**262-267.

68. **Oliveira-Junior IS, Pinheiro BV, Silva ID, Salomao R, Zollner RL, Beppu OS.** 2003. Pentoxifylline decreases tumor necrosis factor and interleukin-1 during high tidal volume. Braz J Med Biol Res **36:**1349-1357.

69. **Rube CE, Wilfert F, Uthe D, Schmid KW, Knoop R, Willich N, Schuck A, Rube C.** 2002. Modulation of radiation-induced tumour necrosis factor alpha (TNF-alpha) expression in the lung tissue by pentoxifylline. Radiother Oncol **64:**177-187.

70. **Ozturk B, Egehan I, Atavci S, Kitapci M.** 2004. Pentoxifylline in prevention of radiation-induced lung toxicity in patients with breast and lung cancer: a double-blind randomized trial. Int J Radiat Oncol Biol Phys **58:**213-219.

71. **Sweitzer NK.** 2003. Cardiology patient page. What is an angiotensin converting enzyme inhibitor? Circulation **108:**e16-18.

72. **Ward WF, Molteni A, Ts'ao CH.** 1989. Radiation-induced endothelial dysfunction and fibrosis in rat lung: modification by the angiotensin converting enzyme inhibitor CL242817. Radiat Res **117:**342-350.

73. **Kharofa J, Cohen EP, Tomic R, Xiang Q, Gore E.** 2012. Decreased risk of radiation pneumonitis with incidental concurrent use of angiotensin-converting enzyme inhibitors and thoracic radiation therapy. Int J Radiat Oncol Biol Phys **84:**238-243.

74. **Yuhas JM, Storer JB.** 1969. Differential chemoprotection of normal and malignant tissues. J Natl Cancer Inst **42:**331-335.

75. **Kouvaris JR, Kouloulias VE, Vlahos LJ.** 2007. Amifostine: the first selective-target and broad-spectrum radioprotector. Oncologist **12:**738-747.

76. **Komaki R, Lee JS, Kaplan B, Allen P, Kelly JF, Liao Z, Stevens CW, Fossella FV, Zinner R, Papadimitrakopoulou V, Khuri F, Glisson B, Pisters K, Kurie J, Herbst**

R, Milas L, Ro J, Thames HD, Hong WK, Cox JD. 2002. Randomized phase III study of chemoradiation with or without amifostine for patients with favorable performance status inoperable stage II-III non-small cell lung cancer: preliminary results. Semin Radiat Oncol **12:**46-49.

77. **Brizel DM, Wasserman TH, Henke M, Strnad V, Rudat V, Monnier A, Eschwege F, Zhang J, Russell L, Oster W, Sauer R.** 2000. Phase III randomized trial of amifostine as a radioprotector in head and neck cancer. J Clin Oncol **18:**3339-3345.

78. **Sanchez-Chino X, Jimenez-Martinez C, Davila-Ortiz G, Alvarez-Gonzalez I, Madrigal-Bujaidar E.** 2015. Nutrient and nonnutrient components of legumes, and its chemopreventive activity: a review. Nutrition and cancer **67:**401-410.

79. **Barnes S.** 2010. The biochemistry, chemistry and physiology of the isoflavones in soybeans and their food products. Lymphat Res Biol **8:**89-98.

80. **Kang J, Badger TM, Ronis MJ, Wu X.** 2010. Non-isoflavone phytochemicals in soy and their health effects. J Agric Food Chem **58:**8119-8133.

81. **Dakora FD, Joseph CM, Phillips DA.** 1993. Alfalfa (Medicago sativa L.) Root Exudates Contain Isoflavonoids in the Presence of Rhizobium meliloti. Plant Physiol **101:**819-824.

82. **Rolfe BG.** 1988. Flavones and isoflavones as inducing substances of legume nodulation. BioFactors (Oxford) **1:**3-10.

83. **Markiewicz L, Garey J, Adlercreutz H, Gurpide E.** 1993. In vitro bioassays of non-steroidal phytoestrogens. J Steroid Biochem Mol Biol **45:**399-405.

84. **Branham WS, Dial SL, Moland CL, Hass BS, Blair RM, Fang H, Shi L, Tong W, Perkins RG, Sheehan DM.** 2002. Phytoestrogens and mycoestrogens bind to the rat uterine estrogen receptor. J Nutr **132:**658-664.

85. **Messina M.** 2010. Isoflavones, p. 439-449. *In* Coates PM, Betz J, Blackman M, Cragg G, Levine M, Moss J, White J (ed.), Encyclopedia of Dietary Supplemets. Informa Healthcare, New York, NY.

86. **Shanle EK, Xu W.** 2011. Endocrine disrupting chemicals targeting estrogen receptor signaling: identification and mechanisms of action. Chem Res Toxicol **24:**6-19.

87. **Omoni AO, Aluko RE.** 2005. Soybean foods and their benefits: potential mechanisms of action. Nutr Rev **63:**272-283.

88. **Dakora FD, Phillips DA.** 1996. Diverse functions of isoflavonoids in legumes transcend anti-microbial definitions of phytoalexins. Physiological and Molecular Plant Pathology **49:**1-20.

89. **Hsu A, Bray TM, Helferich WG, Doerge DR, Ho E.** 2010. Differential effects of whole soy extract and soy isoflavones on apoptosis in prostate cancer cells. Exp Biol Med (Maywood) **235:**90-97.

90. **Raffoul JJ, Banerjee S, Che M, Knoll ZE, Doerge DR, Abrams J, Kucuk O, Sarkar FH, Hillman GG.** 2007. Soy isoflavones enhance radiotherapy in a metastatic prostate cancer model. Int J Cancer **120:**2491-2498.

91. **Hebert JR, Hurley TG, Olendzki BC, Teas J, Ma Y, Hampl JS.** 1998. Nutritional and socioeconomic factors in relation to prostate cancer mortality: a cross-national study. J Natl Cancer Inst **90:**1637-1647.

92. **Kuiper GG, Lemmen JG, Carlsson B, Corton JC, Safe SH, van der Saag PT, van der Burg B, Gustafsson JA.** 1998. Interaction of estrogenic chemicals and phytoestrogens with estrogen receptor beta. Endocrinology **139:**4252-4263.

93. **Banerjee S, Li Y, Wang Z, Sarkar FH.** 2008. Multi-targeted therapy of cancer by genistein. Cancer Letters **269:**226-242.

94. **Perabo FG, Von Low EC, Ellinger J, von Rucker A, Muller SC, Bastian PJ.** 2008. Soy isoflavone genistein in prevention and treatment of prostate cancer. Prostate Cancer Prostatic Dis **11:**6-12.

95. **Lee MM, Gomez SL, Chang JS, Wey M, Wang RT, Hsing AW.** 2003. Soy and isoflavone consumption in relation to prostate cancer risk in China. Cancer epidemiology, biomarkers & prevention : a publication of the American Association for Cancer Research, cosponsored by the American Society of Preventive Oncology **12:**665-668.

96. **Holzbeierlein JM, McIntosh J, Thrasher JB.** 2005. The role of soy phytoestrogens in prostate cancer. Curr Opin Urol **15:**17-22.

97. **Kurosu M.** 2011. Biologically Active Molecules from Soybeans. *In* El-Shemy H (ed.), Biologically Active Molecules from Soybeans, Soybean and Health.

98. **Day JK, Bauer AM, DesBordes C, Zhuang Y, Kim BE, Newton LG, Nehra V, Forsee KM, MacDonald RS, Besch-Williford C, Huang TH, Lubahn DB.** 2002. Genistein alters methylation patterns in mice. J Nutr **132:**2419S-2423S.

99. **Sit KH, Bay BH, Wong KP.** 1993. Effect of genistein, a tyrosine-specific protein kinase inhibitor, on cell rounding by pH upshifting. In Vitro Cell Dev Biol Anim **29A:**395-402.

100. **Coward L, Smith M, Kirk M, Barnes S.** 1998. Chemical modification of isoflavones in soyfoods during cooking and processing. Am J Clin Nutr **68:**1486S-1491S.

101. **Andres S, Abraham K, Appel KE, Lampen A.** 2011. Risks and benefits of dietary isoflavones for cancer. Crit Rev Toxicol **41:**463-506.

102. **Day AJ, DuPont MS, Ridley S, Rhodes M, Rhodes MJ, Morgan MR, Williamson G.** 1998. Deglycosylation of flavonoid and isoflavonoid glycosides by human small intestine and liver beta-glucosidase activity. FEBS Lett **436:**71-75.

103. **Hendrich S.** 2002. Bioavailability of isoflavones. J Chromatogr B Analyt Technol Biomed Life Sci **777:**203-210.

104. **Cooke PS, Selvaraj V, Yellayi S.** 2006. Genistein, estrogen receptors, and the acquired immune response. J Nutr **136:**704-708.

105. **Cui S, Wienhoefer N, Bilitewski U.** 2014. Genistein induces morphology change and G2/M cell cycle arrest by inducing p38 MAPK activation in macrophages. Int Immunopharmacol **18:**142-150.

106. **Lee YW, Lee WH.** 2008. Protective effects of genistein on proinflammatory pathways in human brain microvascular endothelial cells. J Nutr Biochem **19:**819-825.

107. **Chacko BK, Chandler RT, Mundhekar A, Khoo N, Pruitt HM, Kucik DF, Parks DA, Kevil CG, Barnes S, Patel RP.** 2005. Revealing anti-inflammatory mechanisms of soy isoflavones by flow: modulation of leukocyte-endothelial cell interactions. Am J Physiol Heart Circ Physiol **289:**H908-915.

108. **Karin M.** 2009. NF-kappaB as a critical link between inflammation and cancer. Cold Spring Harb Perspect Biol **1:**a000141.

109. **Hillman GG, Singh-Gupta V.** 2011. Soy isoflavones sensitize cancer cells to radiotherapy. Free Radic Biol Med **51:**289-298.

110. **Chun OK, Chung SJ, Song WO.** 2007. Estimated dietary flavonoid intake and major food sources of U.S. adults. J Nutr **137:**1244-1252.

111. **de Kleijn MJ, van der Schouw YT, Wilson PW, Adlercreutz H, Mazur W, Grobbee DE, Jacques PF.** 2001. Intake of dietary phytoestrogens is low in postmenopausal women in the United States: the Framingham study(1-4). J Nutr **131:**1826-1832.

112. **Mulligan AA, Welch AA, McTaggart AA, Bhaniani A, Bingham SA.** 2007. Intakes and sources of soya foods and isoflavones in a UK population cohort study (EPIC-Norfolk). Eur J Clin Nutr **61:**248-254.

113. **Kim J, Kwon C.** 2001. Estimated dietary isoflavone intake of Korean population based on National Nutrition Survey. Nutr Res **21:**947-953.

114. **Lee SA, Wen W, Xiang YB, Barnes S, Liu D, Cai Q, Zheng W, Shu XO.** 2007. Assessment of dietary isoflavone intake among middle-aged Chinese men. J Nutr **137:**1011-1016.

115. **Liu Z, Li W, Sun J, Liu C, Zeng Q, Huang J, Yu B, Huo J.** 2004. Intake of soy foods and soy isoflavones by rural adult women in China. Asia Pac J Clin Nutr **13:**204-209.

116. **Surh J, Kim MJ, Koh E, Kim YK, Kwon H.** 2006. Estimated intakes of isoflavones and coumestrol in Korean population. Int J Food Sci Nutr **57:**325-344.

117. **Marugame T, Katanoda K.** 2006. International comparisons of cumulative risk of breast and prostate cancer, from cancer incidence in five continents Vol. VIII. Jpn J Clin Oncol **36:**399-400.

118. **Akiyama T, Ishida J, Nakagawa S, Ogawara H, Watanabe S, Itoh N, Shibuya M, Fukami Y.** 1987. Genistein, a specific inhibitor of tyrosine-specific protein kinases. J Biol Chem **262:**5592-5595.

119. **Messina M.** 2010. Insights gained from 20 years of soy research. J Nutr **140:**2289S-2295S.

120. **Bradbury RB, White DE.** 1954. Estrogens and related substances in plants. Vitam Horm **12:**207-233.

121. **Curnow DH.** 1954. Oestrogenic activity of subterranean clover. II. The isolation of genistein from subterranean clover and methods of quantitative estimation. Biochem J **58:**283-287.

122. **Bennetts HW, Underwood EJ, Shier FL.** 1946. A specific breeding problem of sheep on subterranean clover pastures in Western Australia. Aust Vet J **22:**2-12.

123. **Wakai K, Egami I, Kato K, Kawamura T, Tamakoshi A, Lin Y, Nakayama T, Wada M, Ohno Y.** 1999. Dietary intake and sources of isoflavones among Japanese. Nutrition and cancer **33:**139-145.

124. **Nagata C, Takatsuka N, Inaba S, Kawakami N, Shimizu H.** 1998. Effect of soymilk consumption on serum estrogen concentrations in premenopausal Japanese women. J Natl Cancer Inst **90:**1830-1835.

125. **Shu XO, Zheng Y, Cai H, Gu K, Chen Z, Zheng W, Lu W.** 2009. Soy food intake and breast cancer survival. Jama **302:**2437-2443.

126. **Caan BJ, Natarajan L, Parker B, Gold EB, Thomson C, Newman V, Rock CL, Pu M, Al-Delaimy W, Pierce JP.** 2011. Soy food consumption and breast cancer prognosis. Cancer epidemiology, biomarkers & prevention : a publication of the American Association for Cancer Research, cosponsored by the American Society of Preventive Oncology **20:**854-858.

127. **Guha N, Kwan ML, Quesenberry CP, Jr., Weltzien EK, Castillo AL, Caan BJ.** 2009. Soy isoflavones and risk of cancer recurrence in a cohort of breast cancer survivors: the Life After Cancer Epidemiology study. Breast cancer research and treatment **118:**395-405.

128. **Boyapati SM, Shu XO, Ruan ZX, Dai Q, Cai Q, Gao YT, Zheng W.** 2005. Soyfood intake and breast cancer survival: a followup of the Shanghai Breast Cancer Study. Breast cancer research and treatment **92:**11-17.

129. **Kang X, Zhang Q, Wang S, Huang X, Jin S.** 2010. Effect of soy isoflavones on breast cancer recurrence and death for patients receiving adjuvant endocrine therapy. CMAJ : Canadian Medical Association journal = journal de l'Association medicale canadienne **182:**1857-1862.

130. **Woo HD, Park KS, Ro J, Kim J.** 2012. Differential influence of dietary soy intake on the risk of breast cancer recurrence related to HER2 status. Nutrition and cancer **64:**198-205.

131. **Zhang YF, Kang HB, Li BL, Zhang RM.** 2012. Positive effects of soy isoflavone food on survival of breast cancer patients in China. Asian Pacific journal of cancer prevention : APJCP **13:**479-482.

132. **Chen M, Rao Y, Zheng Y, Wei S, Li Y, Guo T, Yin P.** 2014. Association between soy isoflavone intake and breast cancer risk for pre- and post-menopausal women: a meta-analysis of epidemiological studies. PloS one **9:**e89288.

133. **Messina M, Caan BJ, Abrams DI, Hardy M, Maskarinec G.** 2013. It's time for clinicians to reconsider their proscription against the use of soyfoods by breast cancer patients. Oncology **27:**430-437.

134. **Hillman GG, Singh-Gupta V, Hoogstra DJ, Abernathy L, Rakowski J, Yunker CK, Rothstein SE, Sarkar FH, Gadgeel S, Konski AA, Lonardo F, Joiner MC.** 2013. Differential effect of soy isoflavones in enhancing high intensity radiotherapy and protecting lung tissue in a pre-clinical model of lung carcinoma. Radiother Oncol **109:**117-125.

135. **Hillman GG, Singh-Gupta V, Lonardo F, Hoogstra DJ, Abernathy LM, Yunker CK, Rothstein SE, Rakowski J, Sarkar FH, Gadgeel S, Konski AA, Joiner MC.** 2013. Radioprotection of lung tissue by soy isoflavones. J Thorac Oncol **8:**1356-1364.

136. **Mahmood J, Jelveh S, Zaidi A, Doctrow SR, Hill RP.** 2013. Mitigation of radiation-induced lung injury with EUK-207 and genistein: effects in adolescent rats. Radiat Res **179:**125-134.

137. **Singh-Gupta V, Joiner MC, Runyan L, Yunker CK, Sarkar FH, Miller S, Gadgeel SM, Konski AA, Hillman GG.** 2011. Soy isoflavones augment radiation effect by inhibiting APE1/Ref-1 DNA repair activity in non-small cell lung cancer. J Thorac Oncol **6:**688-698.

138. **Messina M, Kucuk O, Lampe JW.** 2006. An overview of the health effects of isoflavones with an emphasis on prostate cancer risk and prostate-specific antigen levels. J AOAC Int **89:**1121-1134.

139. **Ahmad IU, Forman JD, Sarkar FH, Hillman GG, Heath E, Vaishampayan U, Cher ML, Andic F, Rossi PJ, Kucuk O.** 2010. Soy isoflavones in conjunction with radiation therapy in patients with prostate cancer. Nutrition and cancer **62:**996-1000.

140. **Hillman GG, Wang Y, Kucuk O, Che M, Doerge DR, Yudelev M, Joiner MC, Marples B, Forman JD, Sarkar FH.** 2004. Genistein potentiates inhibition of tumor

growth by radiation in a prostate cancer orthotopic model. Mol Cancer Ther **3:**1271-1279.

141. **Hill RP, Zaidi A, Mahmood J, Jelveh S.** 2011. Investigations into the role of inflammation in normal tissue response to irradiation. Radiother Oncol **101:**73-79.

142. **Mehta V.** 2005. Radiation pneumonitis and pulmonary fibrosis in non-small-cell lung cancer: pulmonary function, prediction, and prevention. Int J Radiat Oncol Biol Phys **63:**5-24.

143. **Gough MJ, Young K, Crittenden M.** 2013. The impact of the myeloid response to radiation therapy. Clin Dev Immunol **2013:**281958.

144. **Gensel JC, Zhang B.** 2015. Macrophage activation and its role in repair and pathology after spinal cord injury. Brain Res.

145. **Lucas T, Waisman A, Ranjan R, Roes J, Krieg T, Muller W, Roers A, Eming SA.** 2010. Differential roles of macrophages in diverse phases of skin repair. J Immunol **184:**3964-3977.

146. **Duffield JS, Forbes SJ, Constandinou CM, Clay S, Partolina M, Vuthoori S, Wu S, Lang R, Iredale JP.** 2005. Selective depletion of macrophages reveals distinct, opposing roles during liver injury and repair. J Clin Invest **115:**56-65.

147. **Munder M, Eichmann K, Moran JM, Centeno F, Soler G, Modolell M.** 1999. Th1/Th2-regulated expression of arginase isoforms in murine macrophages and dendritic cells. J Immunol **163:**3771-3777.

148. **De Brauwer EI, Jacobs JA, Nieman F, Bruggeman CA, Drent M.** 2002. Bronchoalveolar lavage fluid differential cell count. How many cells should be counted? Anal Quant Cytol Histol **24:**337-341.

149. **Bedoret D, Wallemacq H, Marichal T, Desmet C, Quesada Calvo F, Henry E, Closset R, Dewals B, Thielen C, Gustin P, de Leval L, Van Rooijen N, Le Moine A, Vanderplasschen A, Cataldo D, Drion PV, Moser M, Lekeux P, Bureau F.** 2009. Lung interstitial macrophages alter dendritic cell functions to prevent airway allergy in mice. J Clin Invest **119:**3723-3738.

150. **Rose S, Misharin A, Perlman H.** 2012. A novel Ly6C/Ly6G-based strategy to analyze the mouse splenic myeloid compartment. Cytometry A **81:**343-350.

151. **Ahn GO, Tseng D, Liao CH, Dorie MJ, Czechowicz A, Brown JM.** 2010. Inhibition of Mac-1 (CD11b/CD18) enhances tumor response to radiation by reducing myeloid cell recruitment. Proc Natl Acad Sci U S A **107:**8363-8368.

152. **Cappuccini F, Eldh T, Bruder D, Gereke M, Jastrow H, Schulze-Osthoff K, Fischer U, Kohler D, Stuschke M, Jendrossek V.** 2011. New insights into the molecular pathology of radiation-induced pneumopathy. Radiother Oncol **101:**86-92.

153. **Chiang CS, Liu WC, Jung SM, Chen FH, Wu CR, McBride WH, Lee CC, Hong JH.** 2005. Compartmental responses after thoracic irradiation of mice: strain differences. Int J Radiat Oncol Biol Phys **62:**862-871.

154. **Zaynagetdinov R, Sherrill TP, Kendall PL, Segal BH, Weller KP, Tighe RM, Blackwell TS.** 2013. Identification of myeloid cell subsets in murine lungs using flow cytometry. Am J Respir Cell Mol Biol **49:**180-189.

155. **Gordon S, Taylor PR.** 2005. Monocyte and macrophage heterogeneity. Nat Rev Immunol **5:**953-964.

156. **Wu G, Morris SM, Jr.** 1998. Arginine metabolism: nitric oxide and beyond. Biochem J **336 (Pt 1):**1-17.

157. **Laskin DL, Sunil VR, Gardner CR, Laskin JD.** 2011. Macrophages and tissue injury: agents of defense or destruction? Annu Rev Pharmacol Toxicol **51:**267-288.

158. **Zhang H, Han G, Liu H, Chen J, Ji X, Zhou F, Zhou Y, Xie C.** 2011. The development of classically and alternatively activated macrophages has different effects on the varied stages of radiation-induced pulmonary injury in mice. J Radiat Res **52:**717-726.

159. **Mosser DM.** 2003. The many faces of macrophage activation. J Leukoc Biol **73:**209-212.

160. **Gordon S, Martinez FO.** 2010. Alternative activation of macrophages: mechanism and functions. Immunity **32:**593-604.

161. **Morris SM, Jr.** 2007. Arginine metabolism: boundaries of our knowledge. J Nutr **137:**1602S-1609S.

162. **Ao X, Zhao L, Davis MA, Lubman DM, Lawrence TS, Kong FM.** 2009. Radiation produces differential changes in cytokine profiles in radiation lung fibrosis sensitive and resistant mice. J Hematol Oncol **2:**6.

163. **Wang XP, Chen YG, Qin WD, Zhang W, Wei SJ, Wang J, Liu FQ, Gong L, An FS, Zhang Y, Chen ZY, Zhang MX.** 2011. Arginase I attenuates inflammatory cytokine secretion induced by lipopolysaccharide in vascular smooth muscle cells. Arterioscler Thromb Vasc Biol **31:**1853-1860.

164. **Droke EA, Hager KA, Lerner MR, Lightfoot SA, Stoecker BJ, Brackett DJ, Smith BJ.** 2007. Soy isoflavones avert chronic inflammation-induced bone loss and vascular disease. J Inflamm (Lond) **4:**17.

165. **Bouhlel MA, Derudas B, Rigamonti E, Dievart R, Brozek J, Haulon S, Zawadzki C, Jude B, Torpier G, Marx N, Staels B, Chinetti-Gbaguidi G.** 2007. PPARgamma activation primes human monocytes into alternative M2 macrophages with anti-inflammatory properties. Cell Metab **6:**137-143.

166. **Wang N, Liang H, Zen K.** 2014. Molecular mechanisms that influence the macrophage m1-m2 polarization balance. Frontiers in immunology **5:**614.

167. **Raffoul JJ, Banerjee S, Singh-Gupta V, Knoll ZE, Fite A, Zhang H, Abrams J, Sarkar FH, Hillman GG.** 2007. Down-regulation of apurinic/apyrimidinic endonuclease 1/redox factor-1 expression by soy isoflavones enhances prostate cancer radiotherapy in vitro and in vivo. Cancer research **67:**2141-2149.

168. **Martin M, Lefaix J, Delanian S.** 2000. TGF-beta1 and radiation fibrosis: a master switch and a specific therapeutic target? Int J Radiat Oncol Biol Phys **47:**277-290.

169. **Leask A, Abraham DJ.** 2004. TGF-beta signaling and the fibrotic response. FASEB J **18:**816-827.

170. **Santak G, Santak M, Forcic D.** 2010. The role of interleukin-1beta and platelet-derived growth factor-AB in antifibrosis mediated by native human interferon alpha. Surgery **148:**490-498.

171. **Lemberger T, Desvergne B, Wahli W.** 1996. Peroxisome proliferator-activated receptors: a nuclear receptor signaling pathway in lipid physiology. Annu Rev Cell Dev Biol **12:**335-363.

172. **Hart CM, Roman J, Reddy R, Sime PJ.** 2008. PPARgamma: a novel molecular target in lung disease. J Investig Med **56:**515-517.

173. **Lakatos HF, Thatcher TH, Kottmann RM, Garcia TM, Phipps RP, Sime PJ.** 2007. The Role of PPARs in Lung Fibrosis. PPAR Res **2007:**71323.

174. **Ricketts ML, Moore DD, Banz WJ, Mezei O, Shay NF.** 2005. Molecular mechanisms of action of the soy isoflavones includes activation of promiscuous nuclear receptors. A review. J Nutr Biochem **16:**321-330.

175. **Blanquart C, Barbier O, Fruchart JC, Staels B, Glineur C.** 2003. Peroxisome proliferator-activated receptors: regulation of transcriptional activities and roles in inflammation. J Steroid Biochem Mol Biol **85:**267-273.

176. **Auperin A, Le Pechoux C, Rolland E, Curran WJ, Furuse K, Fournel P, Belderbos J, Clamon G, Ulutin HC, Paulus R, Yamanaka T, Bozonnat MC, Uitterhoeve A, Wang X, Stewart L, Arriagada R, Burdett S, Pignon JP.** 2010. Meta-analysis of concomitant versus sequential radiochemotherapy in locally advanced non-small-cell lung cancer. J Clin Oncol **28:**2181-2190.

177. **Guida C, Maione P, Rossi A, Bareschino M, Schettino C, Barzaghi D, Elmo M, Gridelli C.** 2008. Combined chemo-radiotherapy for locally advanced non-small cell lung cancer: current status and future development. Crit Rev Oncol Hematol **68:**222-232.

178. **Lo SS, Sahgal A, Chang EL, Mayr NA, Teh BS, Huang Z, Schefter TE, Yao M, Machtay M, Slotman BJ, Timmerman RD.** 2013. Serious complications associated with stereotactic ablative radiotherapy and strategies to mitigate the risk. Clin Oncol (R Coll Radiol) **25:**378-387.

179. **Soliman H, Cheung P, Yeung L, Poon I, Balogh J, Barbera L, Spayne J, Danjoux C, Dahele M, Ung Y.** 2011. Accelerated hypofractionated radiotherapy for early-stage non-small-cell lung cancer: long-term results. Int J Radiat Oncol Biol Phys **79:**459-465.

180. **Videtic GM, Stephans KL.** 2010. The role of stereotactic body radiotherapy in the management of non-small cell lung cancer: an emerging standard for the medically inoperable patient? Curr Oncol Rep **12:**235-241.

ABSTRACT

SOY ISOFLAVONES MEDIATE RADIOPROTECTION OF NORMAL LUNG TISSUE BY MODULATING THE RADIATION-INDUCED INFLAMMATORY RESPONSE

by

LISA M. ABERNATHY

August 2015

Advisor: Dr. Gilda Gali Hillman

Major: Immunology and Microbiology

Degree: Doctor of Philosophy

Radiation-induced lung injury (RILI) is caused by an early inflammatory process triggered by damage to lung parenchyma, epithelial cells, vascular endothelial cells and stroma. Initially, oxidative injuries after radiation induce altered expression of pro-inflammatory cytokines. Infiltrating inflammatory cells are stimulated and activated, producing additional mediators, resulting in a cytokine cascade. The expansion and perpetual activation of inflammatory cells, as well as lung parenchyma, lead to clinical pneumonitis. Activated cells produce molecular mediators and growth factors that affect the proliferation and gene expression of lung fibroblasts. This process leads to increased collagen synthesis and deposition, eventually leading to the development of lung fibrosis. These adverse events after radiotherapy affect patients' breathing and their quality of life. Various strategies to decrease the extent of pneumonitis have been investigated but need further research efforts.

We have previously demonstrated in mice receiving a single high dose of thoracic irradiation that supplementation with a mixture soy isoflavones (genistein, daidzein, and glycitein) has the dual capability of protecting normal lung tissue from radiation injury while

simultaneously enhancing radiation damage in the tumor. However, mechanisms of radioprotection by soy isoflavones in normal tissues remained to be elucidated. We hypothesized that soy isoflavones mediate radioprotection via the modulation of radiation-induced inflammatory processes involving macrophages, neutrophils, and myeloid-derived suppressor cells.

The major findings of this work suggest that soy isoflavones can inhibit inflammatory responses triggered by a single dose of thoracic irradiation in the lung, including NF-κB and pro-inflammatory cytokine production. We reveal that soy isoflavones inhibit the infiltration and activation of macrophages and neutrophils in the lung induced by radiation. Radiation induced a pro-inflammatory M1 macrophage phenotype in lungs, while mice receiving soy isoflavones and radiation switched to an anti-inflammatory M2 macrophage subtype. Soy isoflavones had a protective effect on regulatory interstitial macrophages (IM) after irradiation, while inhibiting alveolar macrophage (AM) infiltration and activation induced by radiation. Interestingly, we show that soy isoflavones promote granulocytic myeloid-derived suppressor cells that express Arg-1 after radiation, resulting in subsequent downregulation inflammatory mediators. These data indicate that lung radioprotection by soy isoflavones may occur via the modulation of cellular and molecular mediators involved in the inflammatory response induced by radiation.

AUTOBIOGRAPHICAL STATEMENT

Lisa M. Abernathy

EDUCATION:

Ph.D., Immunology and Microbiology
Wayne State University School of Medicine, Detroit, MI, August 2015

Bachelor of Science in Microbiology and Molecular Genetics
Michigan State University, Lansing, MI, May 2007

WORK EXPERIENCE:

2007 – 2009 Research Associate
Internal Medicine, University of Michigan, Ann Arbor, MI

AWARDS:

2015 First Place, Poster Presentation, Graduate Exhibition
Wayne State University

2013 Conference Scholarship, American Institute for Cancer Research Conference
American Institute for Cancer Research

2007 First Place, Poster Presentation, Undergraduate Research and Arts Forum
Michigan State University

PUBLICATIONS:

2015 **Abernathy LM**, Fountain MD, Rothstein SE, David JM, Yunker CK, Rakowski J, Lonardo F, Joiner MC, Hillman GG. Soy Isoflavones Promote Radioprotection of Normal Lung Tissue by Inhibition of Radiation-Induced Activation of Macrophages and Neutrophils. *Journal of Thoracic Oncology*.

2013 Hillman GG, Singh-Gupta V, Lonardo F, Hoogstra DJ, **Abernathy LM**, Yunker CK, Rothstein SE, Rakowski J, Sarkar FH, Gadgeel S, Konski AA, Joiner MC. Radioprotection of Lung Tissues by Soy Isoflavones. *Journal of Thoracic Oncology*, 8:1356-64.

2013 Hillman GG, Singh-Gupta V, Hoogstra DJ, **Abernathy LM**, Rakowski J, Yunker CK, Rothstein SE, Sarkar FH, Gadgeel S, Konski AA, Lonardo F, Joiner MC. Differential Effect of Soy Isoflavones in Enhancing High Intensity Radiotherapy and Protecting Lung Tissue in a Pre-Clinical Model of Lung Carcinoma. *Radiotherapy and Oncology*, 109:11-25.

2008 Grolleau-Julius A, **Abernathy LM**, Harning E.K., and Yung R.L. Mechanisms of Dendritic Cell Antitumor Dysfunction in Aging. *Journal of Cancer Immunology Immunotherapy*, 58:1935-1939.

2008 Grolleau-Julius A, Harning EK, **Abernathy LM**, and Yung RL, Impaired dendritic cell function in aging lead to defective antitumor immunity. *Cancer Research*, 68:6341-6349.